Yellow Hypergiants and Luminous Blue Variables


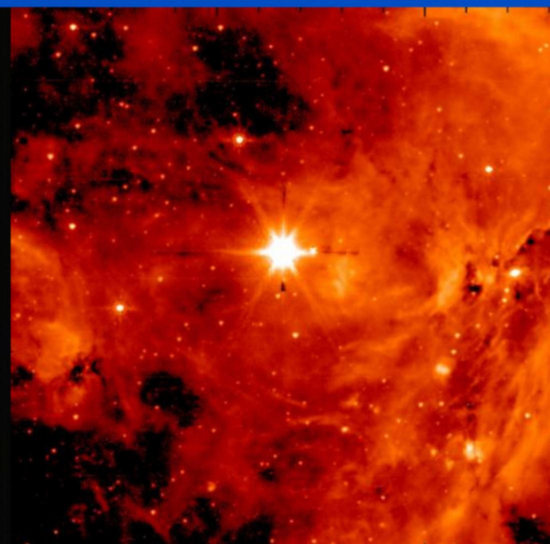
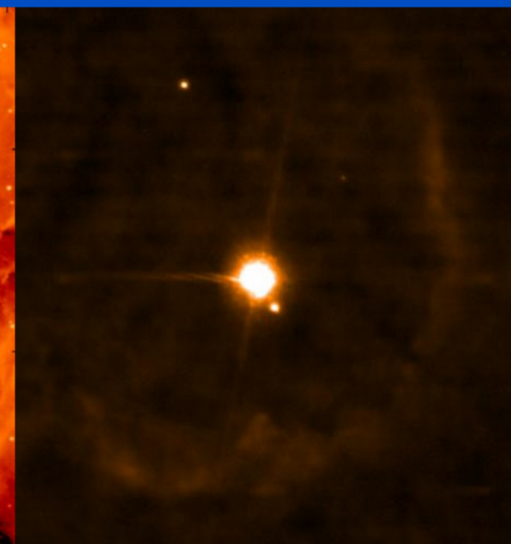
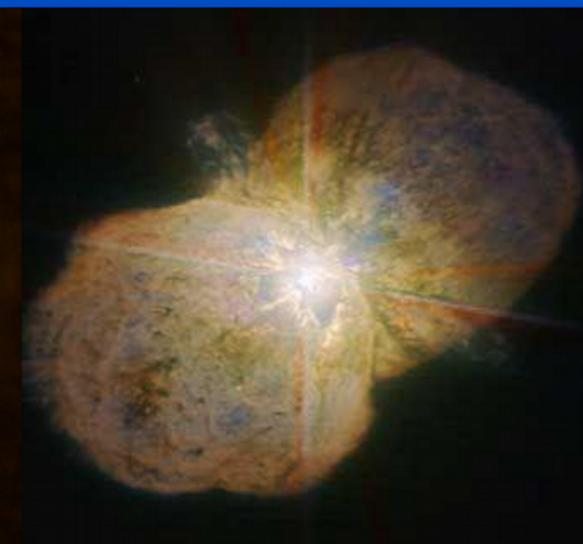

Alex Lobel

Royal Observatory of Belgium, Brussels

POEMS

International Conference

Physics of Extreme Massive Stars

24 - 28 June 2024

Rio de Janeiro, Brazil

Outline

- **What are Yellow Hypergiants (YHG) and Luminous Blue Variables (LBV)? Where do they live in the H-R diagram? Investigate notorious YHGs : Rho Cas, HR 8752, HR 5171A, and some well-studied (c)LBVs : S Dor, P Cyg, HD 168607, MWC 314.**

- **What can long-term high-resolution spectroscopic monitoring of YHGs, LBVs, and cLBVs tell us about their atmospheres and the wind physics of these exceptional massive stars close to the stellar luminosity limit?**

- **Investigate atmospheric dynamics, pulsation properties, wind structures, mass-loss rates, outburst events, etc. by combining long-term spectroscopy and multi-band photometry.**

- **What can multi-D radiative transfer modelling of large-scale hydrodynamic wind structures in massive B-stars learn?**

Yellow Hypergiants in the upper H-R diagram

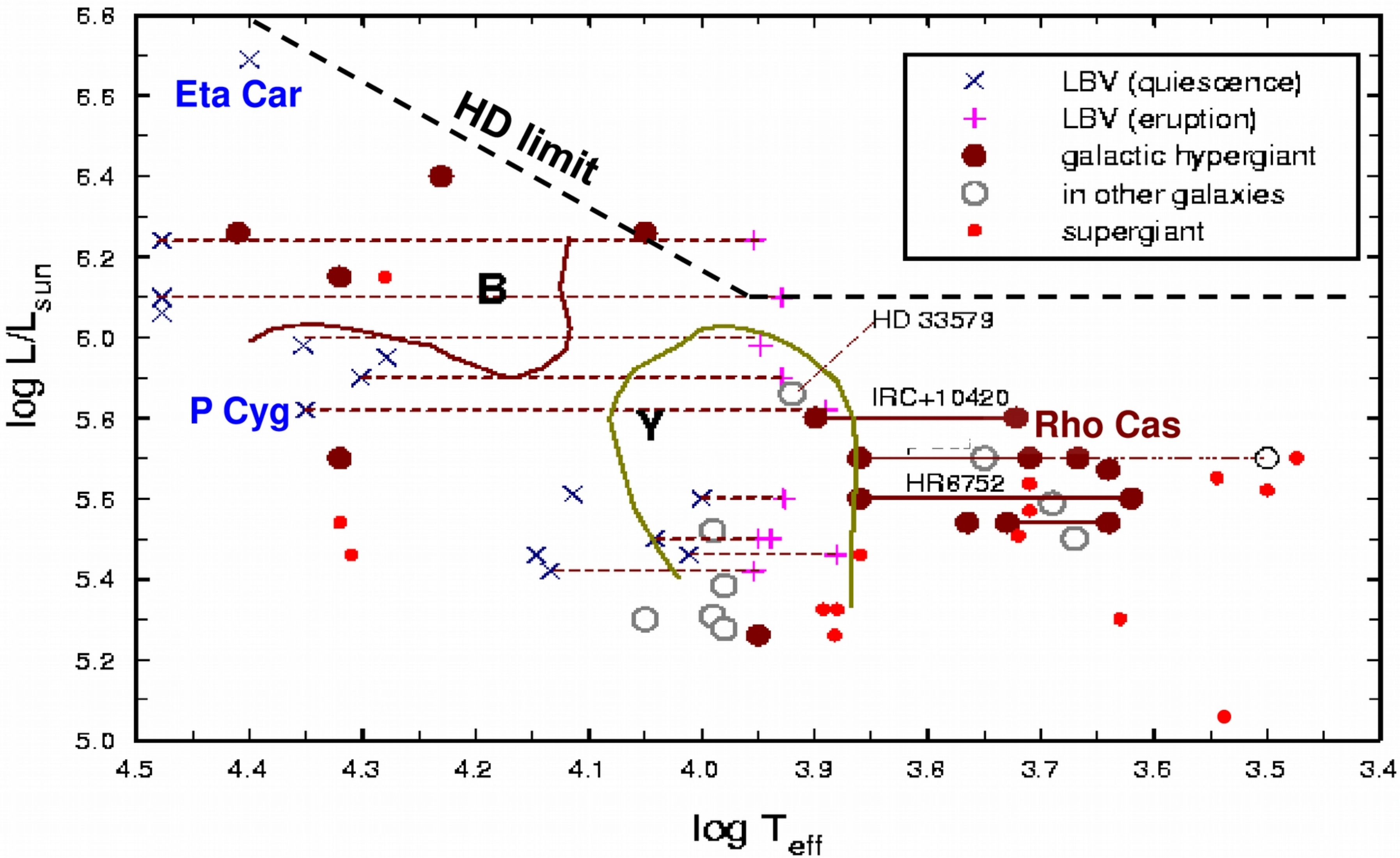

- **Most massive and luminous supergiants near upper luminosity limit (F-G Ia^{+}).**
- **Show strong spectral variability and semi-regular *V*-brightness curves.**
- **Recurrent eruption events with exceptionally large mass-loss rates to ~10^{-3} $M_{\odot}$ /y**

The Yellow Hypergiant Void

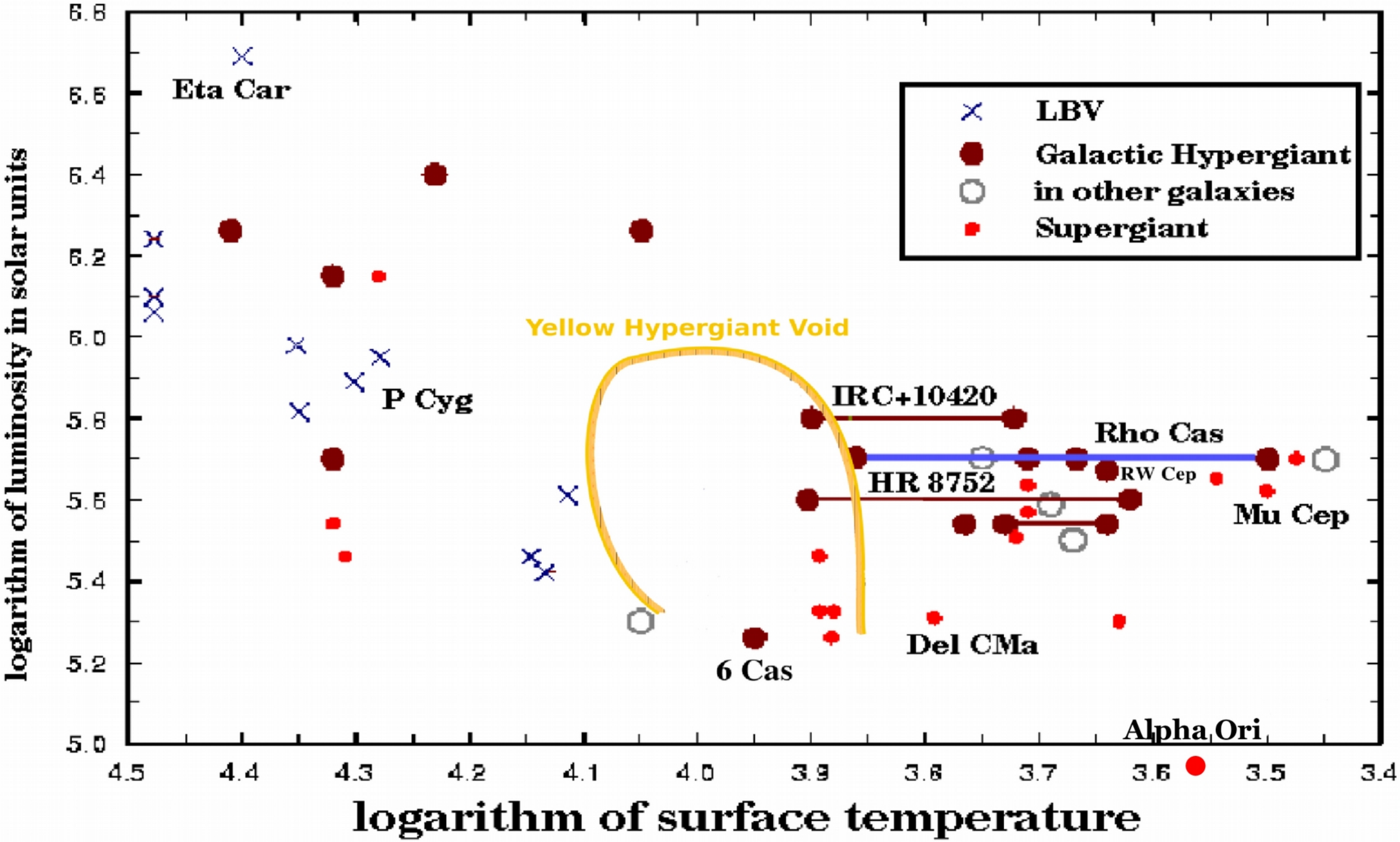

- **Most Yellow Hypergiants cluster near cool border of Yellow Void.**
- **The Yellow Void is a region devoid of Yellow Hypergiants (evolving blueward).**
- **Cool Hypergiants thought be on fast blueward evolutionary tracks (de Jager 1998).**

Atmospheric Instability in front of Yellow Evolutionary Void

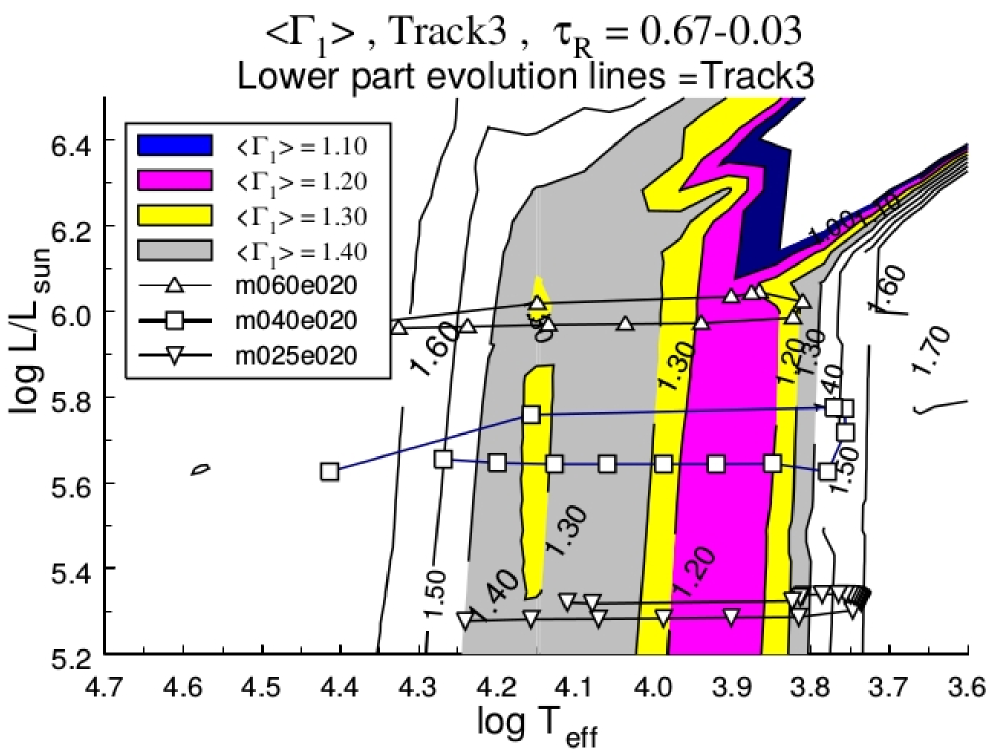

Fig. 17. Evolutionary model tracks for ZAMS masses of 25, 40, and 60 solar masses (Meynet et al. 1994) are superimposed on a background grid with values of Γ_1, as described in the text. Γ_1 is given for the full calculation, no radiation, and following Lobel et al. (1992) and Lobel (2001). The graph should be considered with the lower parts of the evolutionary tracks (track 3).

- **YEV is observational phenomenon for blueward evolving post-RGB stars. The models show a very extended partial H-ionization zone in an extended atmosphere with volumetric pressure-weighted heat-capacity integral $<\Gamma_1>$ very close to 4/3.**
- **Cool boundary of YEV at Teff ~ 8100 K with large compressibility or small bulk modulus.**
- **Redward evolving SGs do not feel YEV, while blueward evolving post-RSGs bounce off.**

LUMINOUS BLUE VARIABLE

P Cygni B1 Ia+

T_{eff} = 19,300 K Log g = 0.0

$R_* = 76\ R_\odot$ $L_* = 630{,}000\ L_\odot$

RED SUPERGIANT

Alpha Ori M2 Iab

T_{eff} = 3500 K Log g = - 0.5

$R_* = 700\ R_\odot$ $L_* = 40{,}000\ L_\odot$

YELLOW HYPERGIANT

Rho Cas F - G Ia+

T_{eff} = 7200 K Log g = 0.5

$R_* = 400\ R_\odot$ $L_* = 100{,}000\ L_\odot$

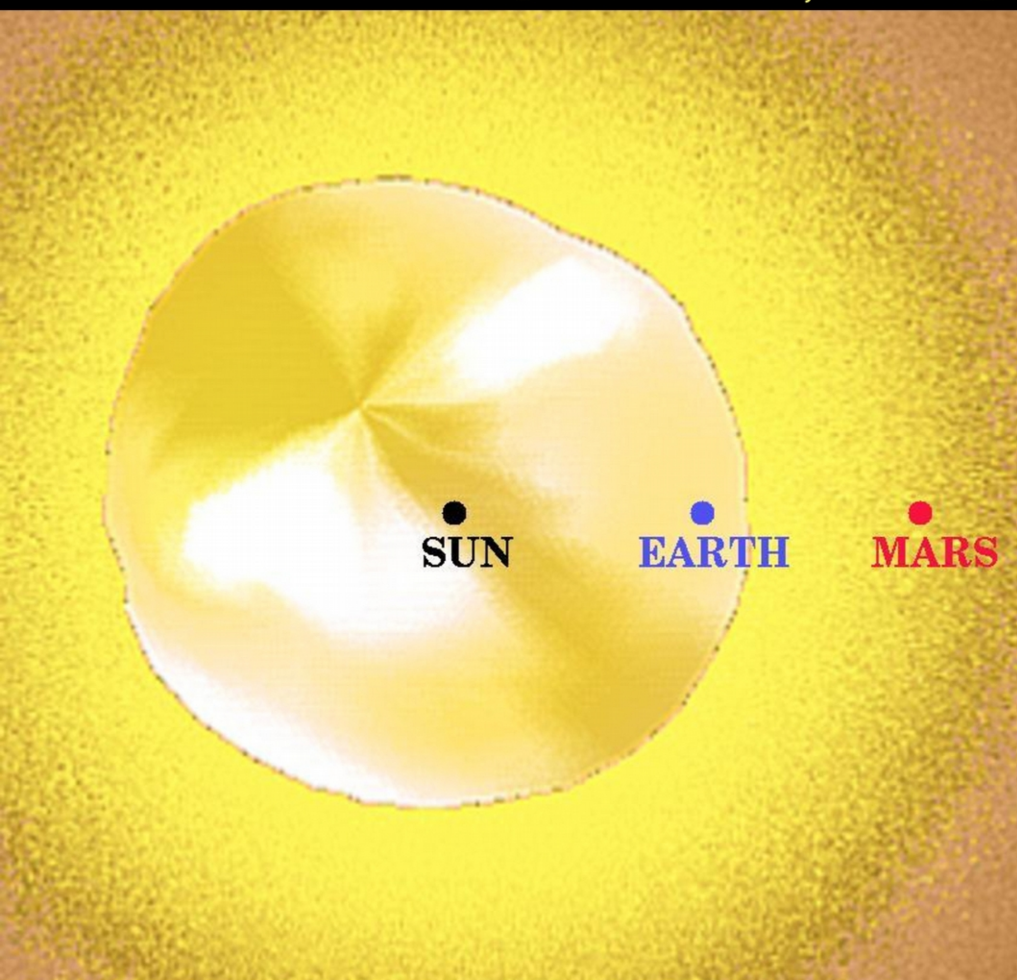

V brightness curves of YHGs Rho Cas and HR 5171

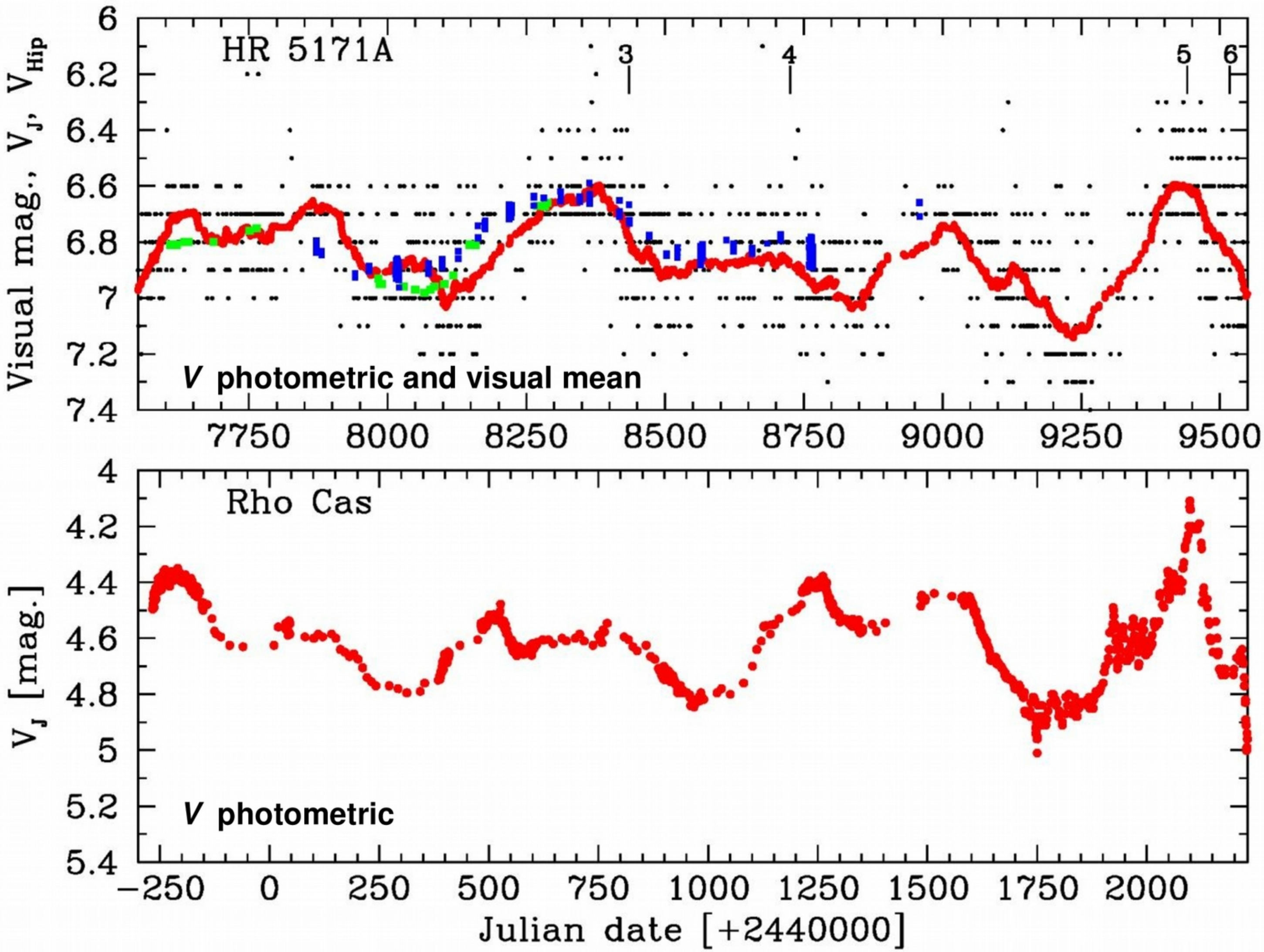

- **Quasi-periodic *V*-variability over several years with P_q = 240 d – 520+ d.**
- ***V* lightcurve amplitudes of $0^m.2$ to $0^m.5$ due to atmospheric pulsations.**
- ***V* lightcurve can occasionally resemble RV Tau stars with double minima.**
- ***V* amplitudes can decrease and increase over years and result in … outbursts.**

Quiescence Pulsations of Rho Cas

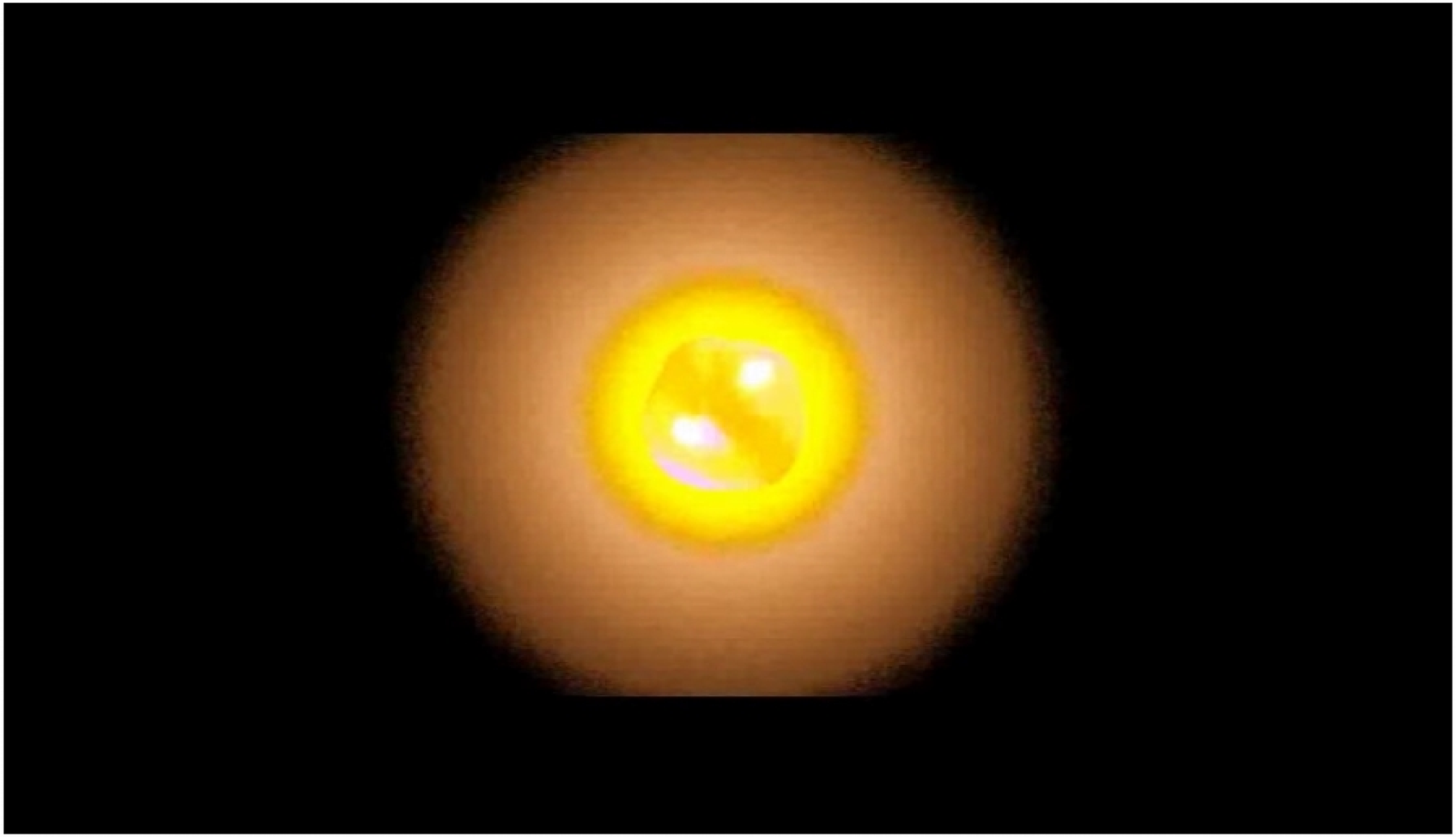

- Atmospheric pulsations show velocity stratification in metal vs. Hα lines.
- Pulsations initiate large steady mass-loss rates of ~10^{-5} $M_{\odot}$/y.
- Non-radial pulsations in quiescence variability phases.
- Pulsations are linked with strong convective movements and line broadening.

Quiescence Pulsations of Rho Cas

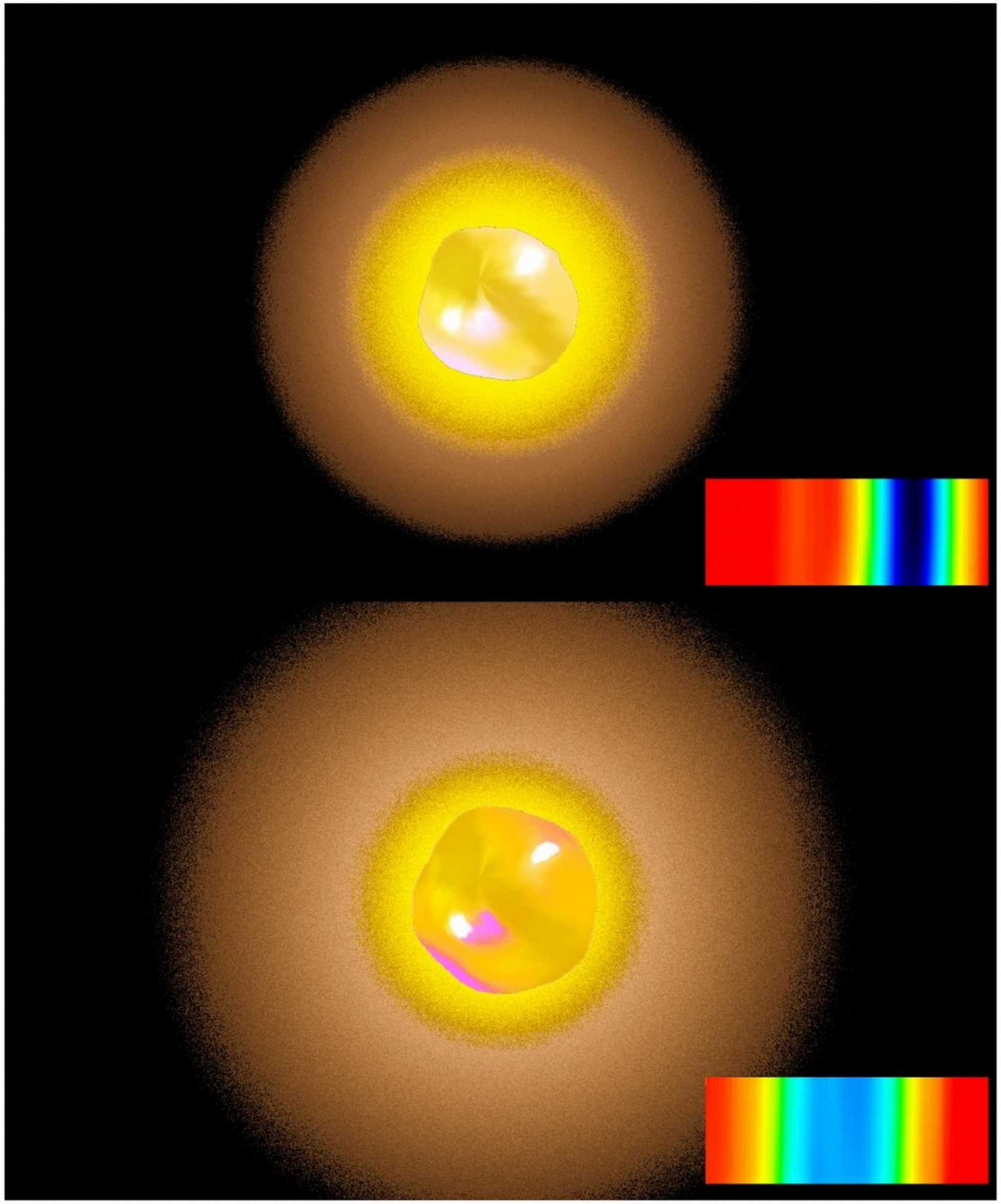

- Photospheric metal lines show strong Doppler shifts in absorption cores.
- *V* lightcurve follows and lags the radial velocity curve of metal lines.

Spectroscopic Sisters Rho Cas, HR 5171A, HR 8752

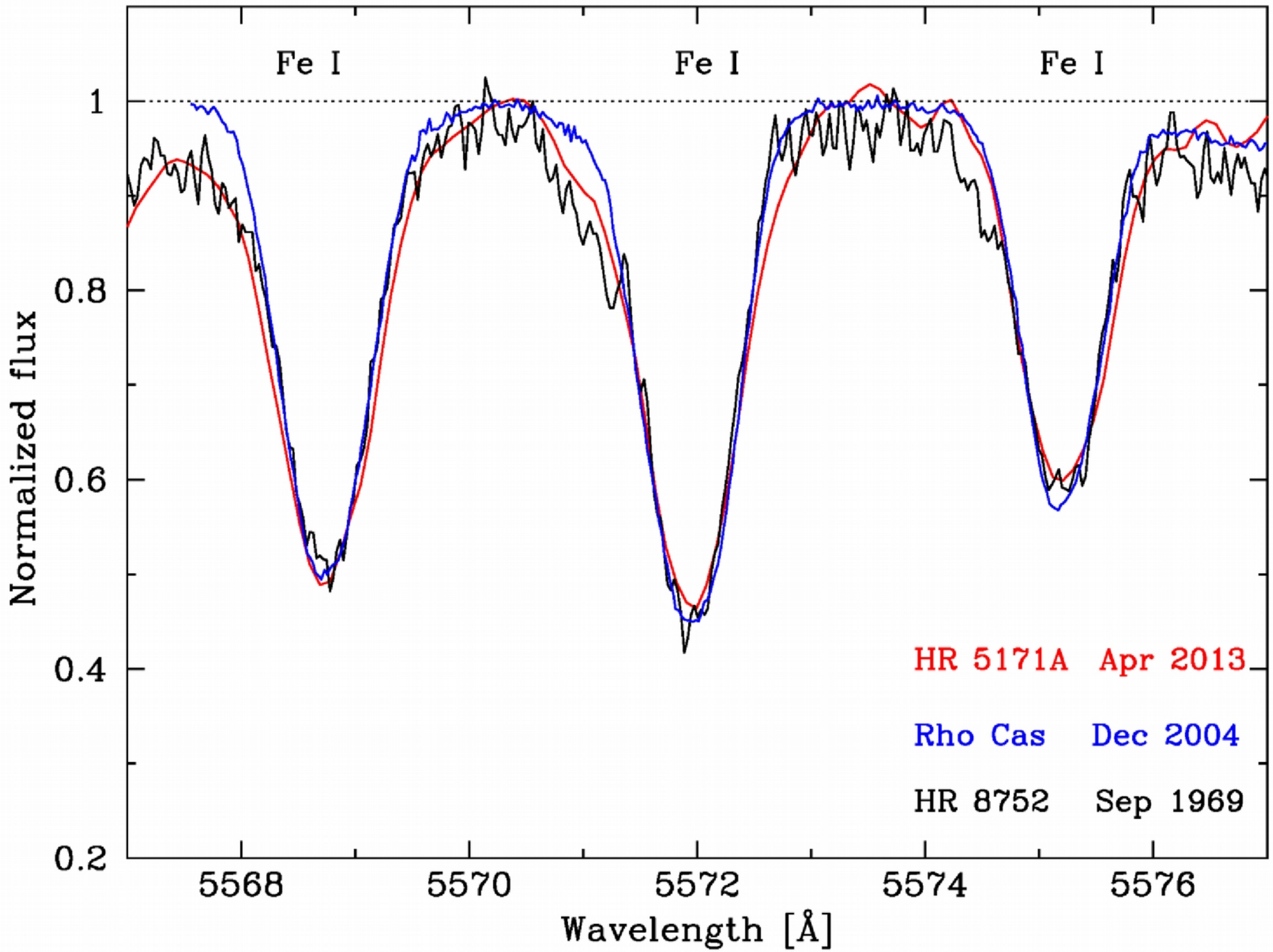

- **Photospheric Fe absorption lines show same shapes and widths in 3 YHGs.**
- **Spectroscopic sister stars during epochs of similar Teff.**
- **Around AMBER observations HR 5171A spectroscopically identical to Rho Cas.**

Long-term Spectroscopic Monitoring of Rho Cas

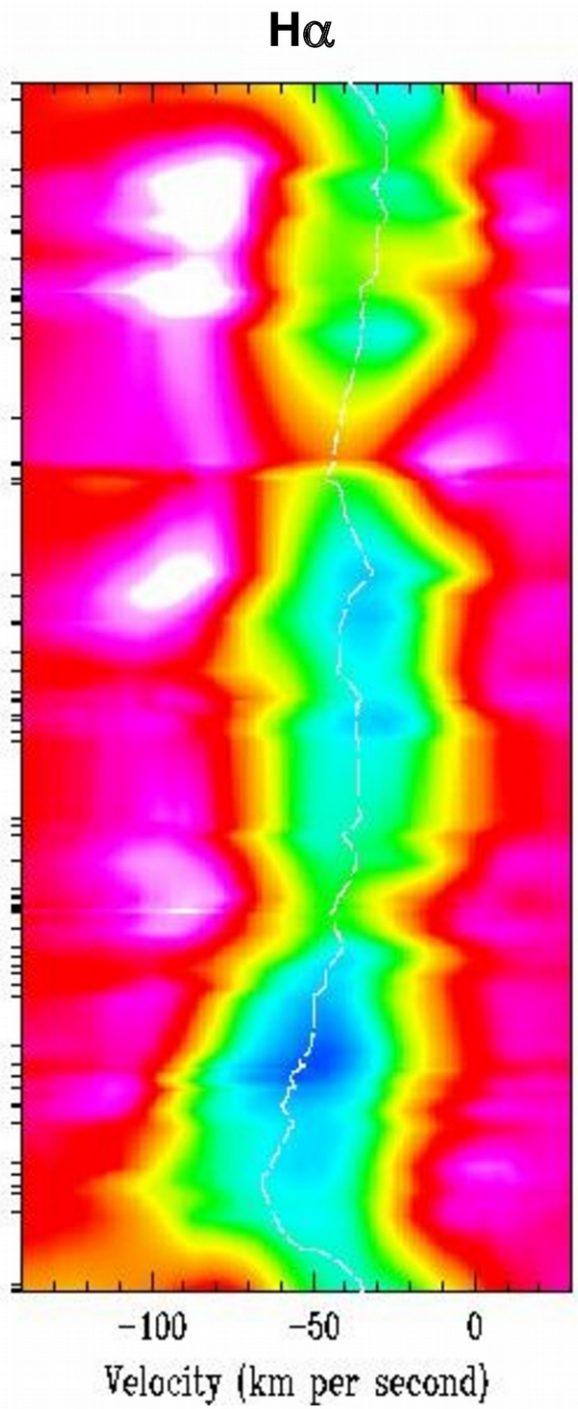

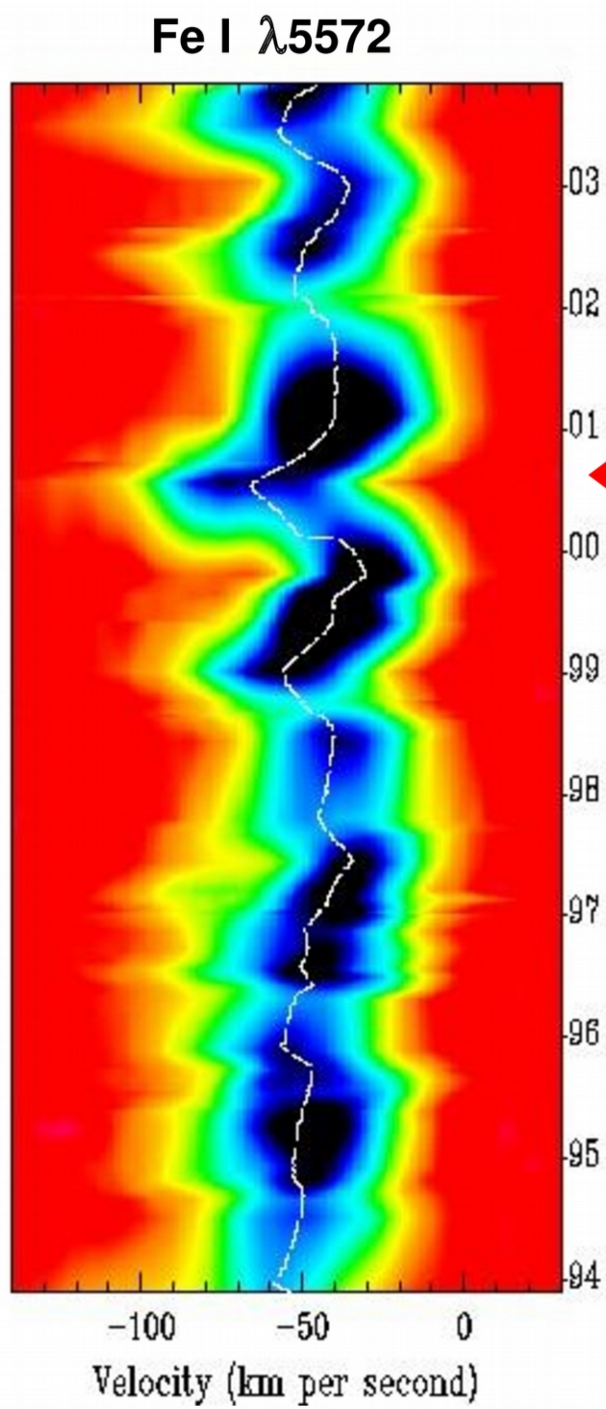

- Striking variability of photospheric lines with P_q = 300 to 500 d.
- Hα variability very different from photospheric metal lines.

Millennium Outburst
ApJ 2003, 583, 923

- Hα line formation region more extended and velocity stratified compared to photospheric lines.
- Yellow hypergiants have very broad abs. lines due to unusually strong broadening mechanism causing supersonic 'micro'- and 'macro'-turbulence velocity values.
- Far violet extended wings develop in photospheric lines during outburst events related to strong radial pulsations with <u>global</u> cooling of entire atmosphere.

Millennium Outburst of Rho Cas

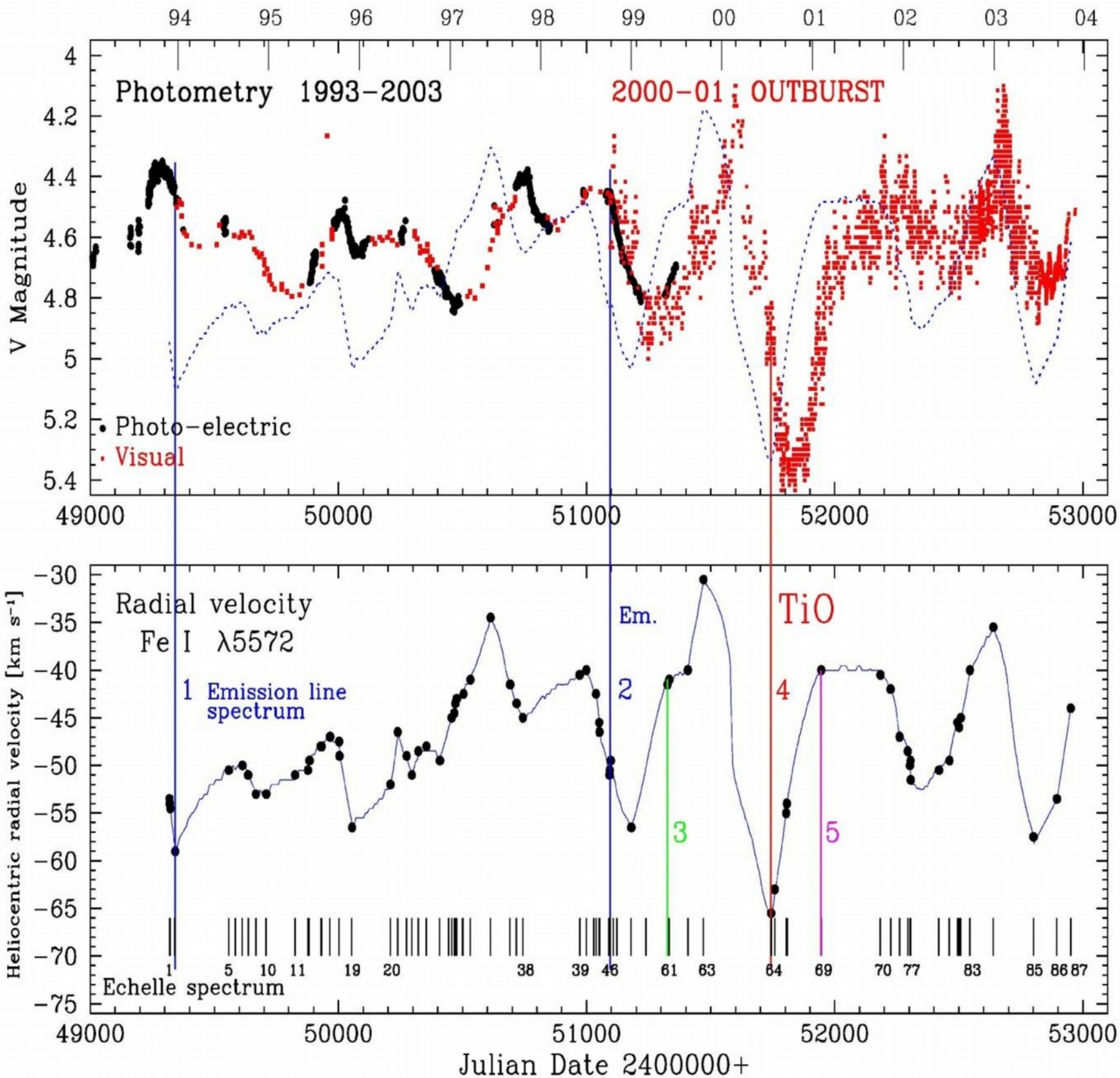

- **Outburst related to very large amplitude of phot. Vrad curve with strong radial pulsation.**
- ***V* dims by 1.5 mag. in 200 d.**
- **T_{eff} decreases from ~7000 K to below 4000 K from RT modeling.**
- **Shell event with 35 ± 2 km/s observed in new TiO bands.**
- **Mdot increases from ~10^{-5} $M_{\odot}$/y to 5.4 10^{-2} $M_{\odot}$/y.**
- **Total gas-mass expelled by shell event ~5 % of $M_{\odot}$ from TiO bands and violet wings of phot. lines.**
- **Radiative line driving mechanism too weak and dust driving mechanism not efficient.**
- **Mechanical wind driving plays important role during outburst events.**

Millennium Outburst of Yellow Hypergiant Rho Cas

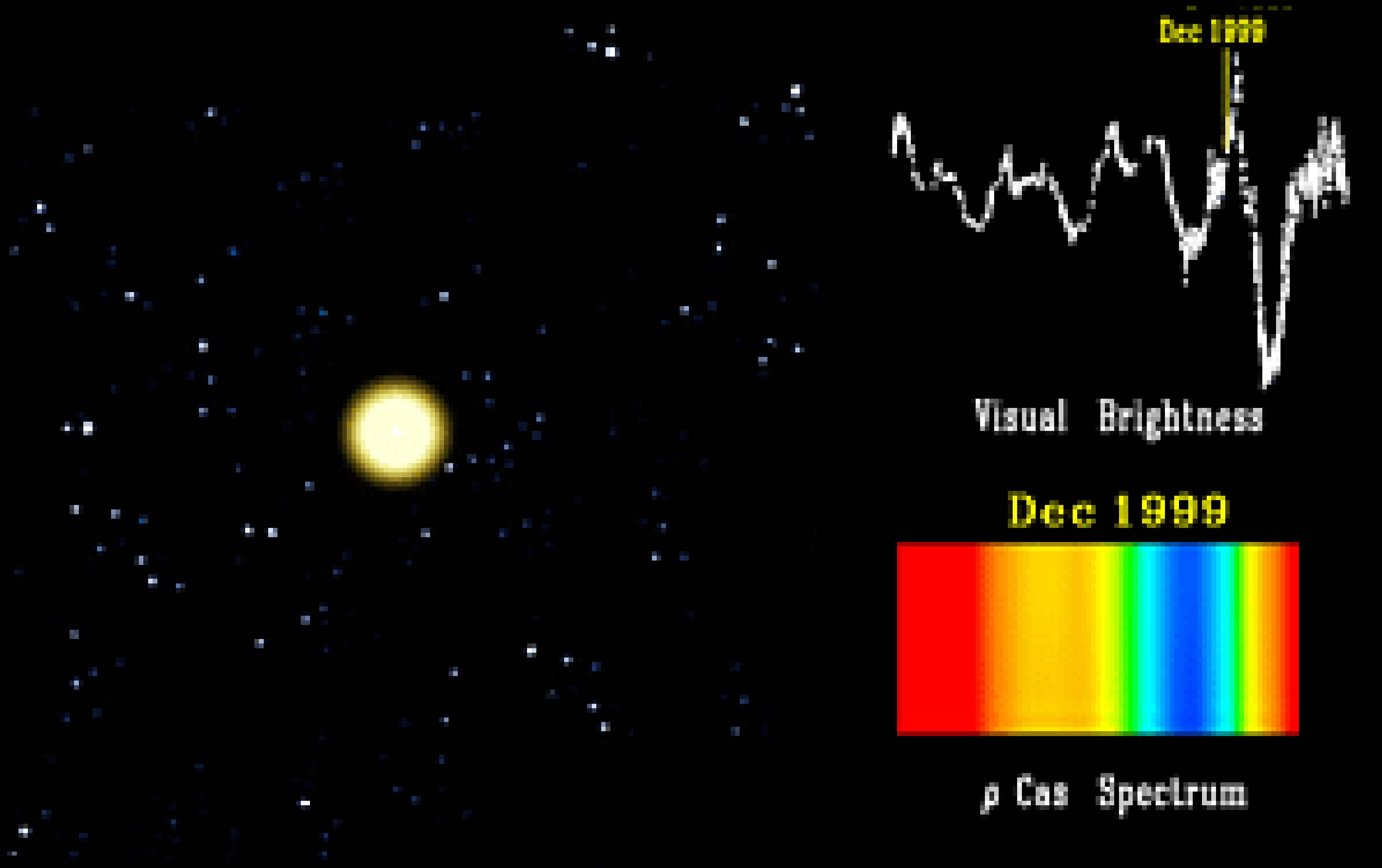

Millennium Outburst of Yellow Hypergiant Rho Cas

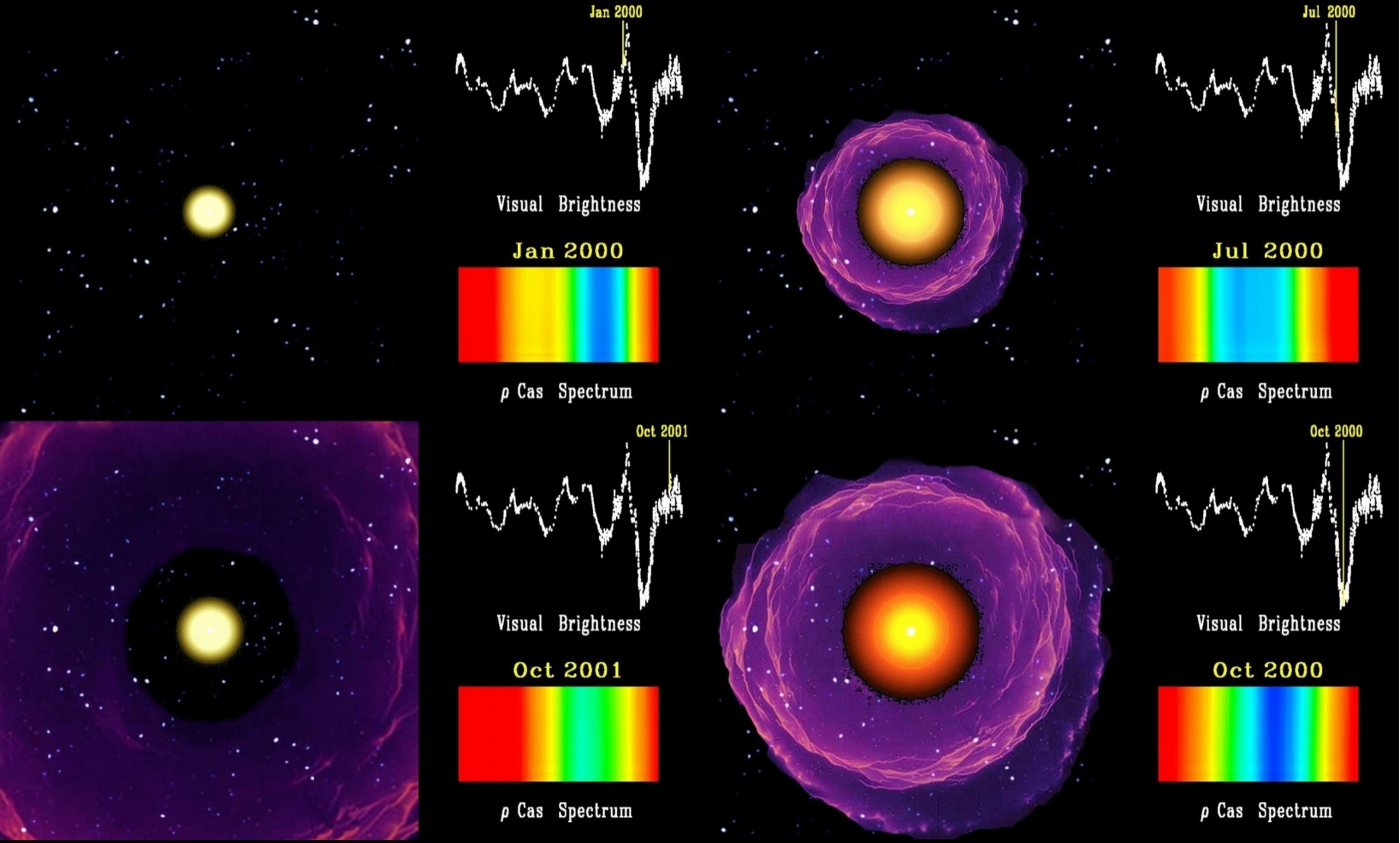

New TiO Bands in Brightness Minimum of Outburst

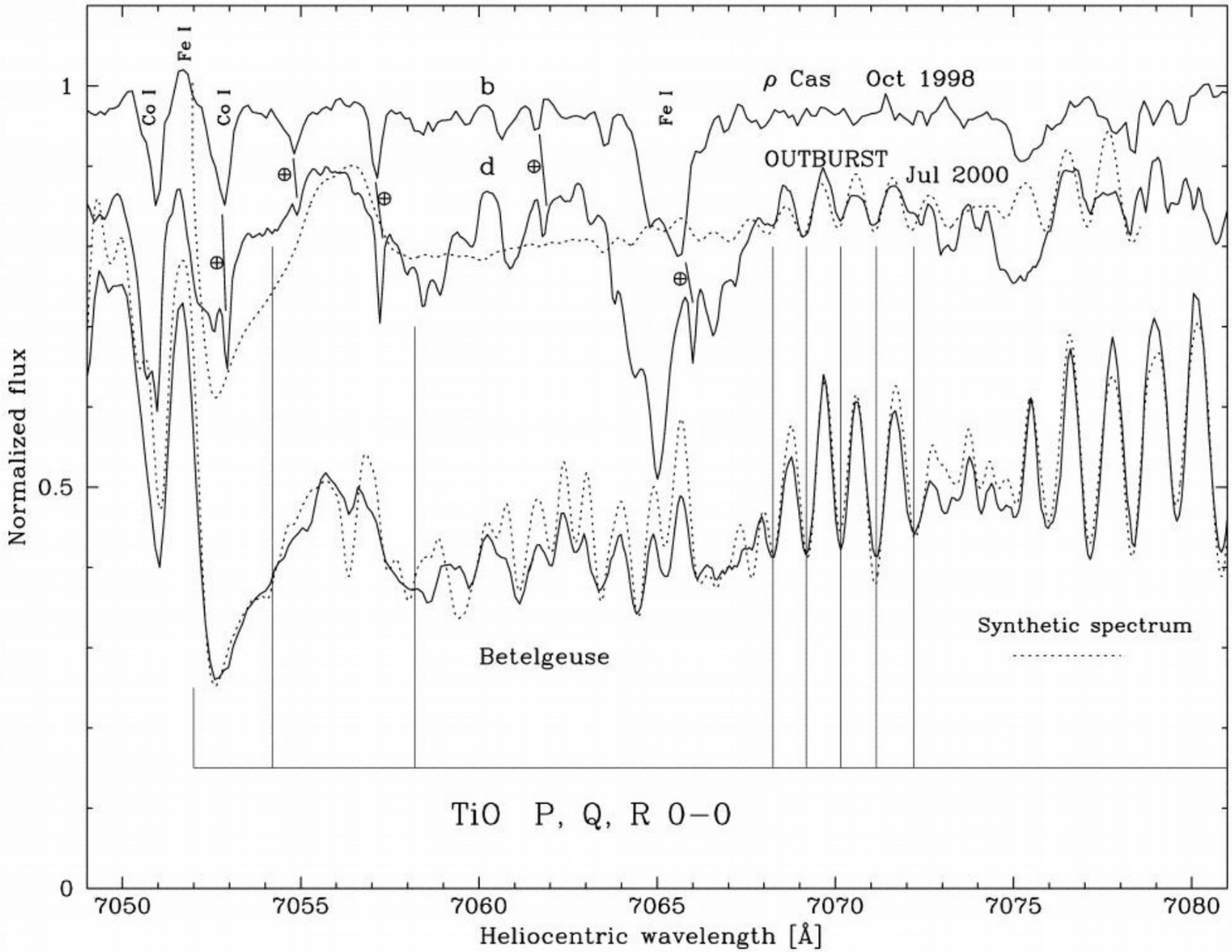

- Near-IR TiO bands appear during deep *V* brightness minimum, and vanish again.
- TiO bands are observed only in M-type stars (Betelgeuse) with Teff < 4000 K.
- Line blue-shifts yields increase of mass-loss rate by factor >100.
- Major mass-loss mechanism of YHG is due to punctuated mass-loss events.

Historical Outbursts and TiO in Rho Cas

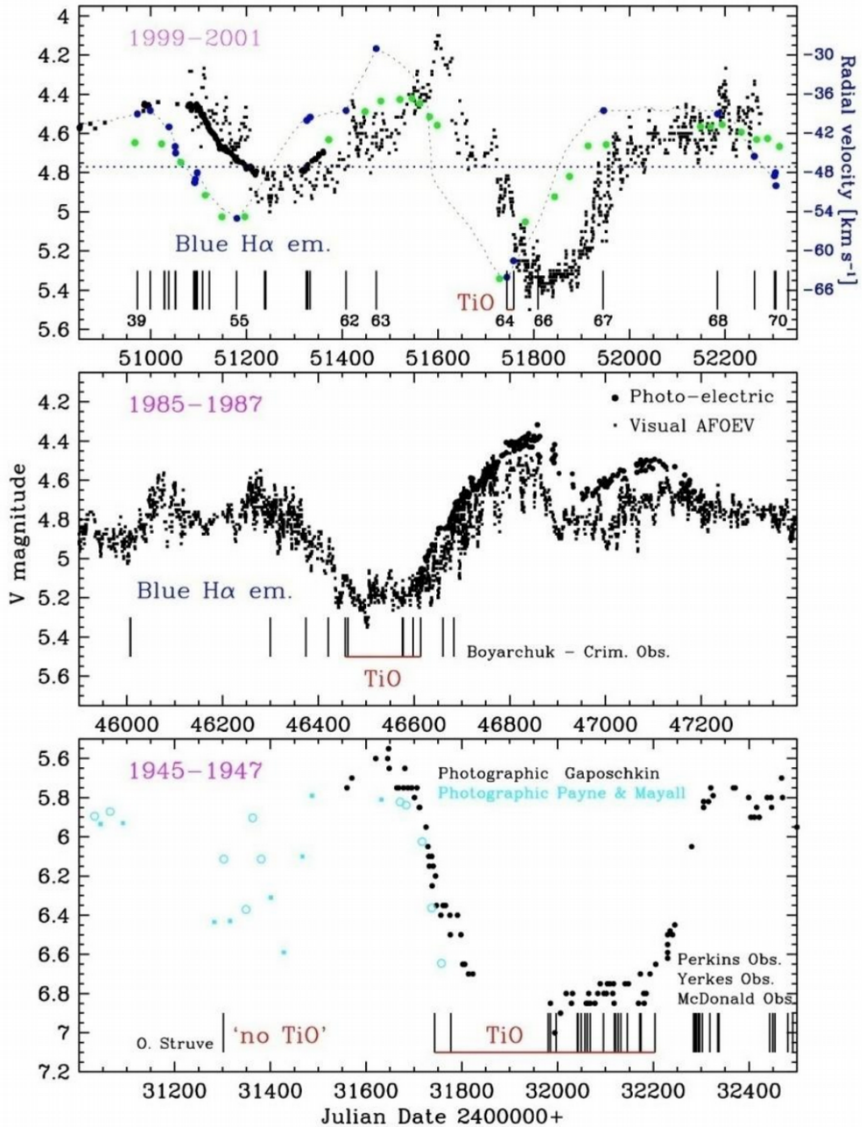

- 4 outbursts on record with spectroscopic observations in 1946, 1986, 2000, 2013.
- New TiO bands appear & disappear observed in spectra during all 4.
- Strong blue Hα emission (inverse P Cyg) in 1985 and 1999 signal strong atmospheric contraction prior to outburst events.

Historical outbursts of Rho Cas after 1941

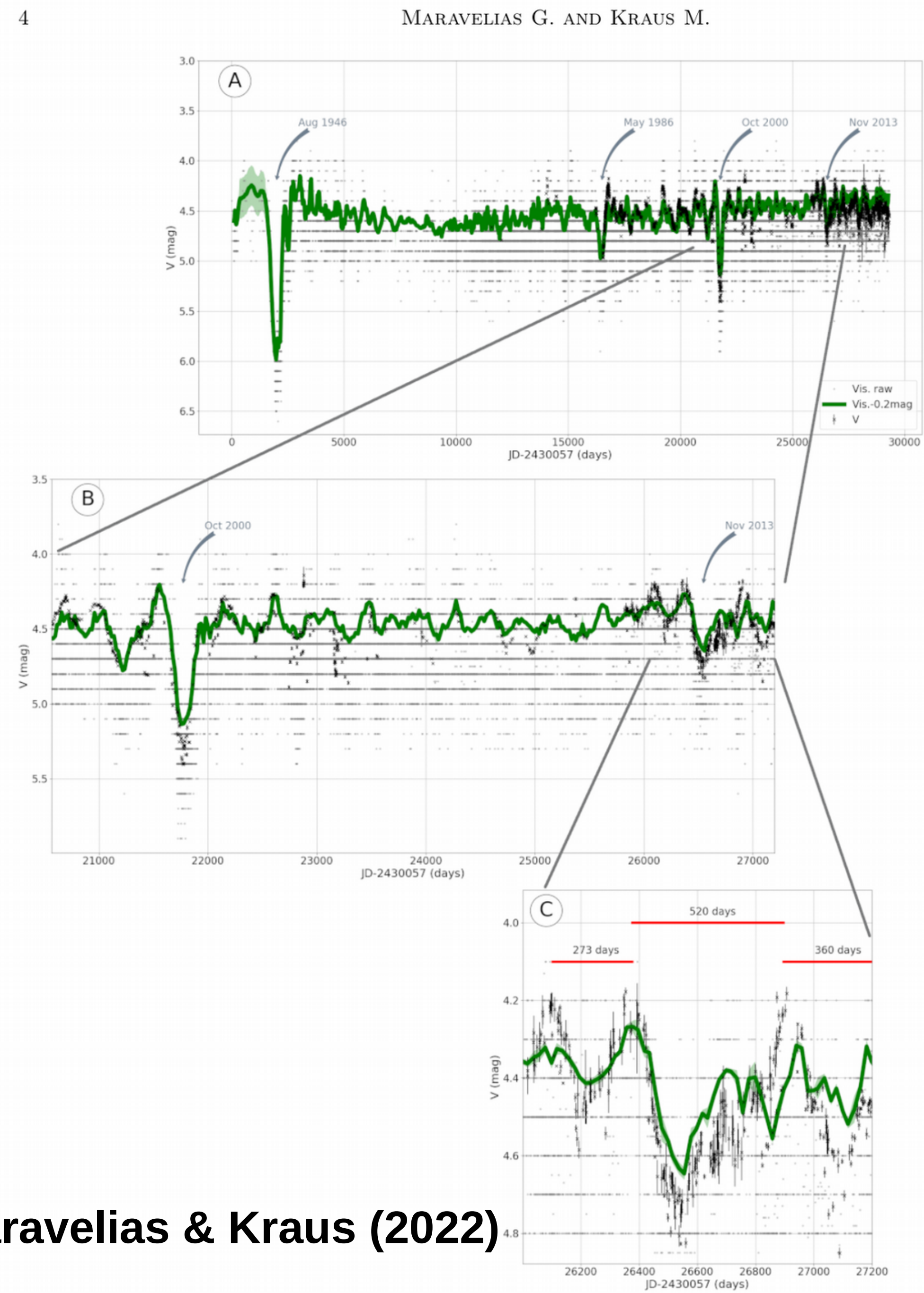

Maravelias & Kraus (2022)

- Photometric comparison of outbursts 1946, 1986, 2000, & 2013.
- Became shorter and more frequent.
- Bouncing against YEV, transition to other phase B[e], LBV?

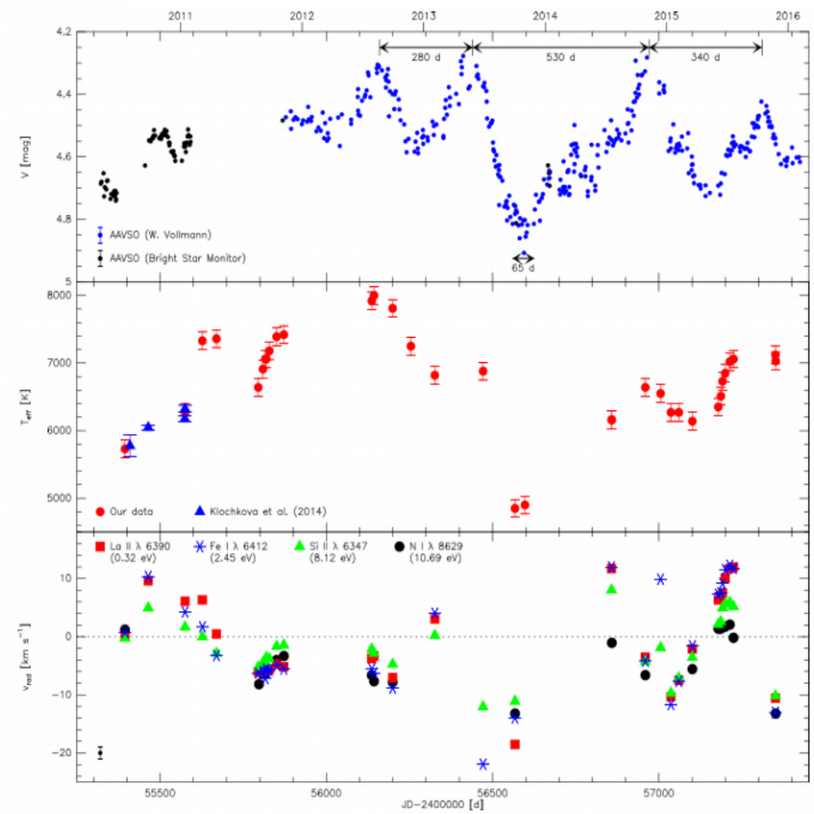

Kraus et al. (A&A 2019)

Historical outbursts of Rho Cas after 1941

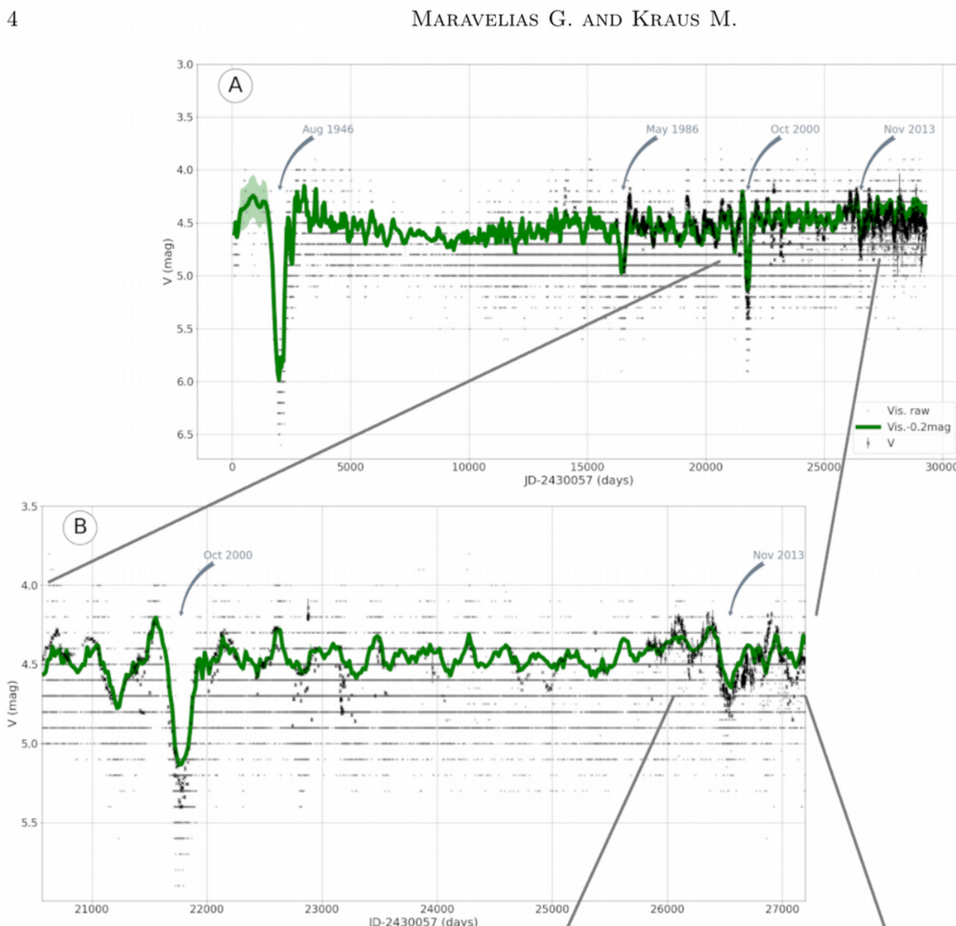

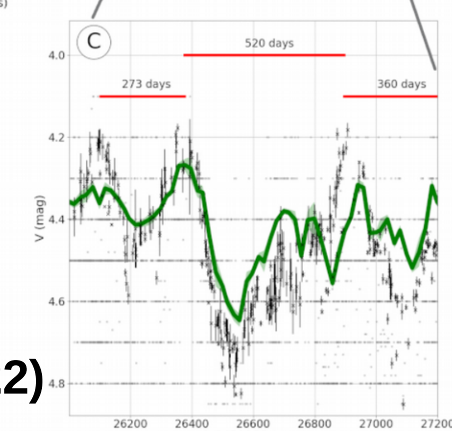

Maravelias & Kraus (2022)

- **Photometric comparison of outbursts 1946, 1986, 2000, & 2013.**
- **Became shorter and more frequent.**
- **Bouncing against YEV, transition to other phase B[e], LBV?**

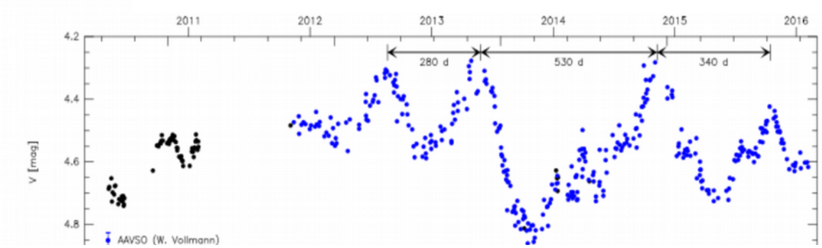

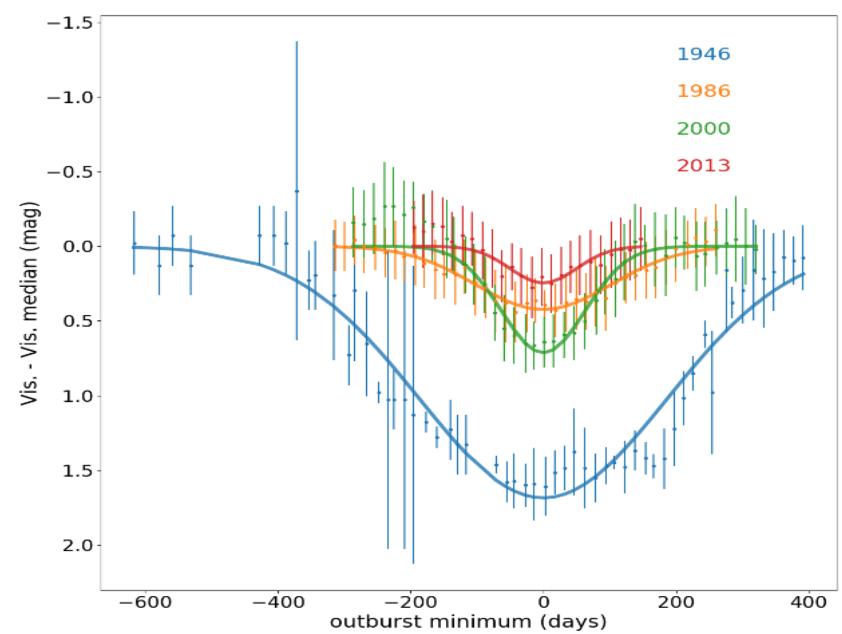

Historical outbursts of Rho Cas after 1941

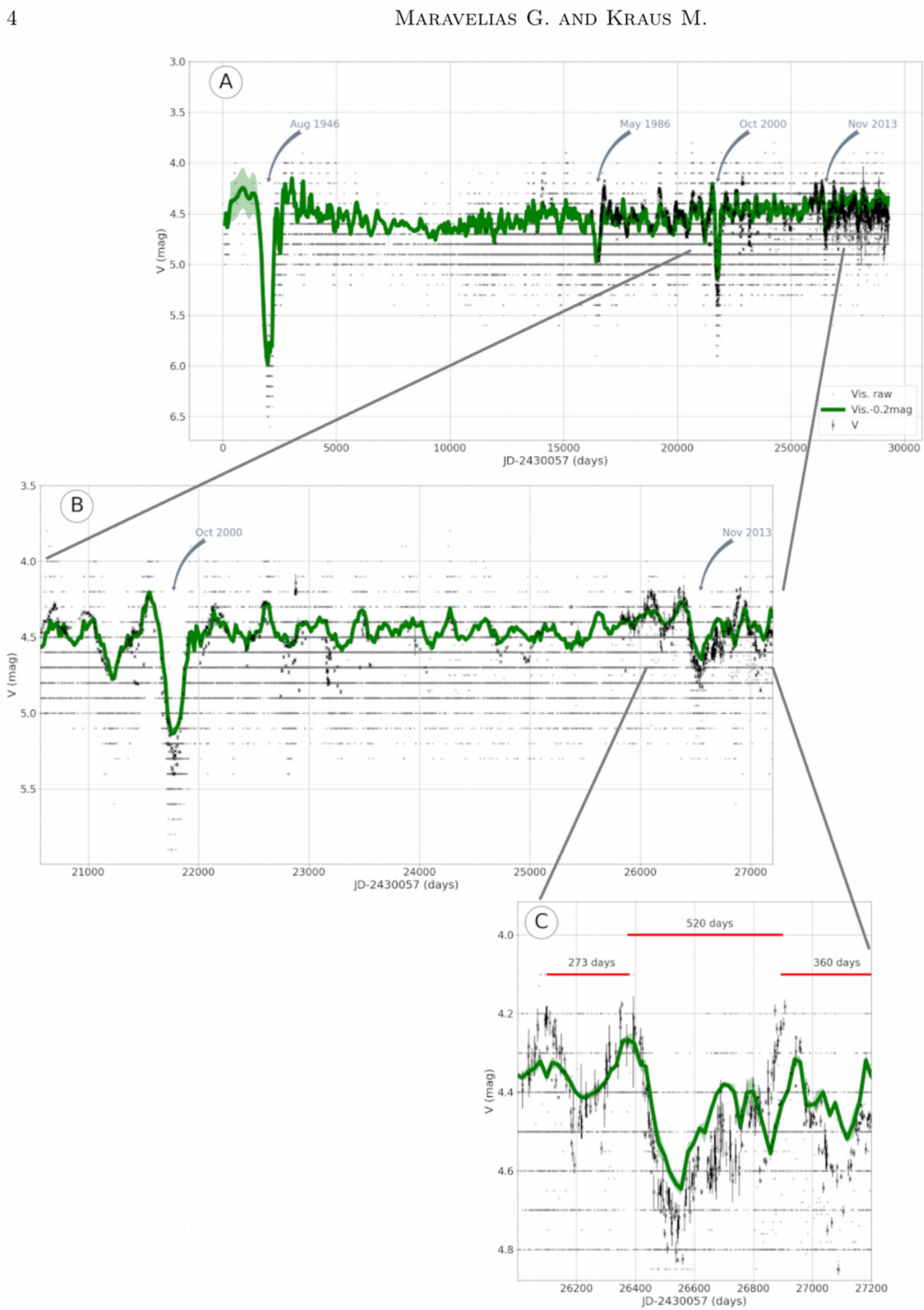

- **Photometric comparison of outbursts 1946, 1986, 2000, & 2013.**
- **Became shorter and more frequent.**
- **Bouncing against YEV, transition to other phase B[e], LBV?**

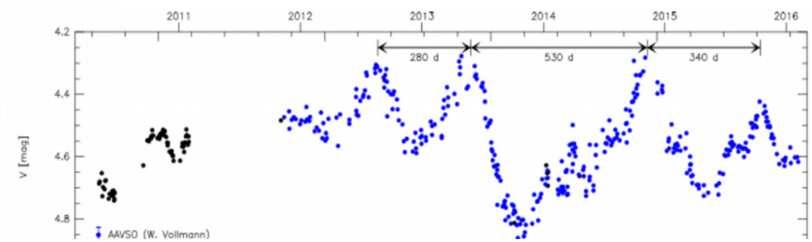

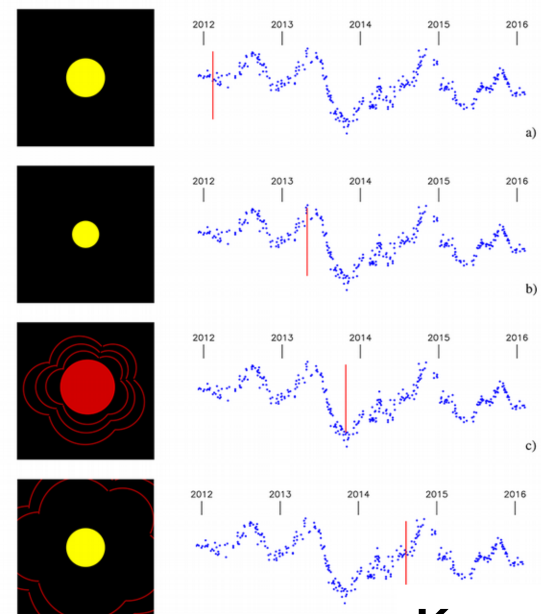

Kraus (2024)

Long-term Hα line variability in Rho Cas

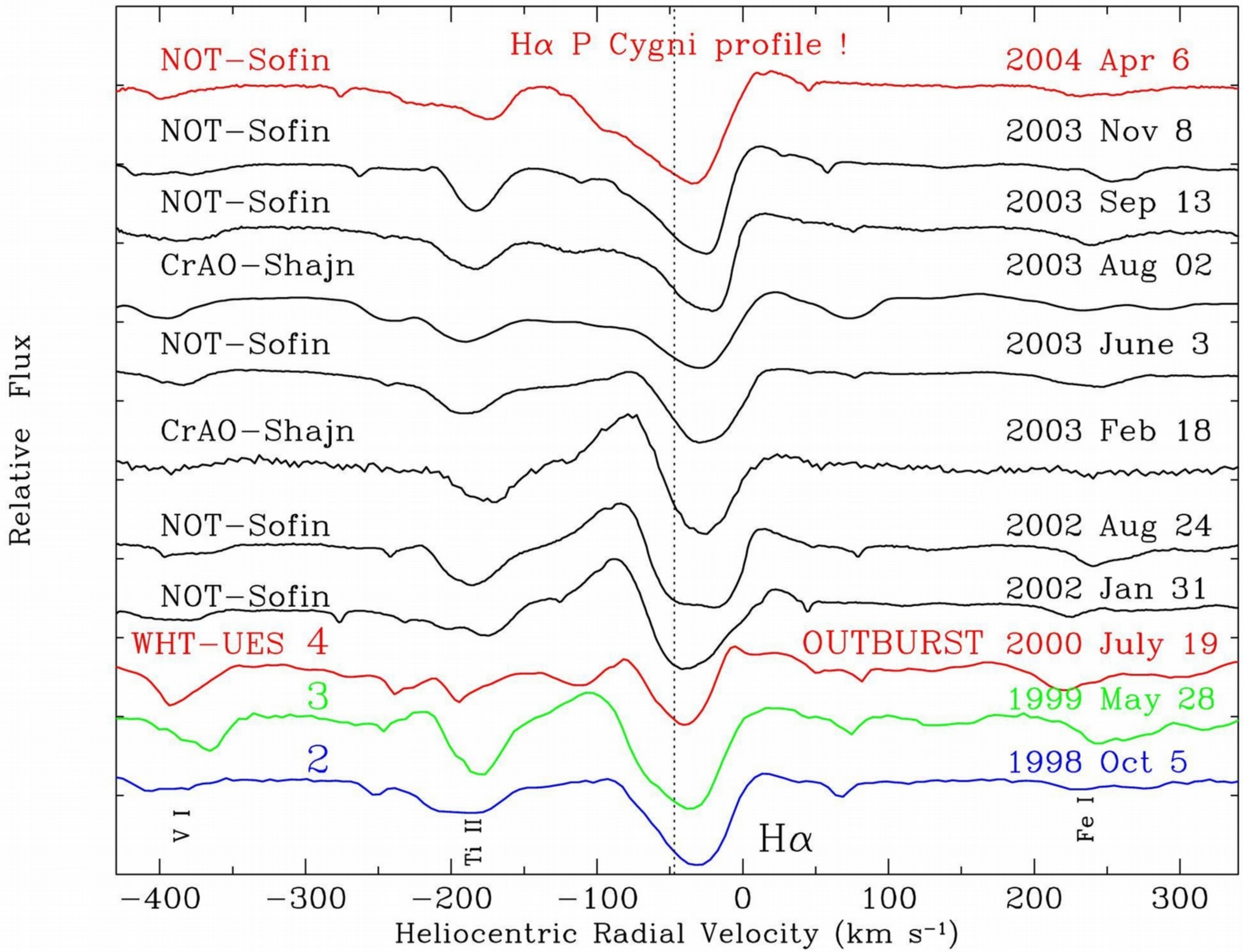

- Strong Hα profile variability due to variable mass-loss & extended-wind opacity.
- Hα line monitoring reveals P Cyg and inverse P Cyg profiles over years.
- Hα absorption very weak during 2000 outburst due to very strong Teff decrease.

Long-term Hα line variability in Rho Cas

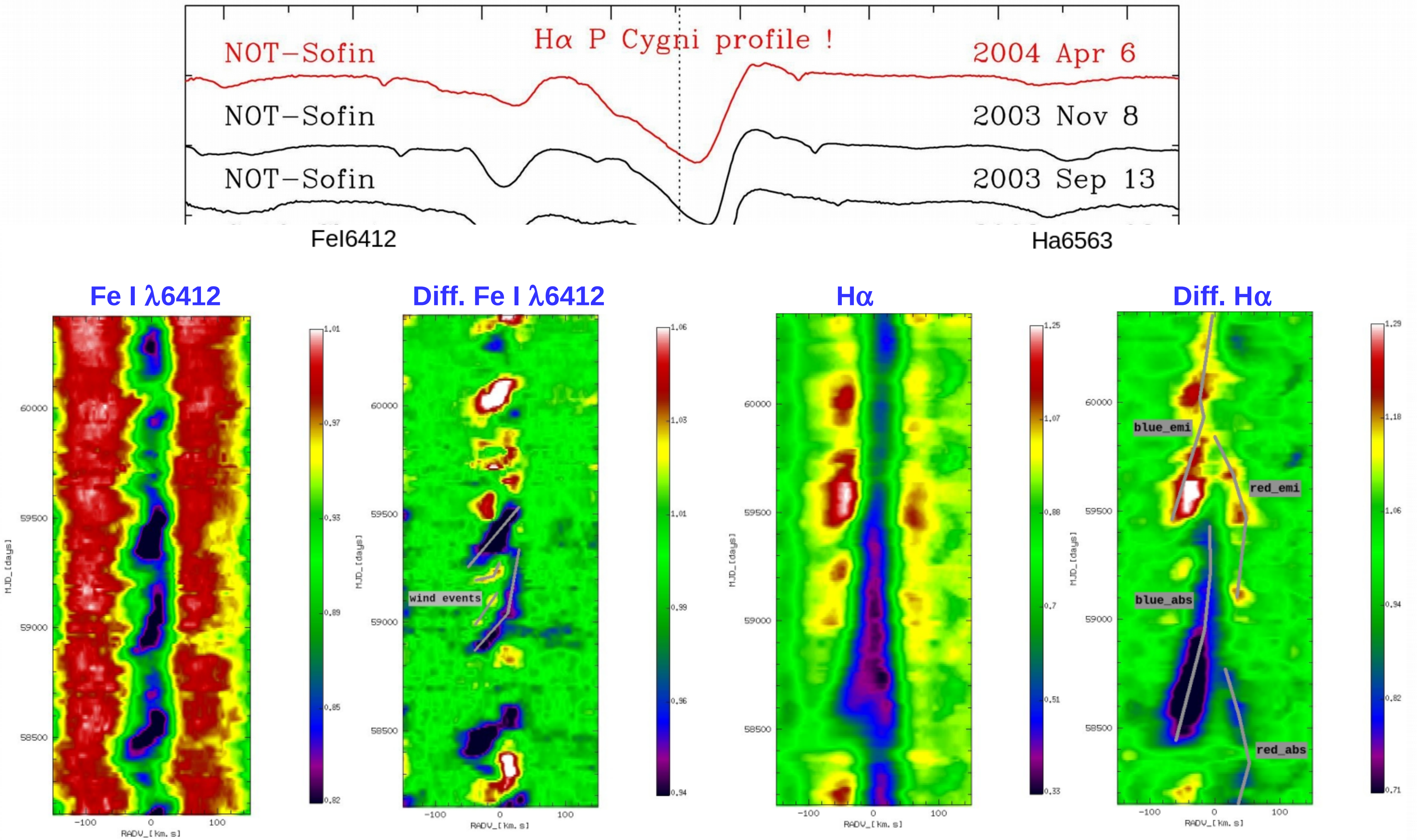

- **Strong Hα profile variability due to variable mass-loss & extended-wind opacity.**
- **Hα line monitoring reveals P Cyg and inverse P Cyg profiles over years.**
- **Hα absorption very weak during 2000 outburst due to very strong Teff decrease.**

Teff variability from Fe I and Ca I absorption lines

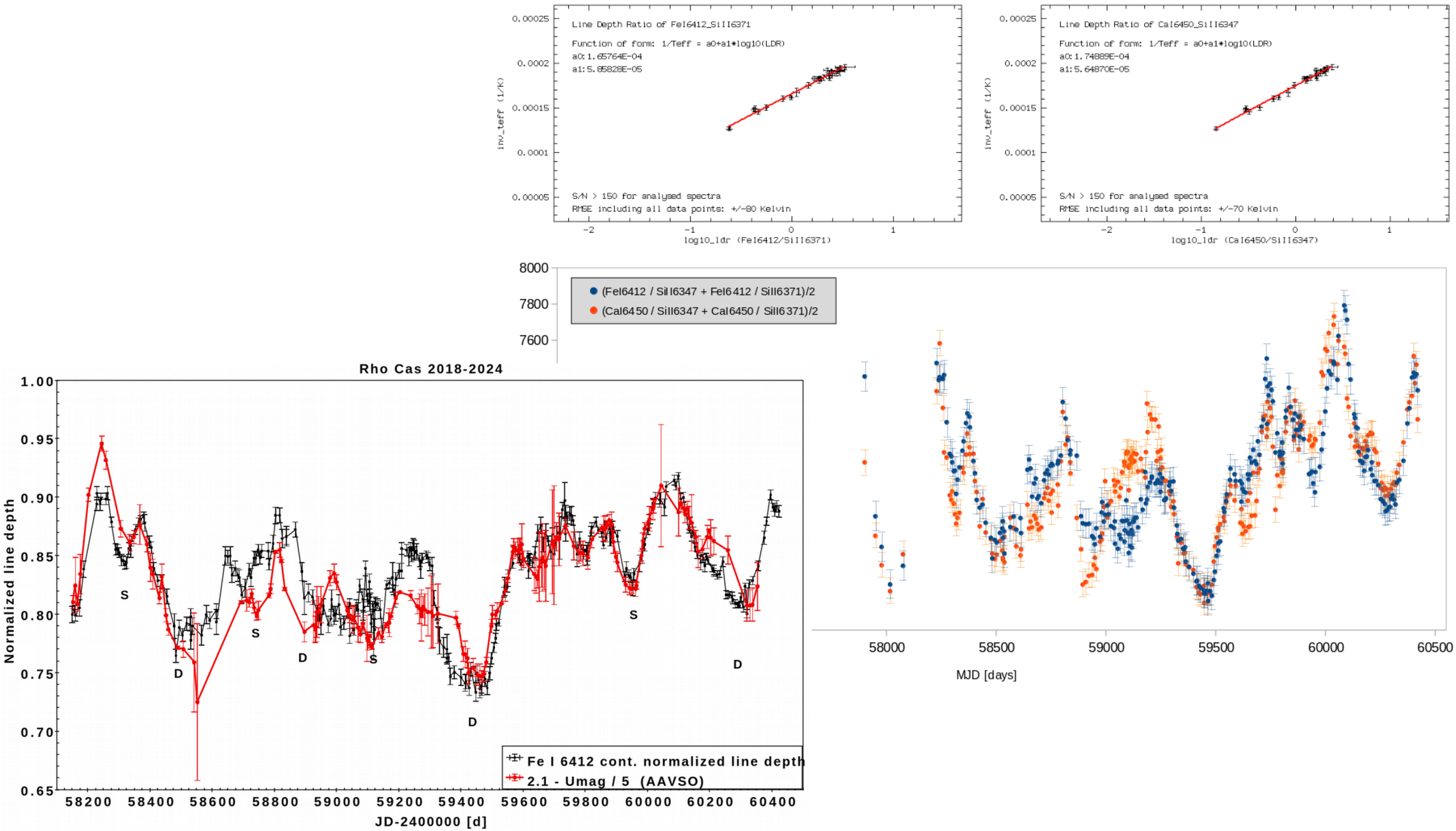

- **Teff from abs. line depth ratios of ~320 spectra in 2018-2024; Teff = 6200 K – 7800 K.**
- **UBV-magnitude curves strongly correlated to Fe I λ6412 line depth variability.**
- **Quandt et al., 2024 (conf. Poster: *Ten years of spectroscopic monitoring of Rho Cas*).**

Radiative transfer modelling of variable wind conditions

- **Modelling of detailed metal line profile variability in Rho Cas.**
- **Central core of Fe I absorption lines blue-shift and deploy far violet extended line wings when Teff increases > 7200 K.**
- **Fe I cores red-shift and become more symmetrical towards lower Teff ~6500 K & decrease of Mdot.**

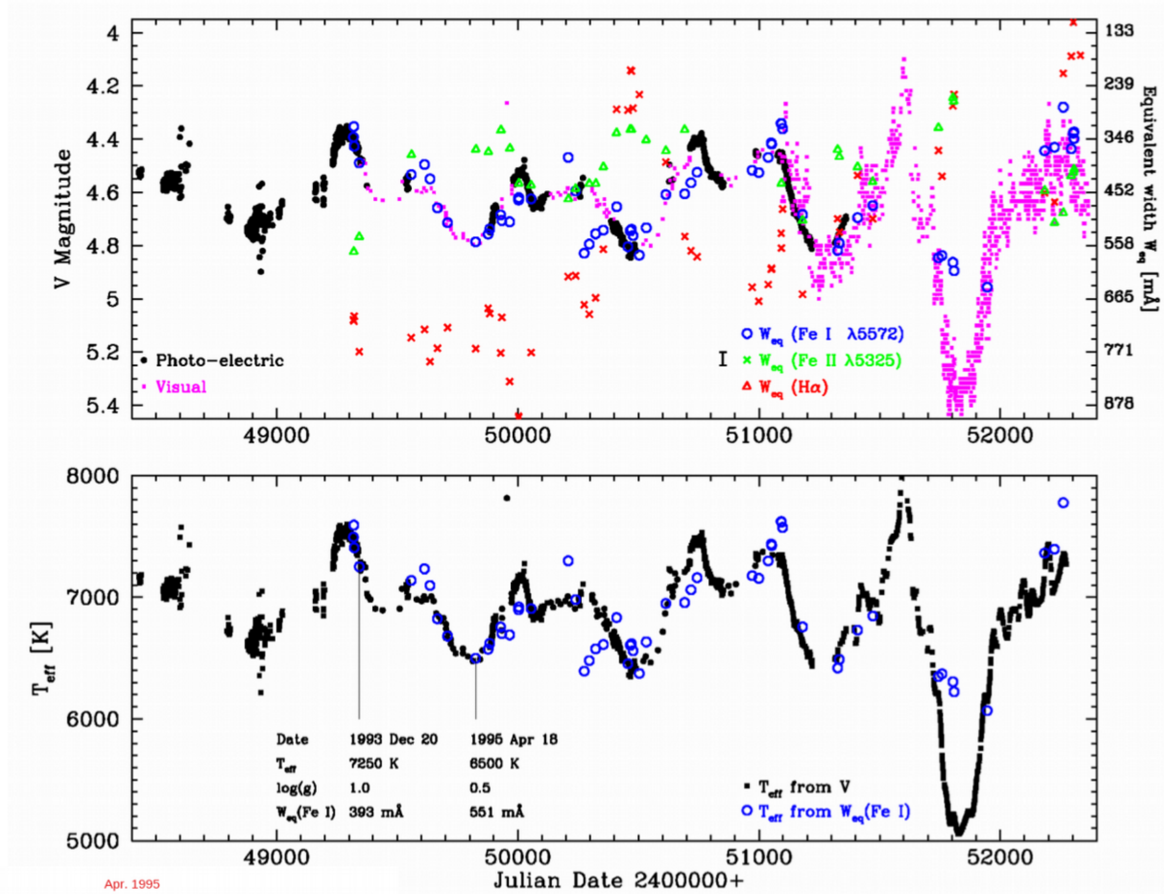

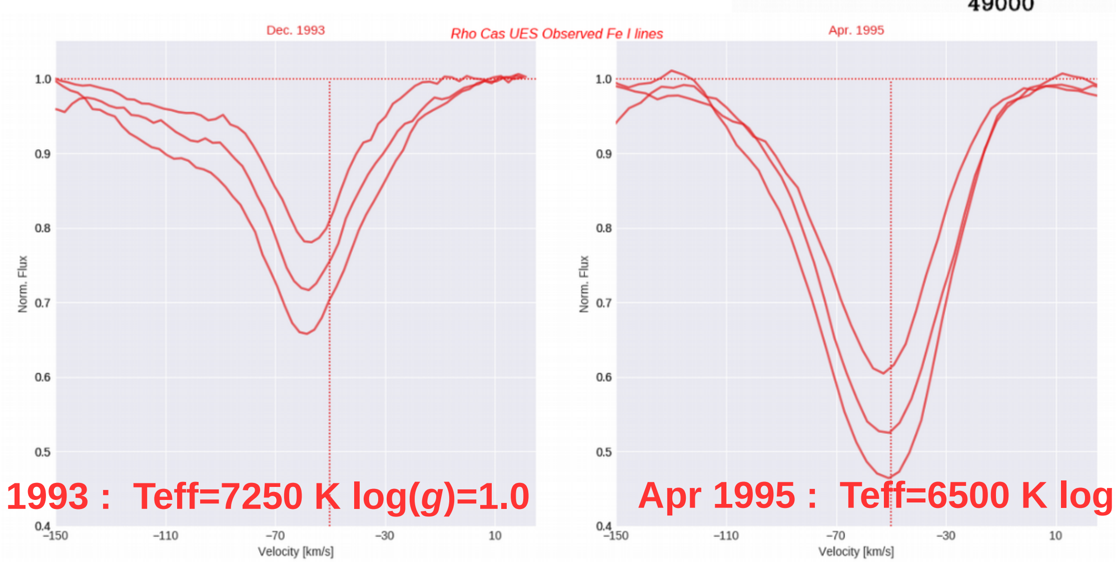

Dec 1993 : Teff=7250 K log(*g*)=1.0

Apr 1995 : Teff=6500 K log(*g*)=0.5

Radiative transfer modelling of variable wind conditions

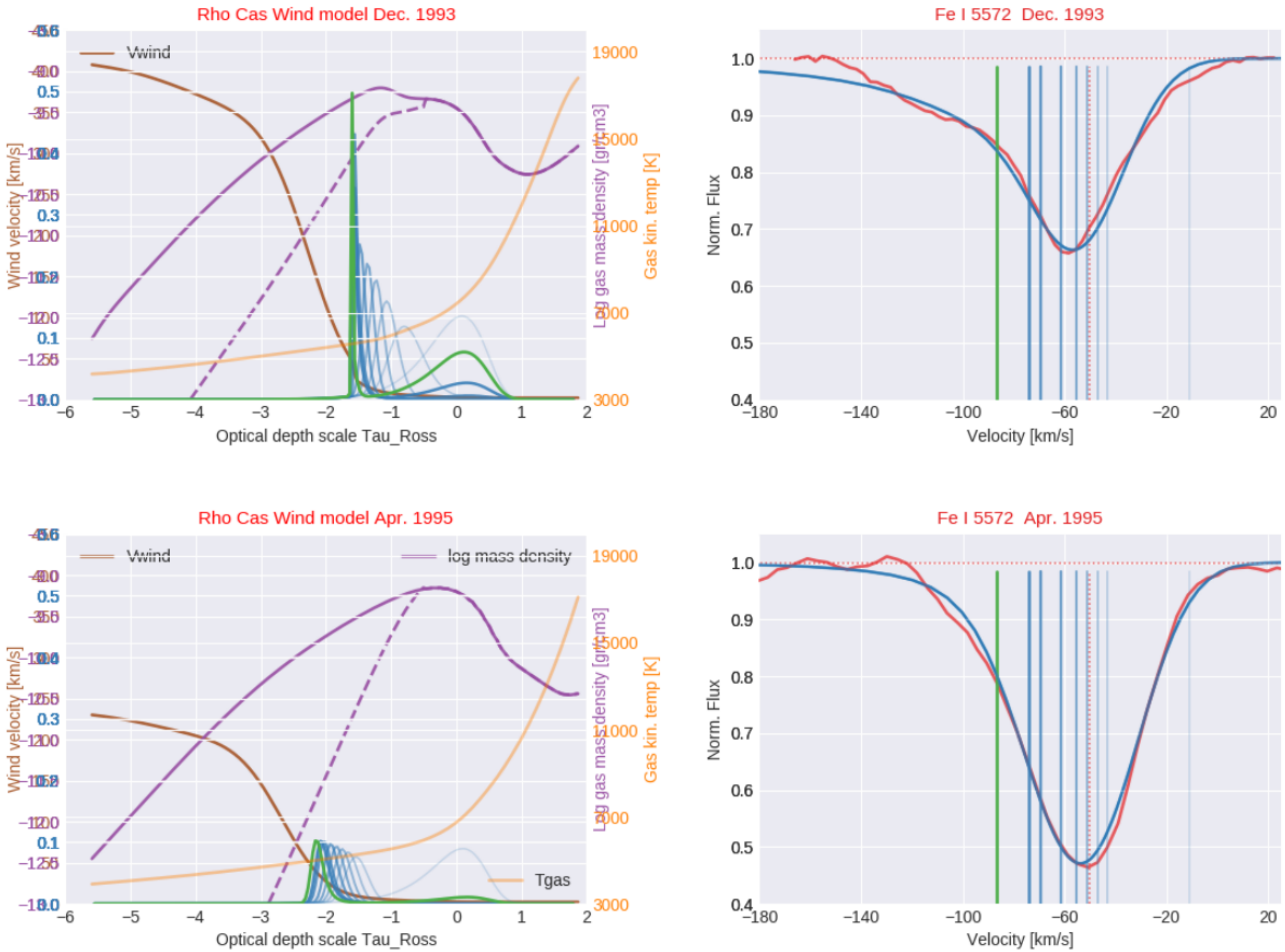

- **Semi-empiric modelling of Tgas-, ρ density-, Ne-, and Vwind-structure from line fitting.**
- **Non-LTE, plane-parallel, 1-D, hydro-static atmosphere+wind models for line formation.**
- **Stellar mass-flux ρ × Vwind can vary by factor of ~5 around mean Mdot ≃ 10^{-5} $M_{\odot}$/y.**

Long-term H Balmer lines variability in YHG 6 Cas

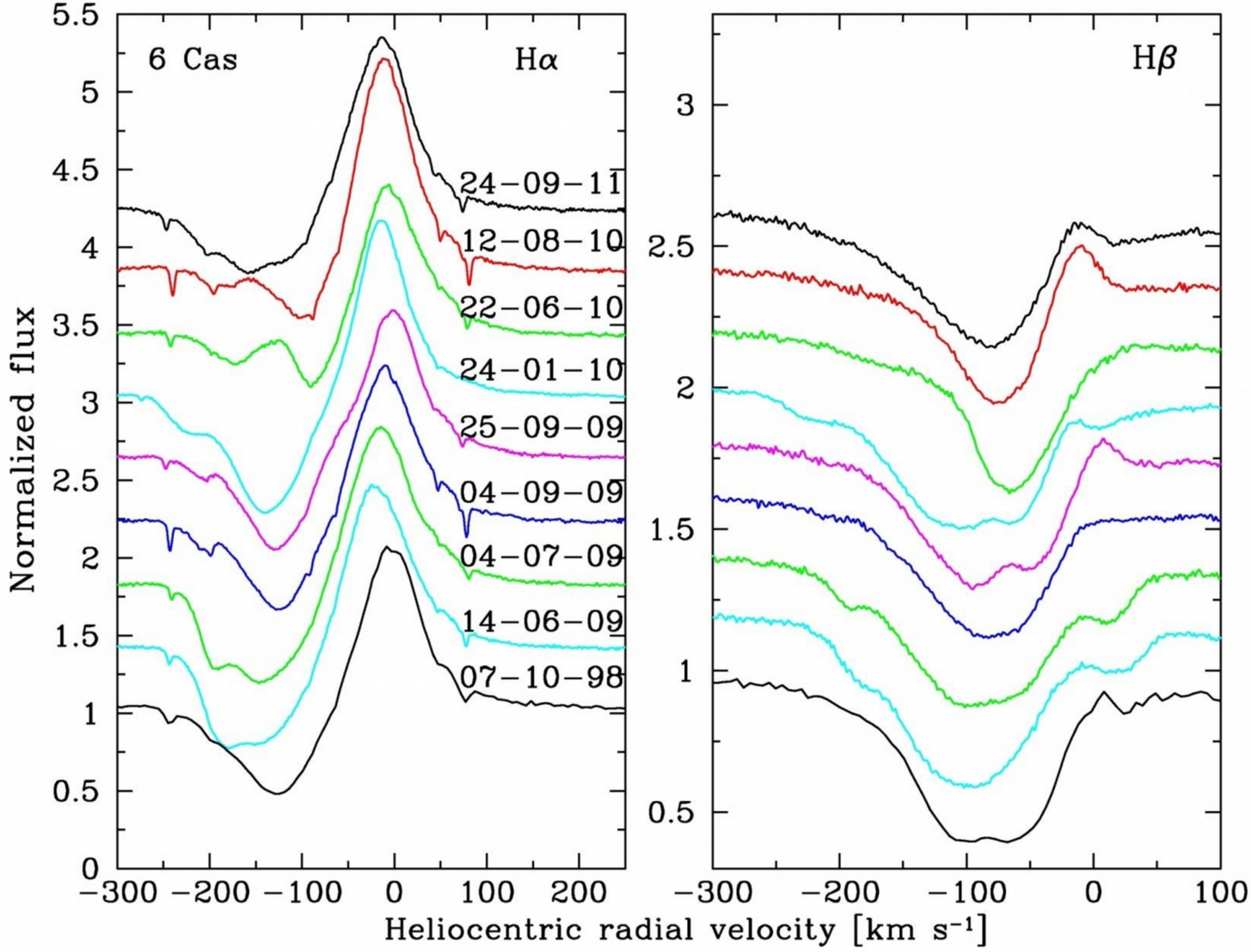

- **Hα P Cyg and Hβ profile variability in 6 Cas due to atmospheric pulsations.**
- **6 Cas is less luminous than Rho Cas with similarly large wind mass-loss rates.**

Long-term H Balmer lines variability in YHG 6 Cas

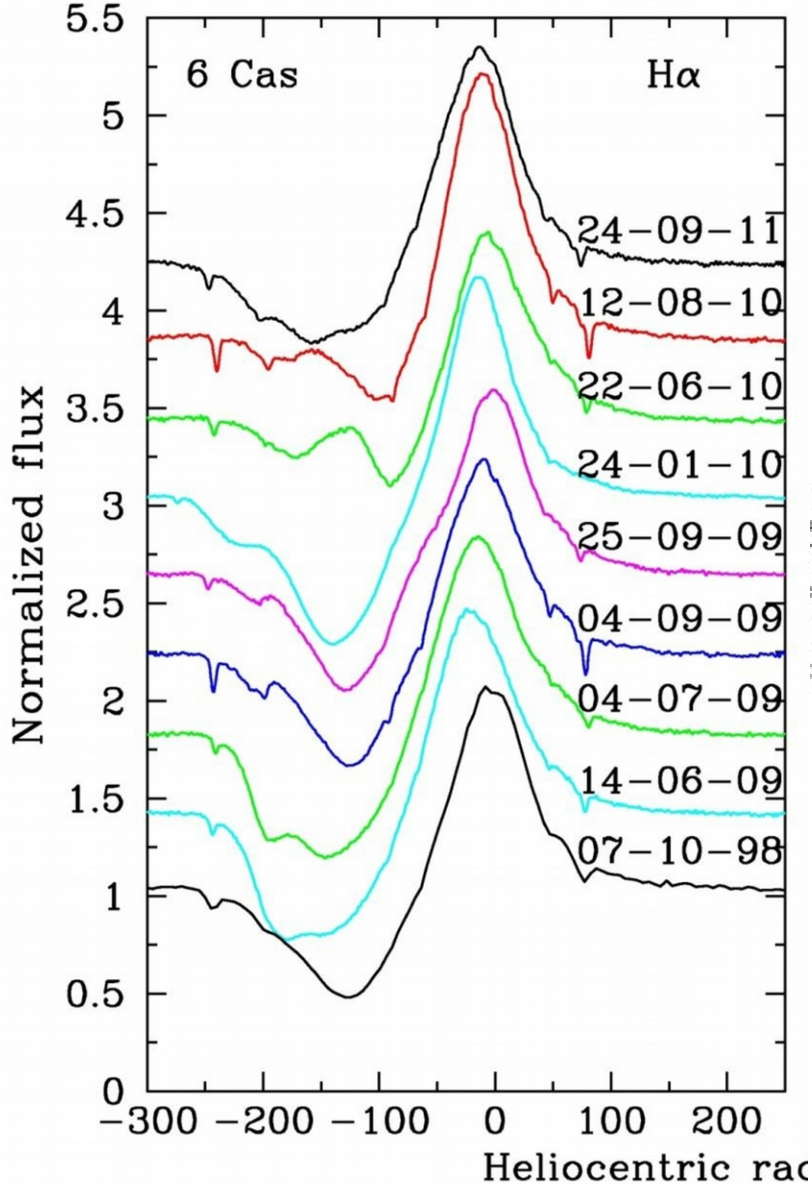

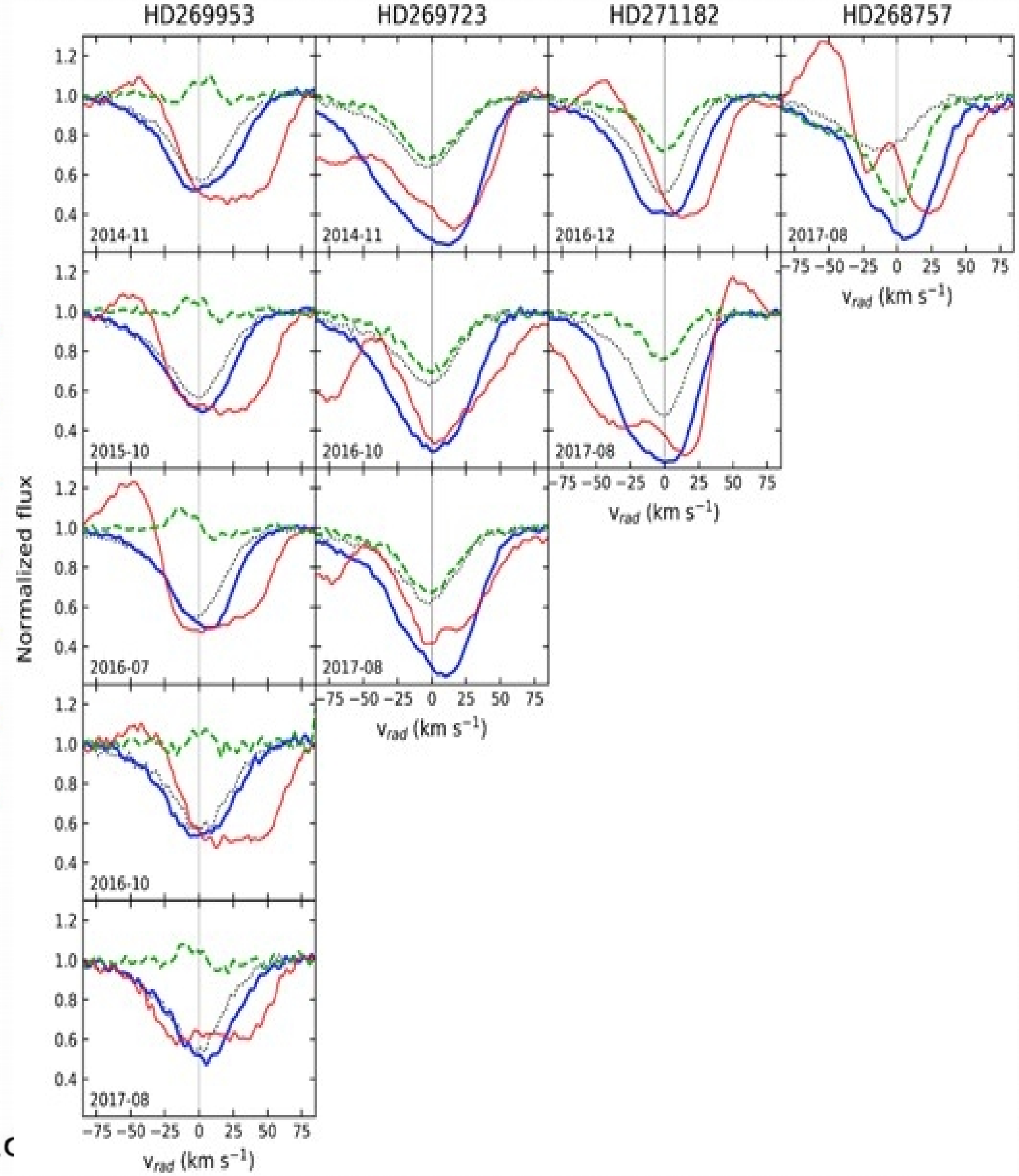

- **Modelling of metal lines in 4 luminous LMC stars (Kourniotis et al., 2022, MNRAS).**
- **HD 269953 is post-RSG binary of Teff = 7050 - 7300 K (2014 – 2017).**
- **HD 271182 is ‘Rho Cas analog’ of Teff = 6100 - 6500 K & dims by ~0^{m}.4 (very promising).**

Long-term Teff increase of YHG HR 8752

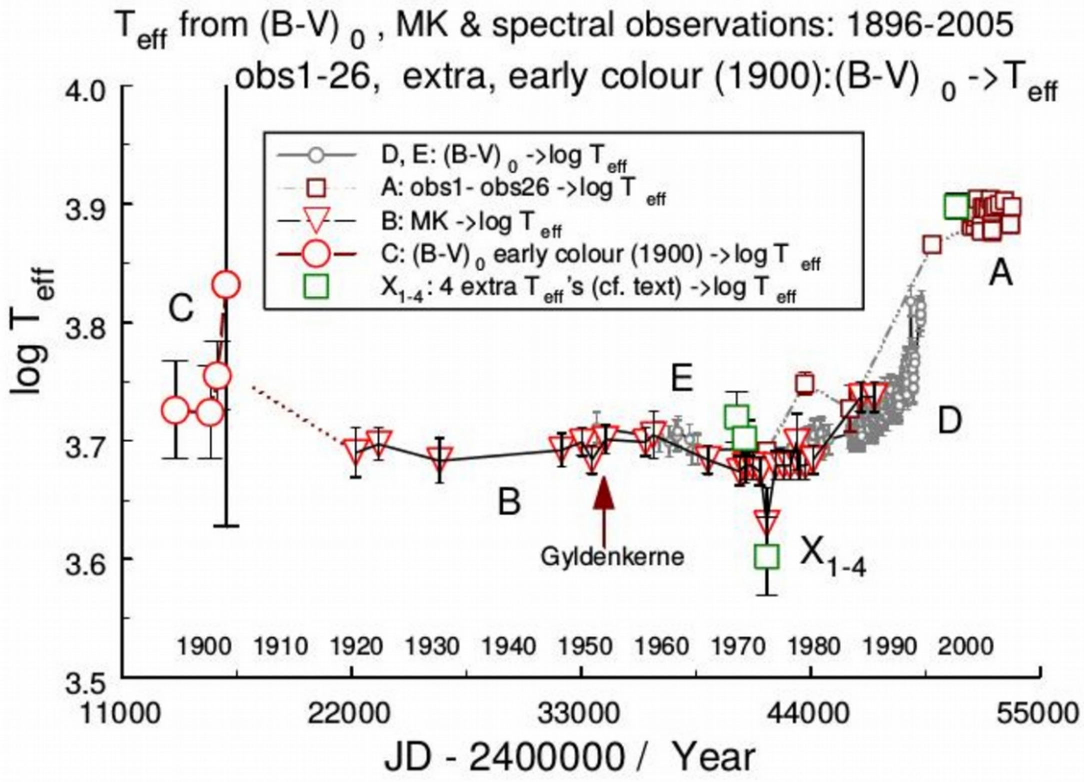

Fig. 10. Combination of the temperatures in one plot: from B–V corrected for interstellar extinction, from MK-> $T_{\rm eff}$, from obs1-obs26 (Section 2), and from some extra data (indicated by 'X'(X_{1-4}), cf. text). The temperatures derived from the B–V and MK data combine reasonably well. The temperatures for obs1-obs2, obs4-obs6 also seem to follow the combined data, and the values for obs7-obs26 extend the data. The difference from obs2 is relatively large. This forms step 5.

- **Teff increase over last 40 years from photometric and spectroscopic data.**
- **Superfast evolution of YHG on blueward track ?**
- **Slow clearing of ejected shells revealing hot supergiant ? (Nieuwenhuijzen et al. 2012)**

Long-term Teff increase of YHG HR 8752

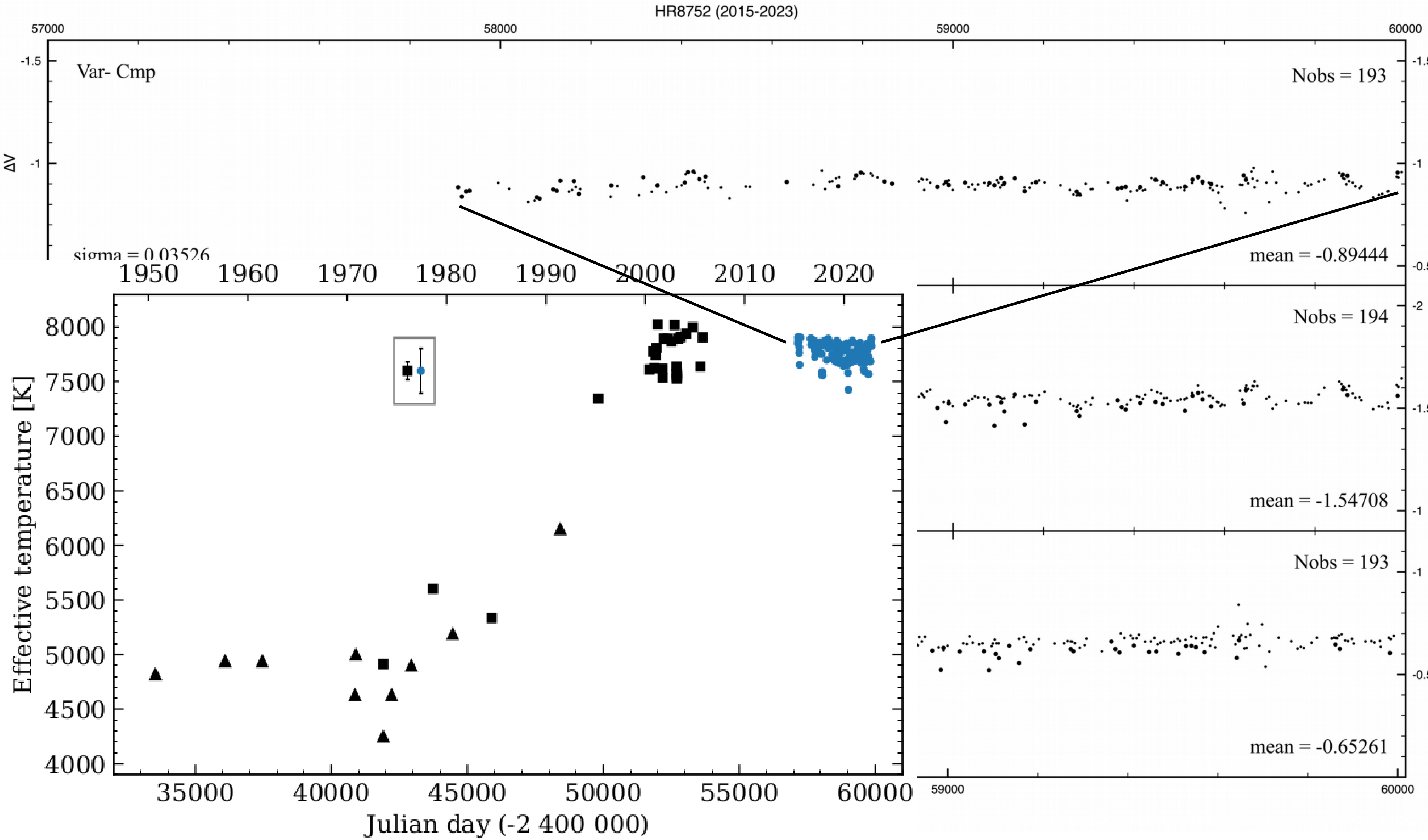

- **Kasikov et al. 2024 (A&A, in press)** ***YHG V509 Cas – stable in the 'yellow void'***
- **Stable pulsations around Teff ~ 7800 K. Is HR 8752 starting to traverse the yellow void?**

Long-term Teff increase of YHG HR 8752

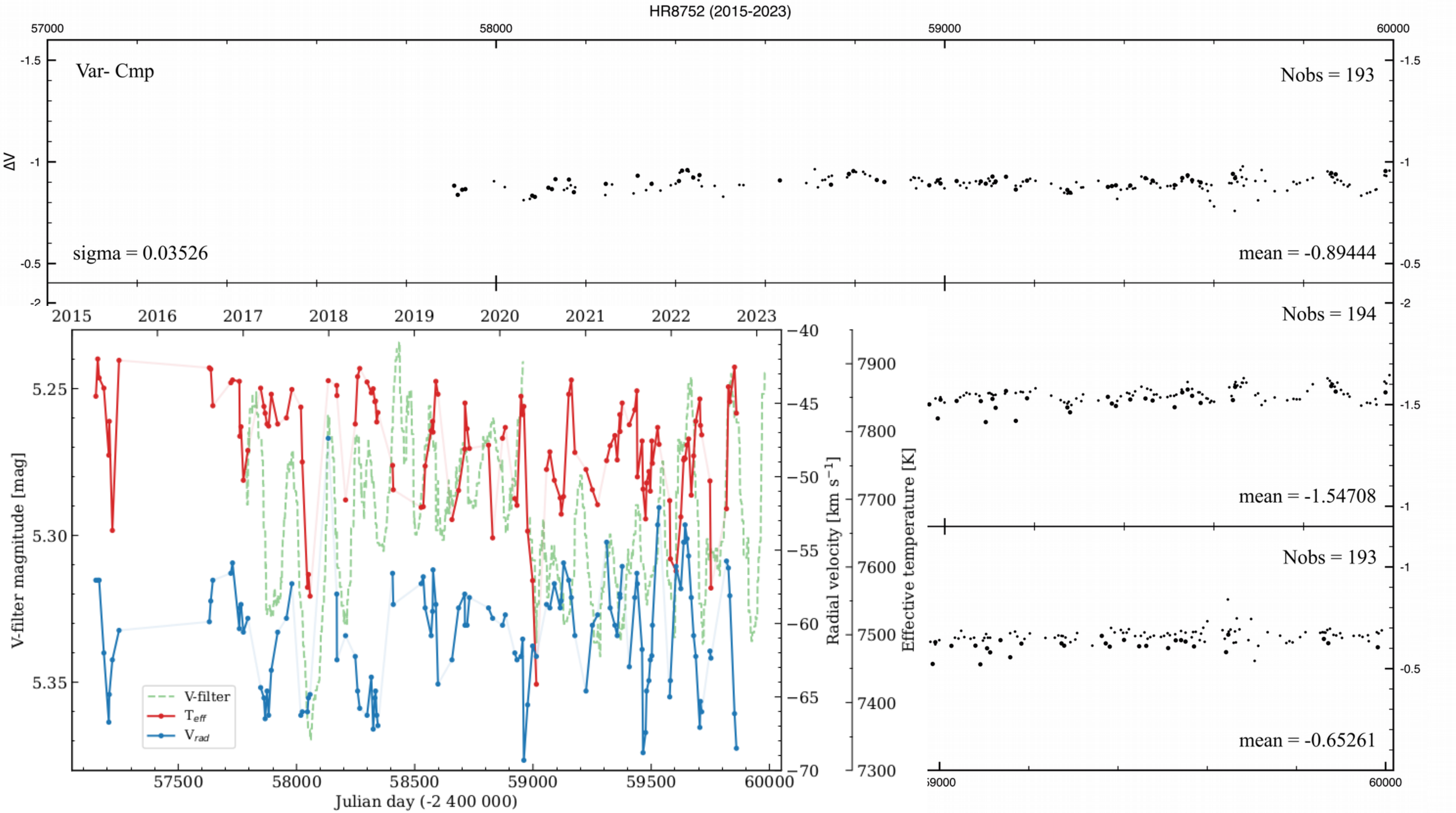

- ***V*-band magnitude variability follows the Vrad-curve, or *V* - Vrad phase shift observed.**

Long-term Teff increase of YHG HR 8752

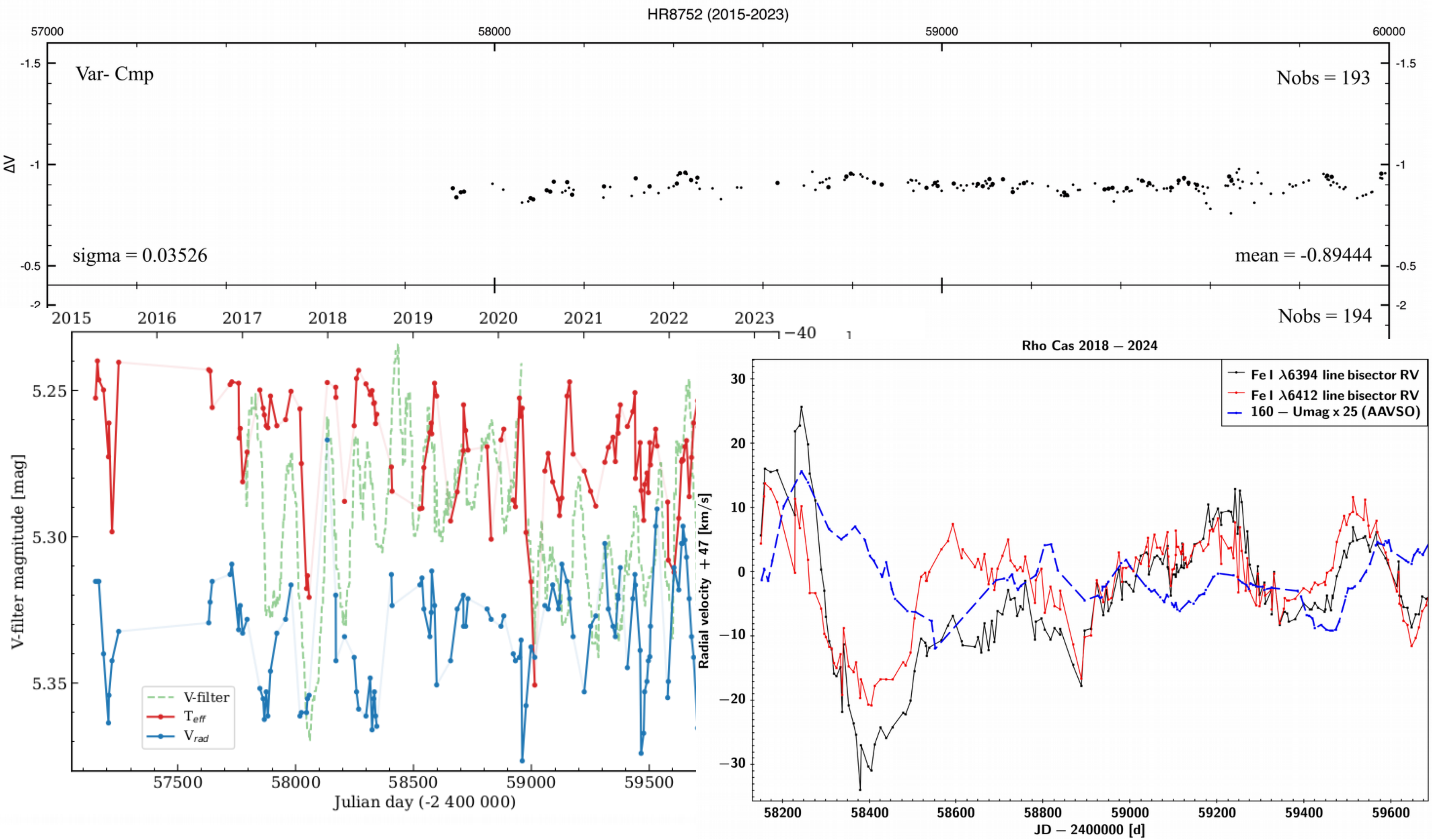

- ***V*-band magnitude variability follows the Vrad-curve, or *V* - Vrad phase shift observed.**
- **Phase shift also observed in Rho Cas in 1993-2003 (spectroscopic twins in 1970ies).**
- **Signaling quasi-periodic variability phases with radial pulsations.**

Historical Outburst Event in YHG HR 5171A ?

4 Chesneau et al.: HR 5171 A: a massive interacting system in common envelope phase

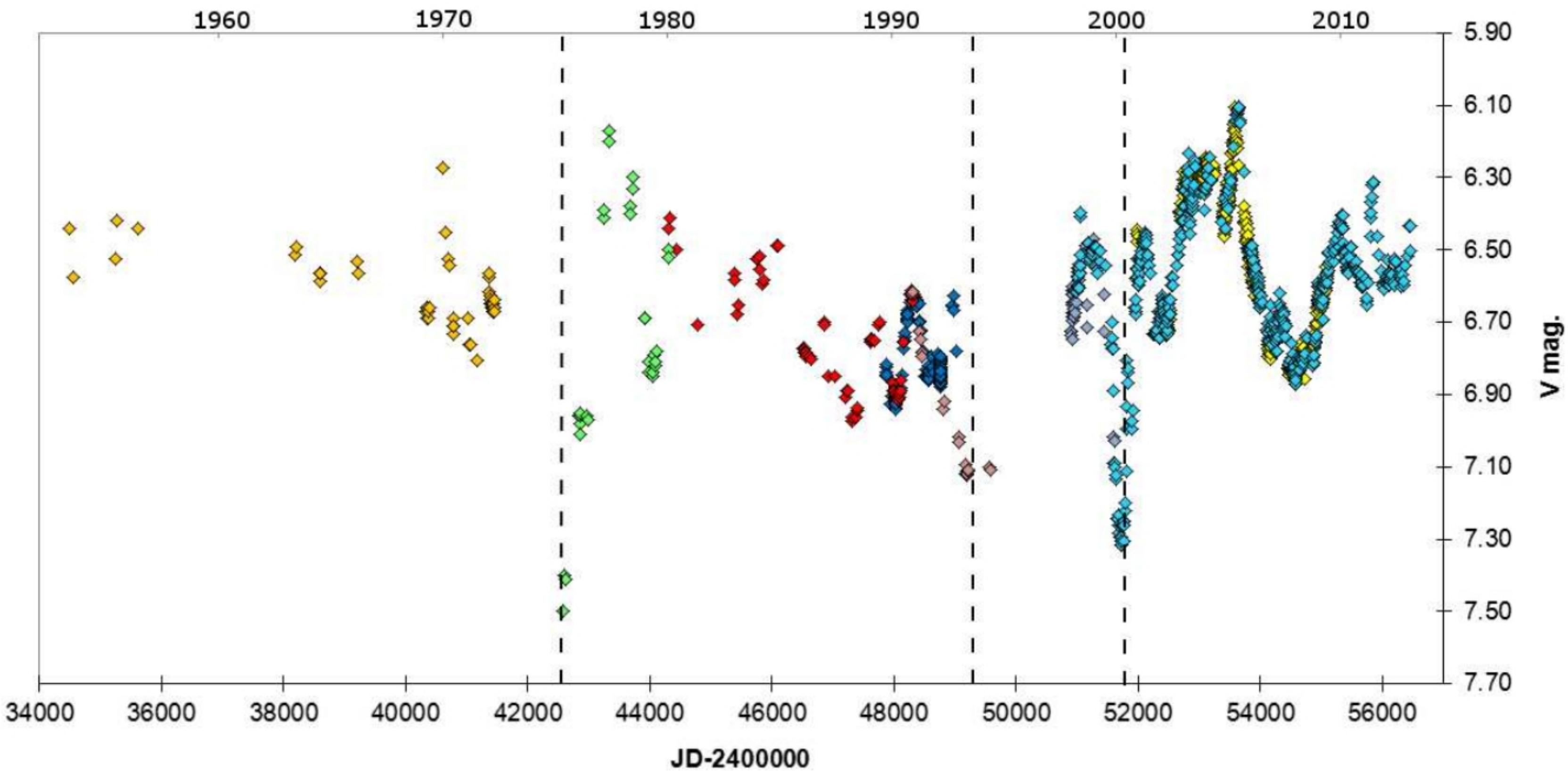

Fig. 3. Visual light curve spanning more than 60yrs. The colors are described in Table A.2. The low flux events are indicated named the Dean, Steken and Otero minima, that occurred in ~1975, ~1994 and ~2000, respectively.

- **Visual lightcurve of 60+ years reveals two deep *V*-brightness minima.**
- **Long- & short-term photometric and spectroscopic variability very similar to Rho Cas.**
- **Dean and Otero dimming are reminiscent of *V*-lightcurve in Rho Cas during outbursts.**

Historical Outburst Event in YHG HR 5171A ?

4 Chesneau et al.: HR 5171 A: a massive interacting system in common envelope phase

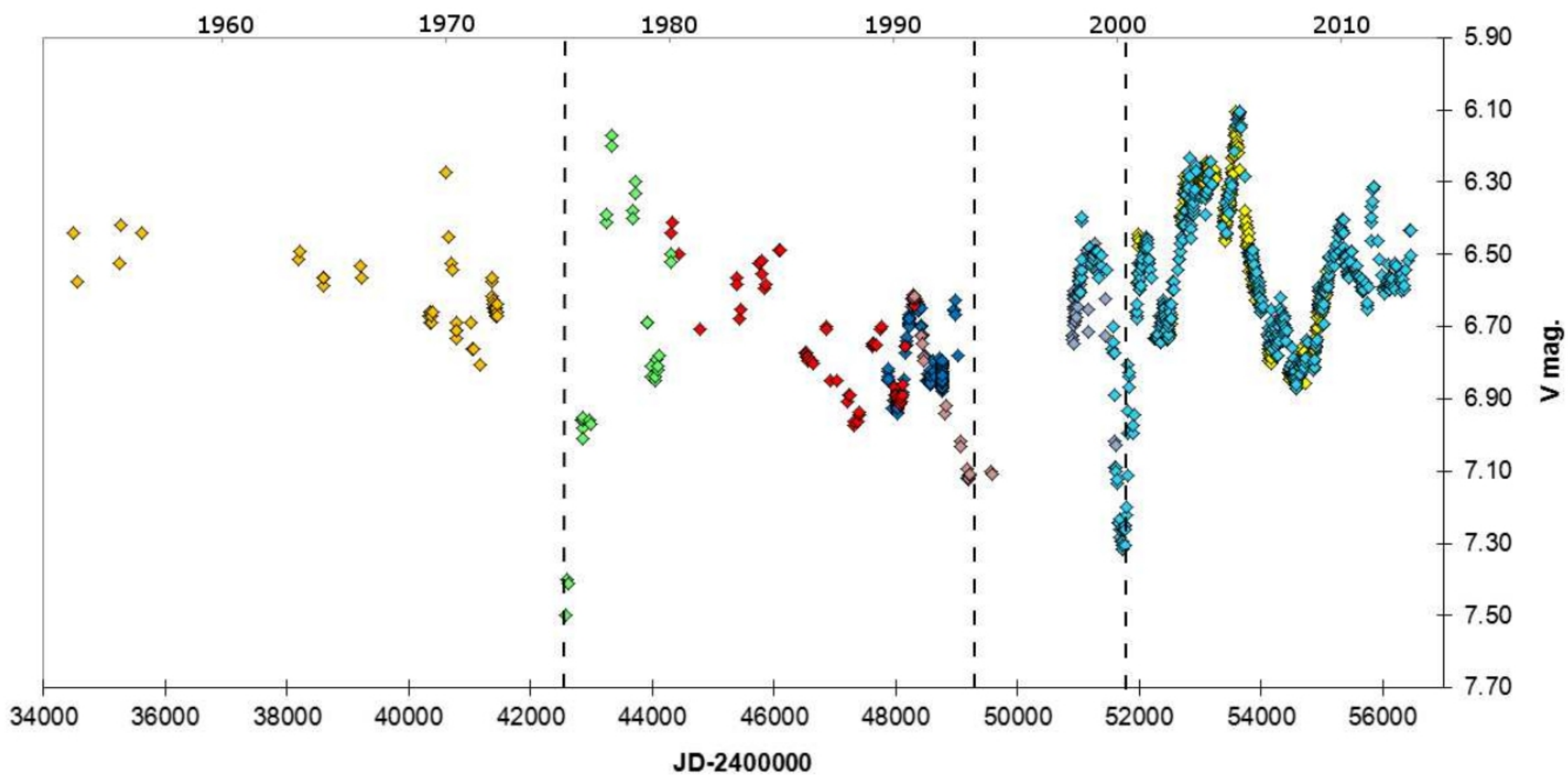

Fig. 3. Visual light curve spanning more than 60yrs. The colors are described in Table A.2. The low flux events are indicated named the Dean, Steken and Otero minima, that occurred in ~1975, ~1994 and ~2000, respectively.

- **Visual lightcurve of 60+ years reveals two deep *V*-brightness minima.**
- **Long- & short-term photometric and spectroscopic variability very similar to Rho Cas.**
- **Dean and Otero dimming are reminiscent of *V*-lightcurve in Rho Cas during outbursts.**
- **Investigation ongoing comparing Rho Cas millennium outburst and HR 5171 dimmings.**
  → Same physical phenomenon in single YHGs ? (Lobel et al., in prep.)

What are LVBs and candidate LBVs ?

- LBV = luminous blue star showing S-Doradus cycles: irregular photometric and spectroscopic variability on time scales of ~10 yr
  Entire spectrum changes dramatically between "*quiescent*" and "*outburst*" state

- cLBV = stellar parameters found in LBVs but without observed S-Dor cycle ("*dormant LBV*")

- Galactic LBVs and cLBVs are often found in bi-polar or spherical circumstellar nebulae signaling past eruptive events

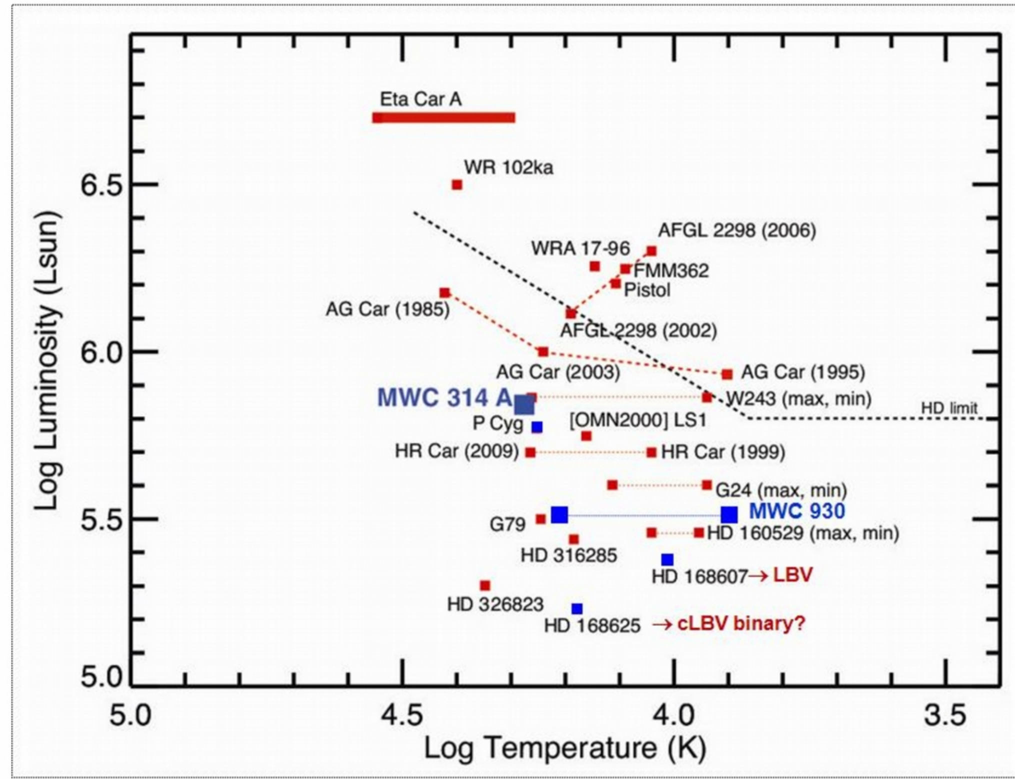

Mercator-HERMES high-resolution spectroscopic monitoring of LBVs and cLBVs

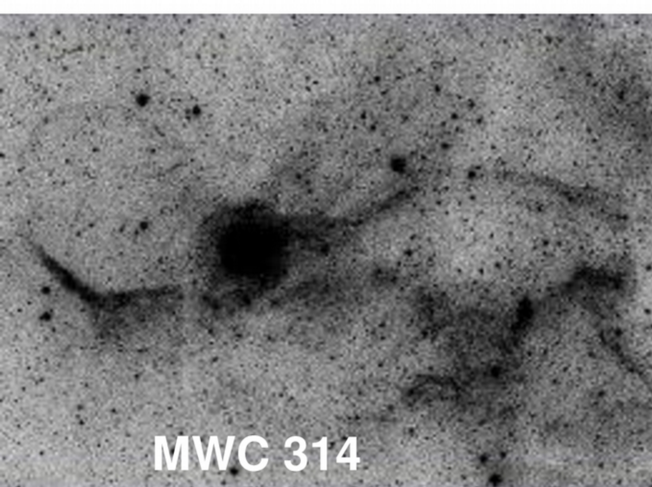

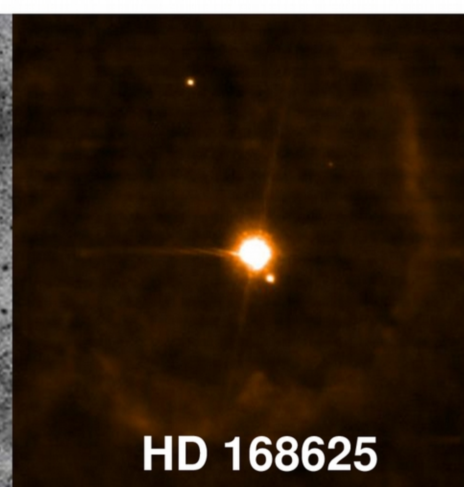

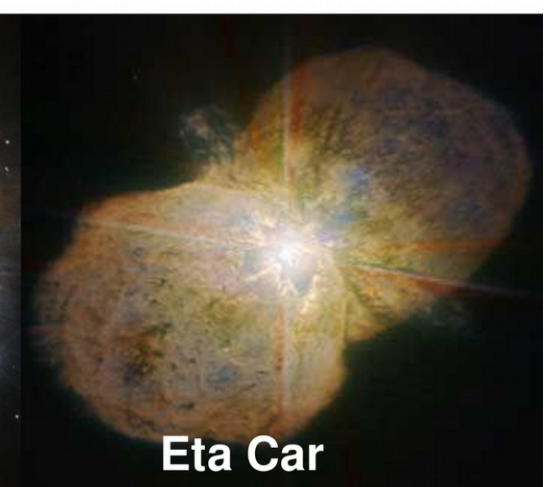

Long-term *V* brightness cycles of LBV S Dor

***V* brightness changes of ~$1^m.5$ over last 50 years**

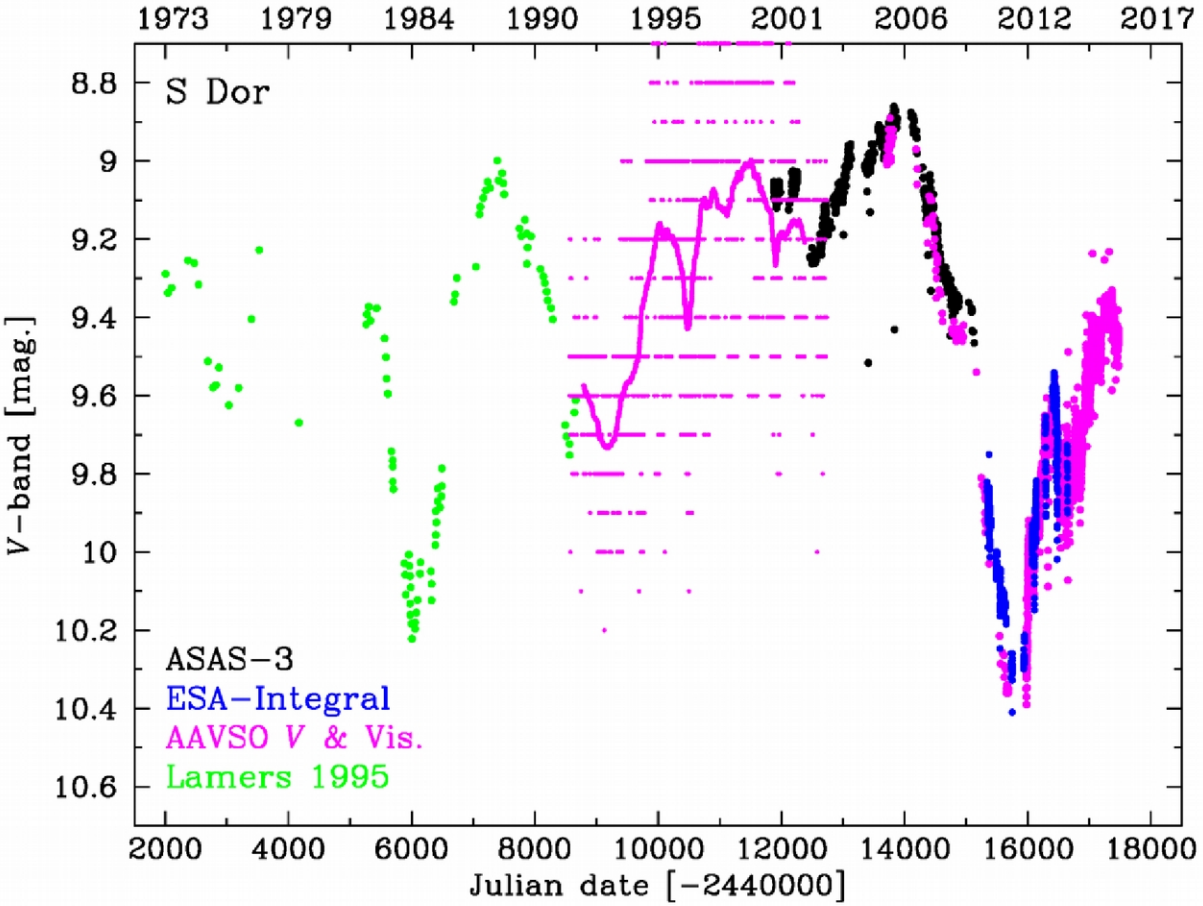

Spectroscopic variability of LBV S Dor

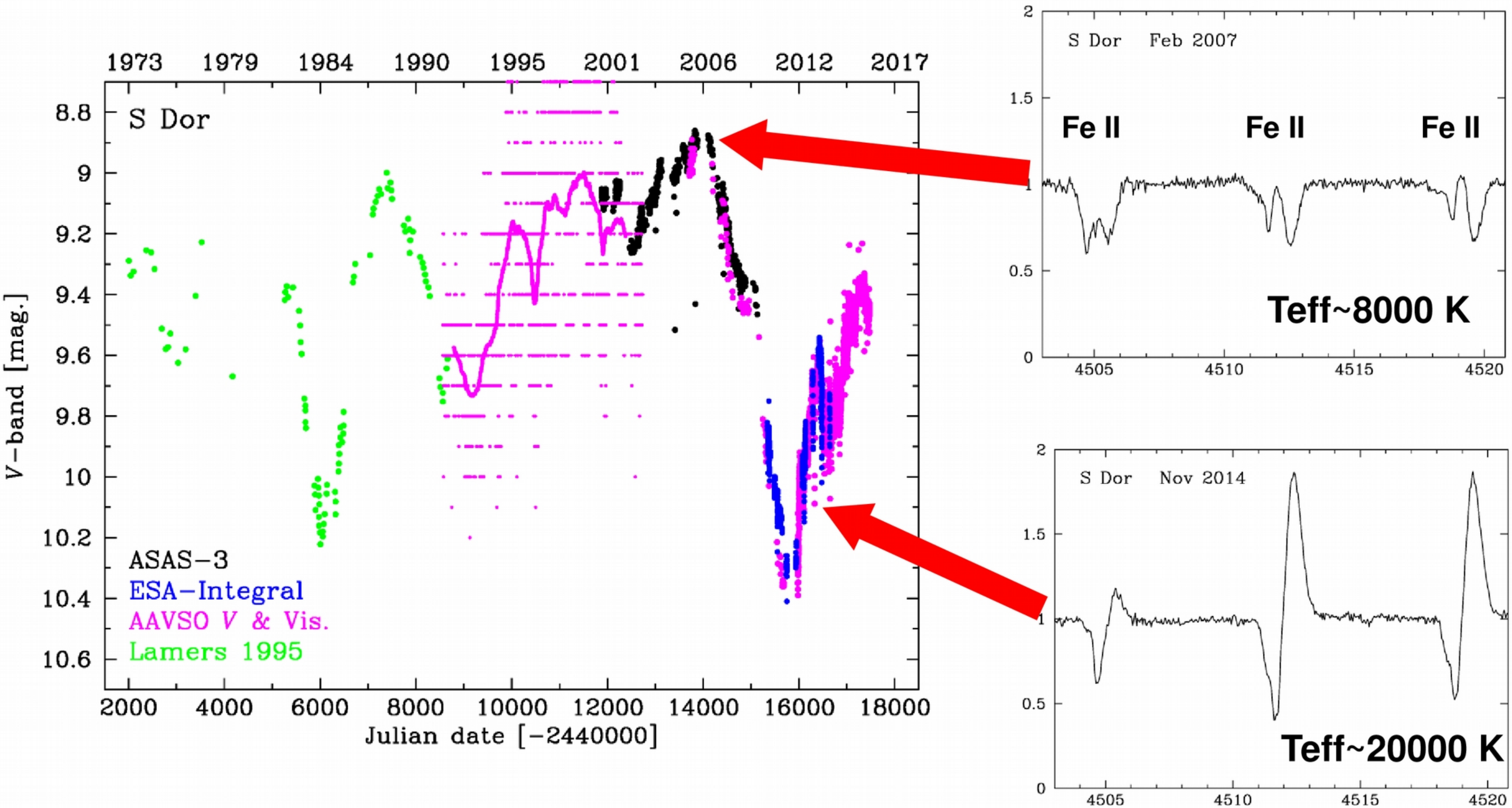

Strong P Cyg emission lines spectrum observed around minimum *V* brightness = “quiescent state”
Metallic absorption line spectrum around maximum *V* brightness = “outburst phase”
Increase of visible R_* from 100 $R_\odot$ to 380 $R_\odot$ in 1985-1989 and in 2006-2011 ? Or binary interaction?

Beccari & Boffin, 2019

Line profile variability in LBV S Dor

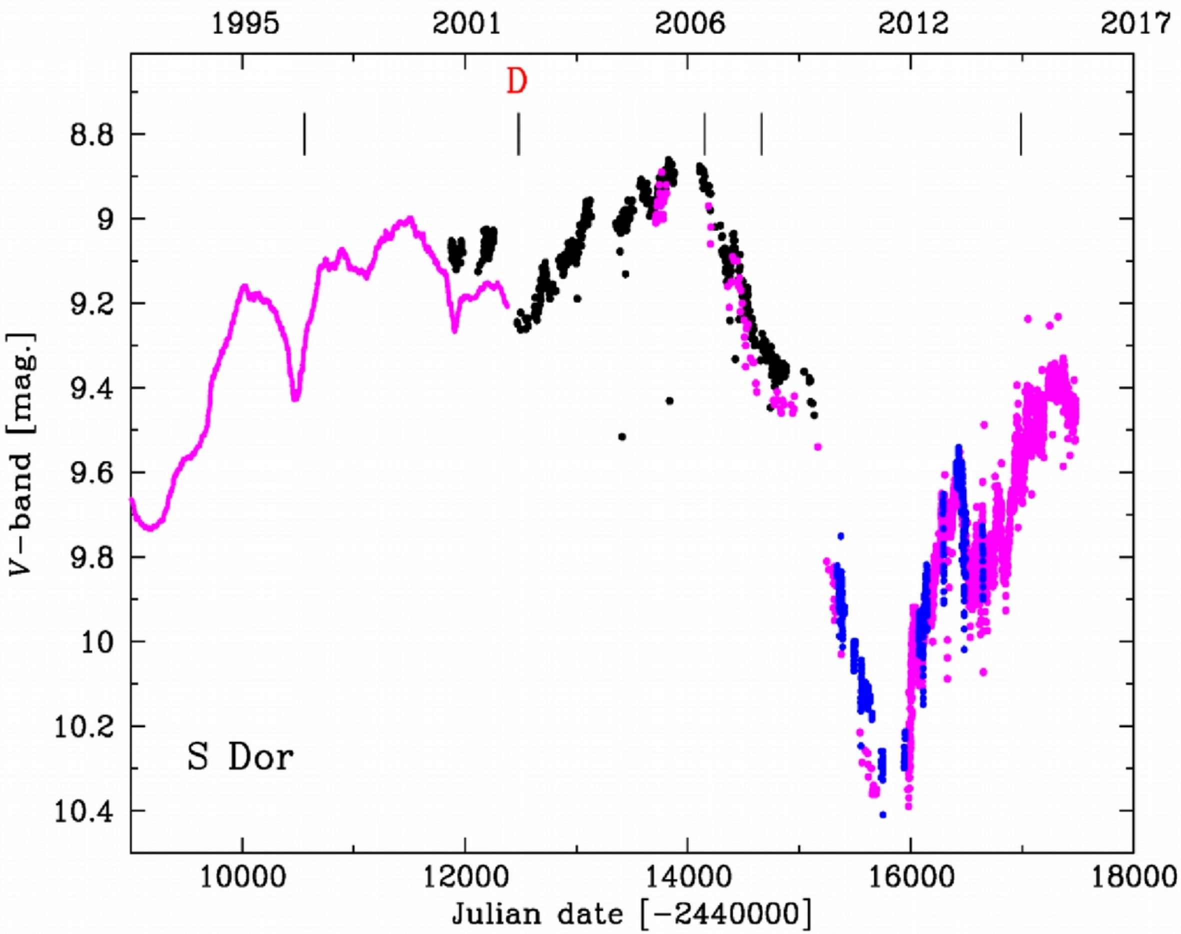

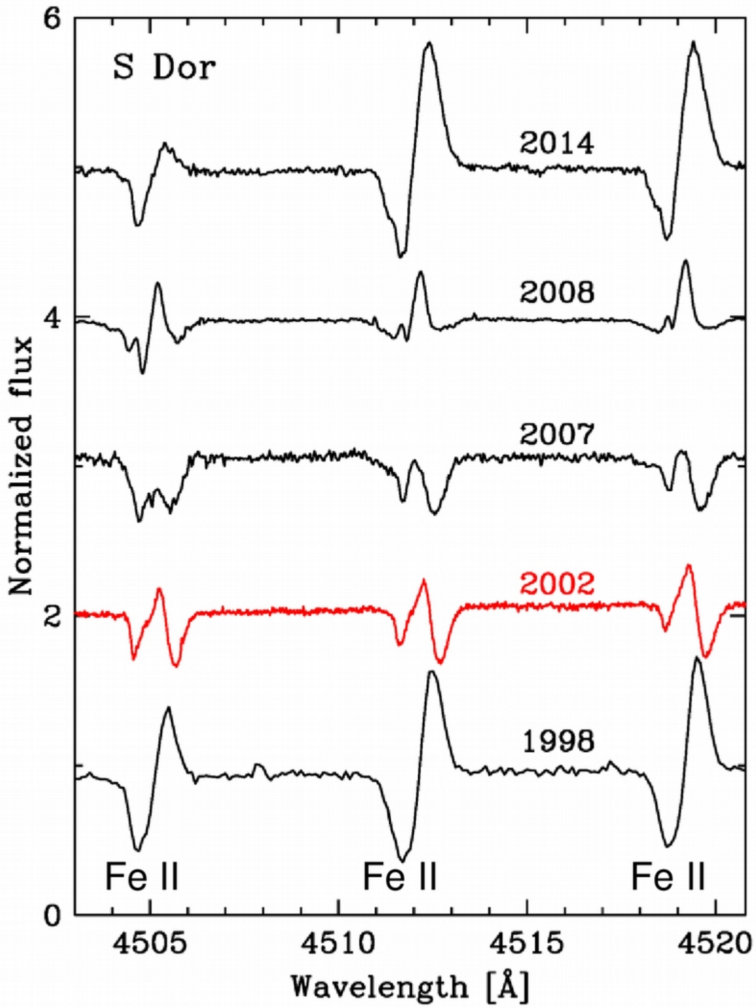

- **During *V*-brightness increase before 2006 maximum, the Fe II P Cyg line profiles transform into split absorption lines with central emission cores.**

- **Is there a physical link with split metal lines observed in various YHG?**

Monitoring of 'wind lines' in P Cygni

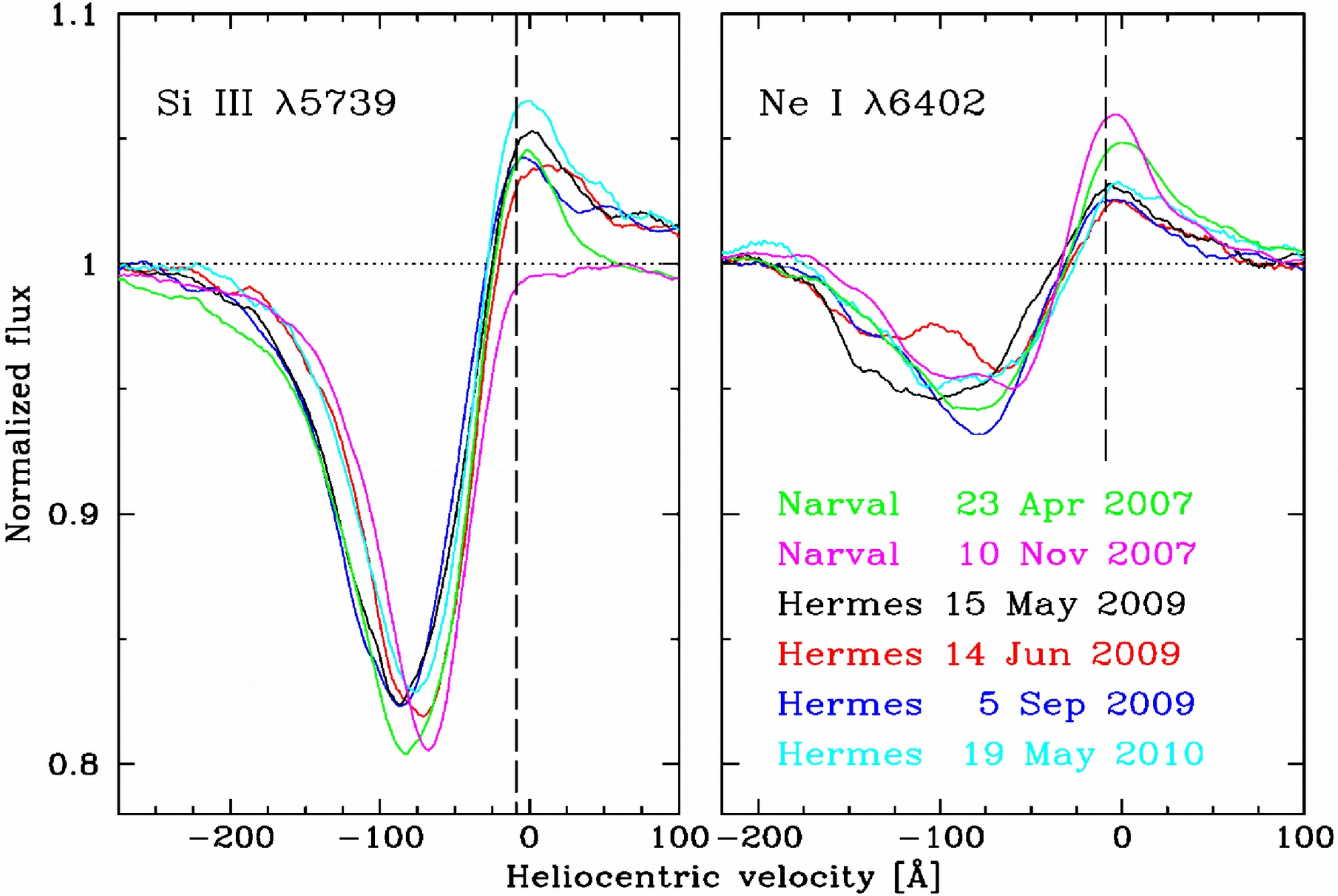

Use large spectral resolution spectrographs to investigate physical properties and variability of slow-wind regions close to the stellar surface from weak P Cyg profiles observed with large S/N ratios.

S Dor -like *V* brightness cycle of MWC 930

V **brightness increase of ~1^m.3 between 2000 and 2014**

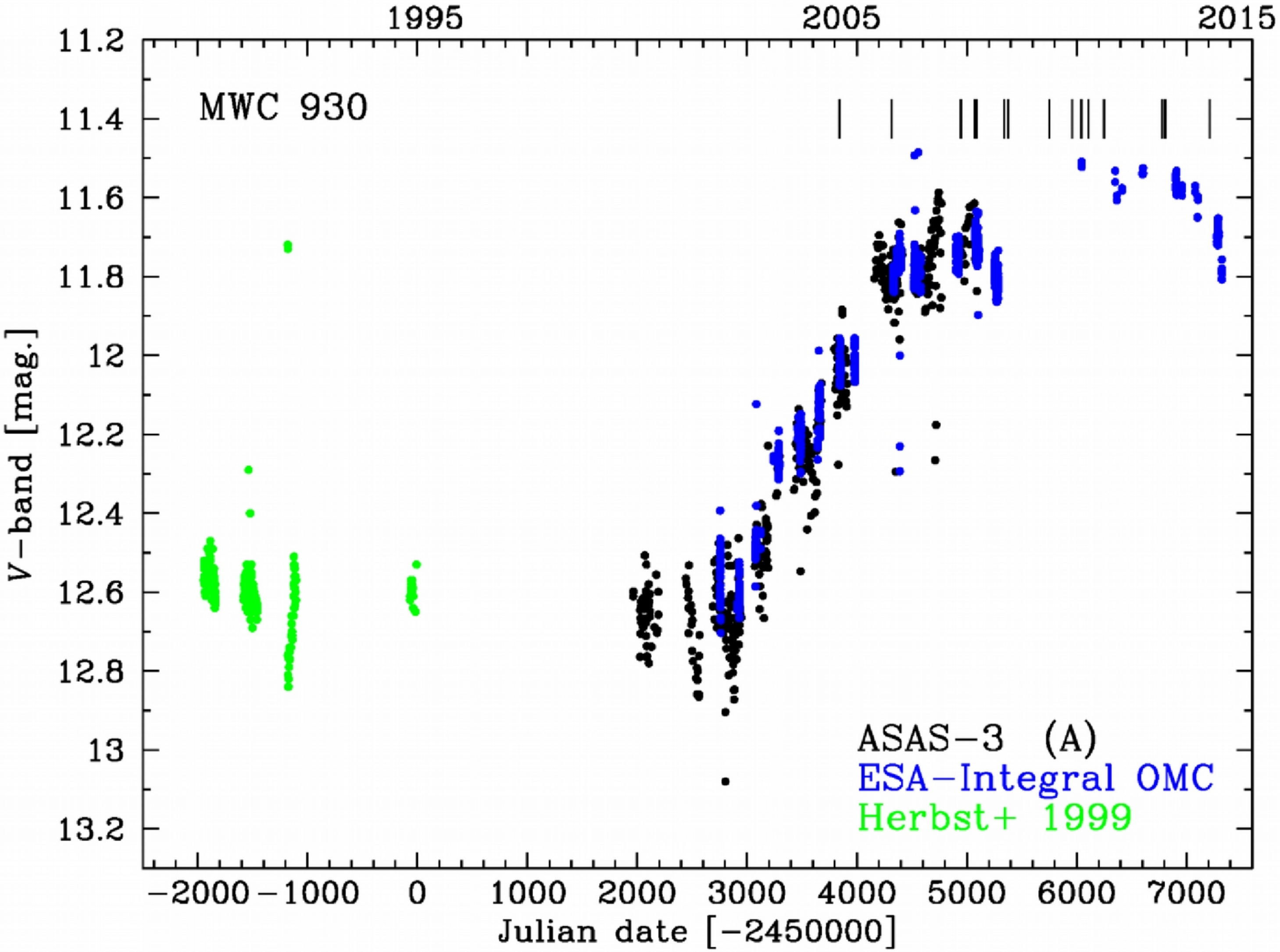

High-resolution spectroscopic monitoring ongoing with Mercator-HERMES since 2009.

Spectroscopic monitoring of LBV MWC 930

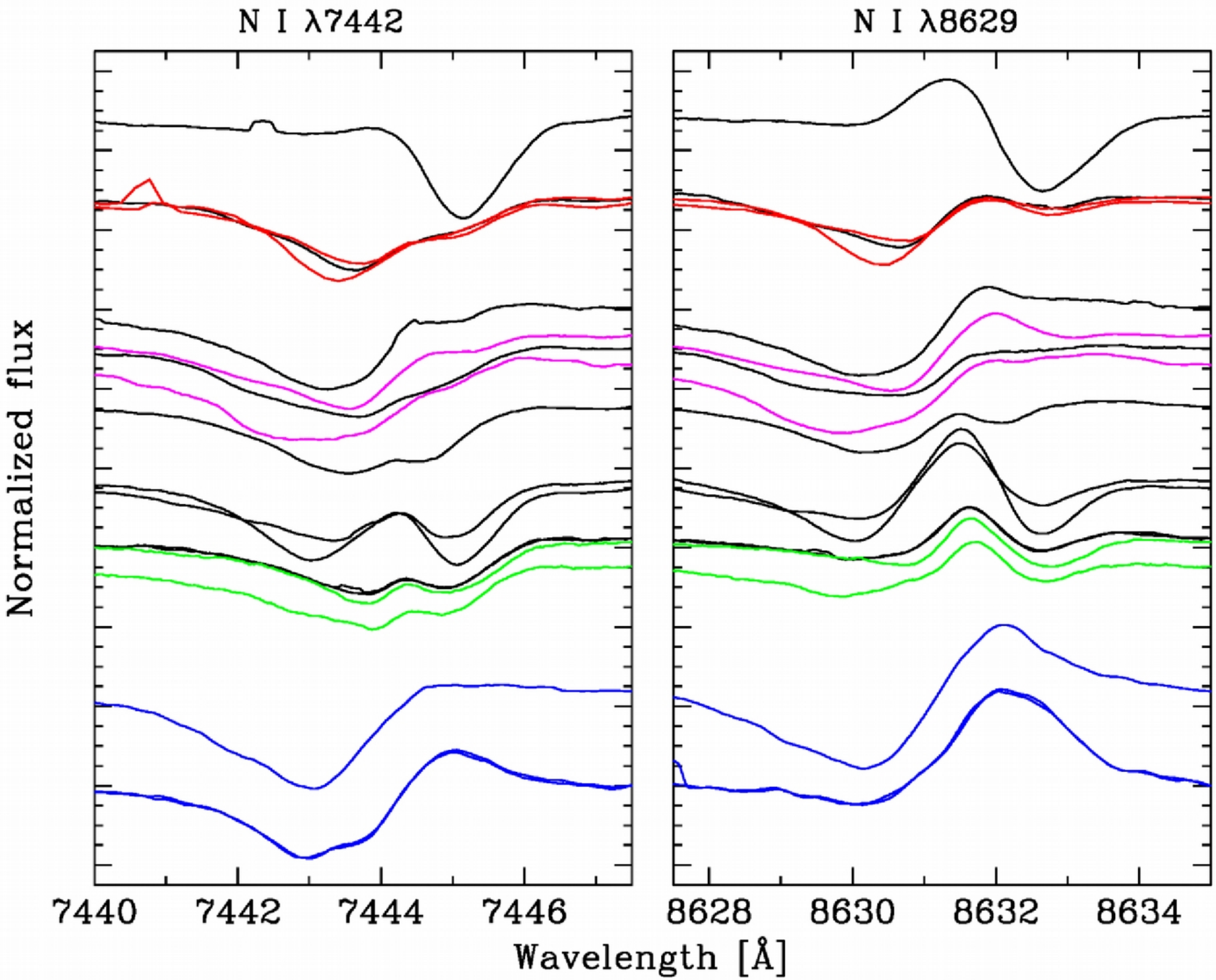

9 HERMES (2009-)
2 ESO-Feros (2006-2007)
2 VLT-UVES (2009)
2 CFHT-Espadons
2 VLT-XShooter

N I near-IR lines show remarkable shape transformations from P Cyg profiles to inverse P Cyg profiles over periods over several years, but without indications of binarity.

Wind expansion and contraction phases => cyclic wind variability in massive stars

HD 168625 and HD 168607 in the upper HRD

LBVs and candidate LBVs

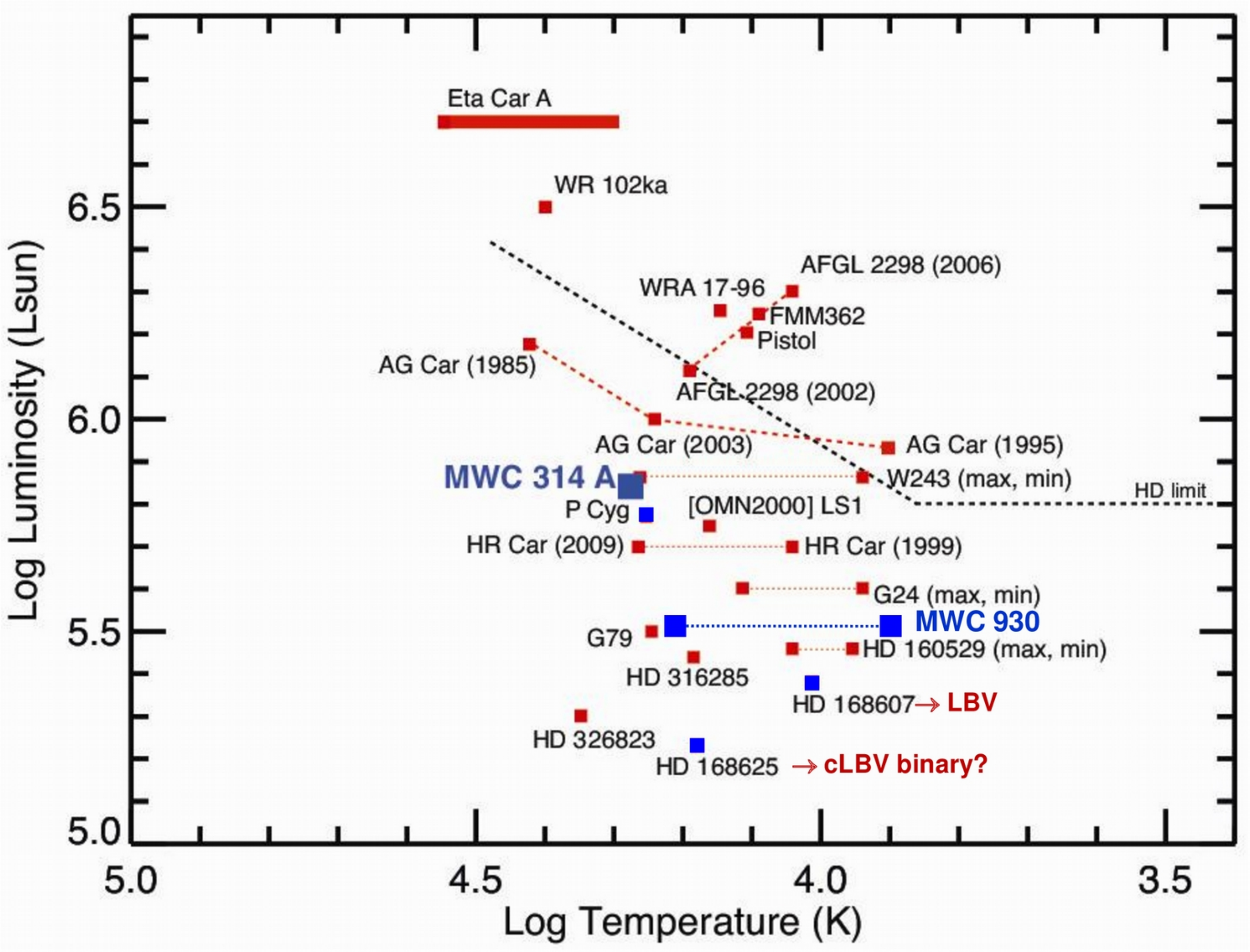

Mercator-HERMES long-term spectroscopic monitoring 2009-2023

HD 168607

LBV of S Dor-type

Teff = 9300 K.

log $L_*/L_\odot$= 5.4

No nebula, but shows *V* micro-variability.

HD 168625

cLBV

Teff = 13500 K.

log $L_*/L_\odot$= 5.1

$\dot{M}$ = 1.4 10^{-6} $M_\odot$ /yr

Loop-like inner and outer (bi-polar) nebulae.

LBV HD 168607 and cLBV HD 168625

• Remarkable close pair. HD 168607 LBV without nebula & Teff = 9300 K B9.5 (van Genderen, A&A 2001)

• HD 168625 (B5.5) dormant LBV? Ring-like nebular structures observed with IRAC-Spitzer (Smith+ 2007)

Discrete Absorption Components in LBV HD 168607

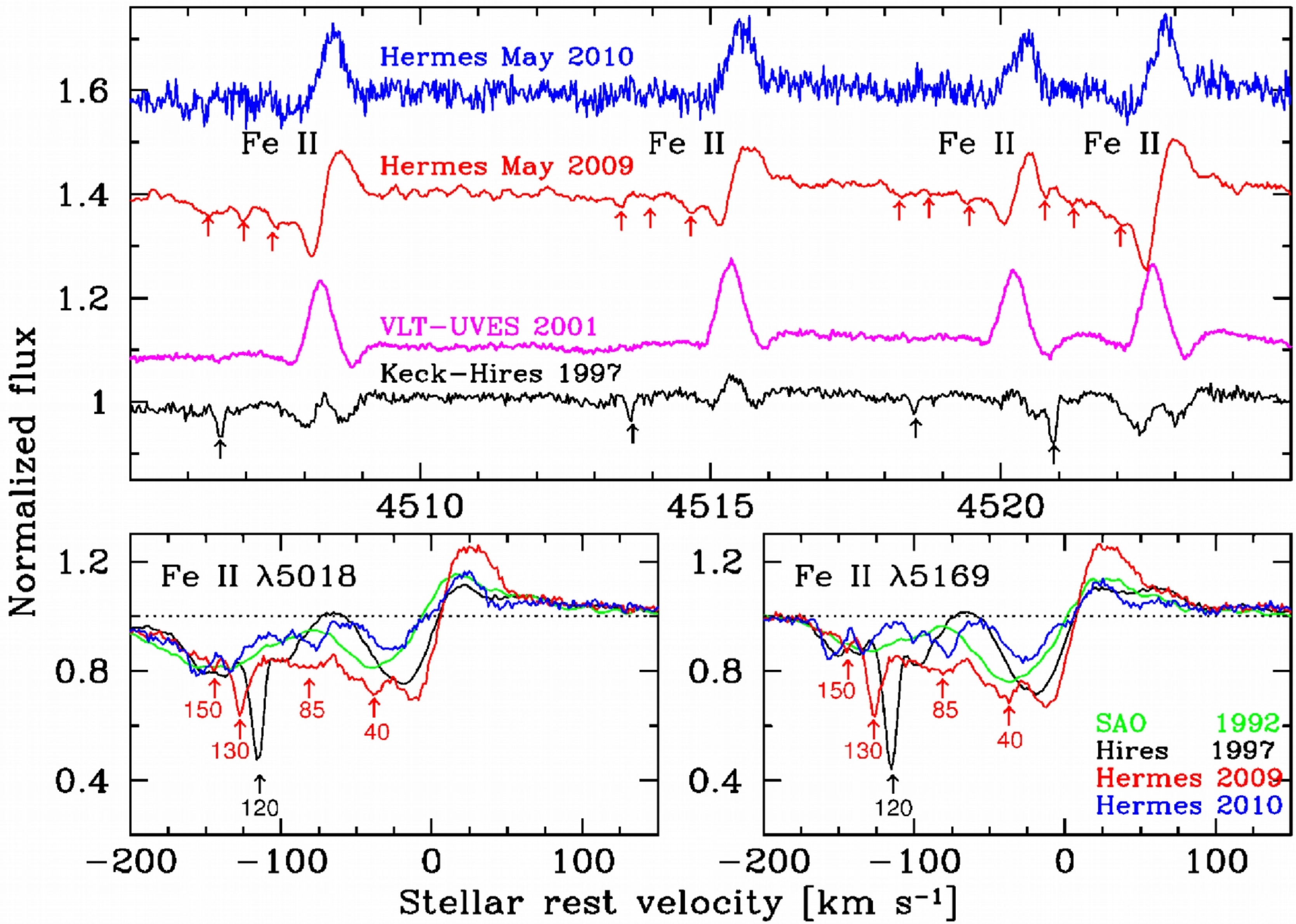

- DACs signal large-scale wind structures. DAC acceleration can help to constrain large-scale structured wind model (i.e. rotating wind interaction regions = CIRs).

Discrete Absorption Components in LBV HD 168607

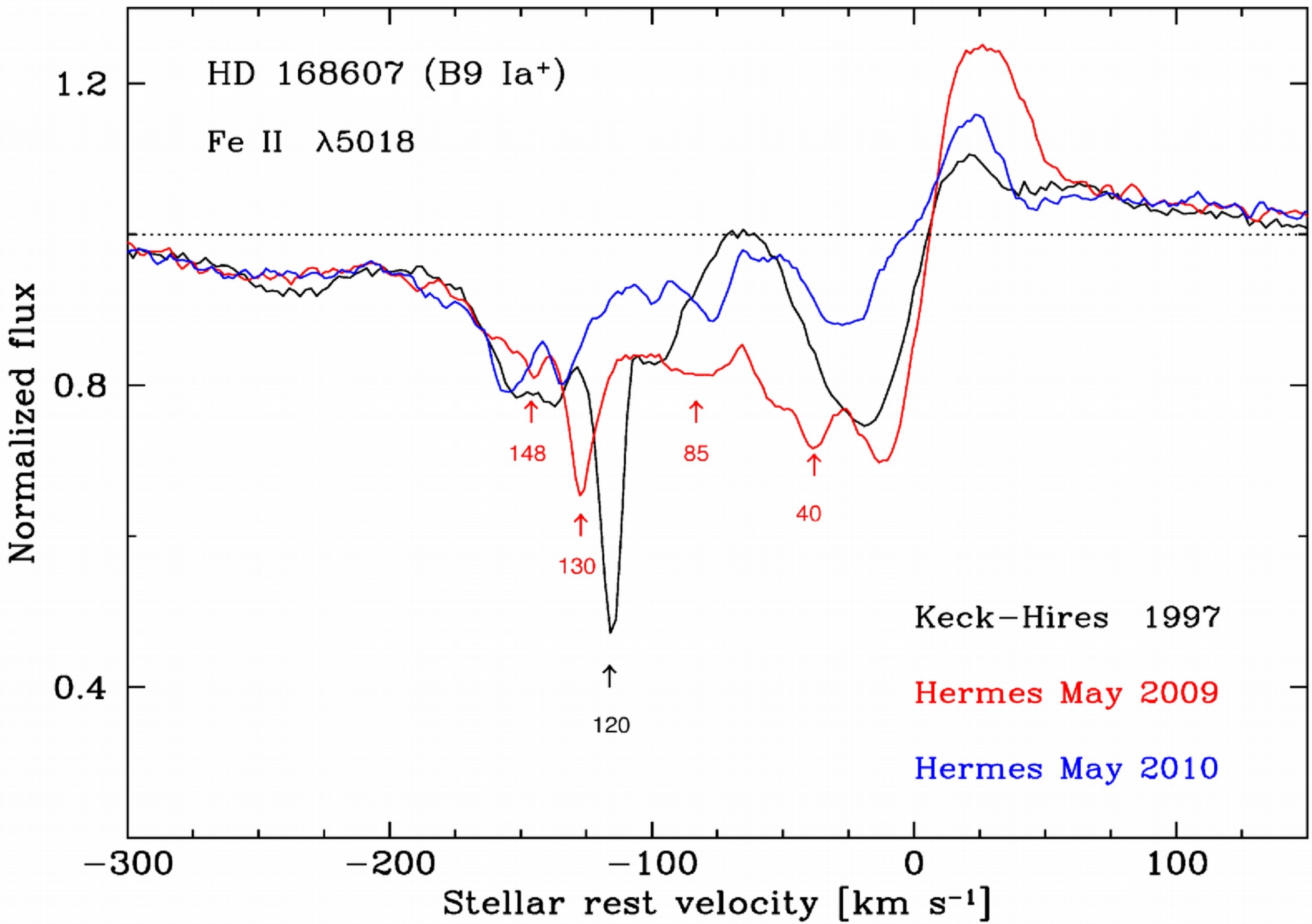

Monitoring of DACs required for detailed 3-D RT wind modeling of DAC acceleration.

Discrete Absorption Components in LBV HD 168607

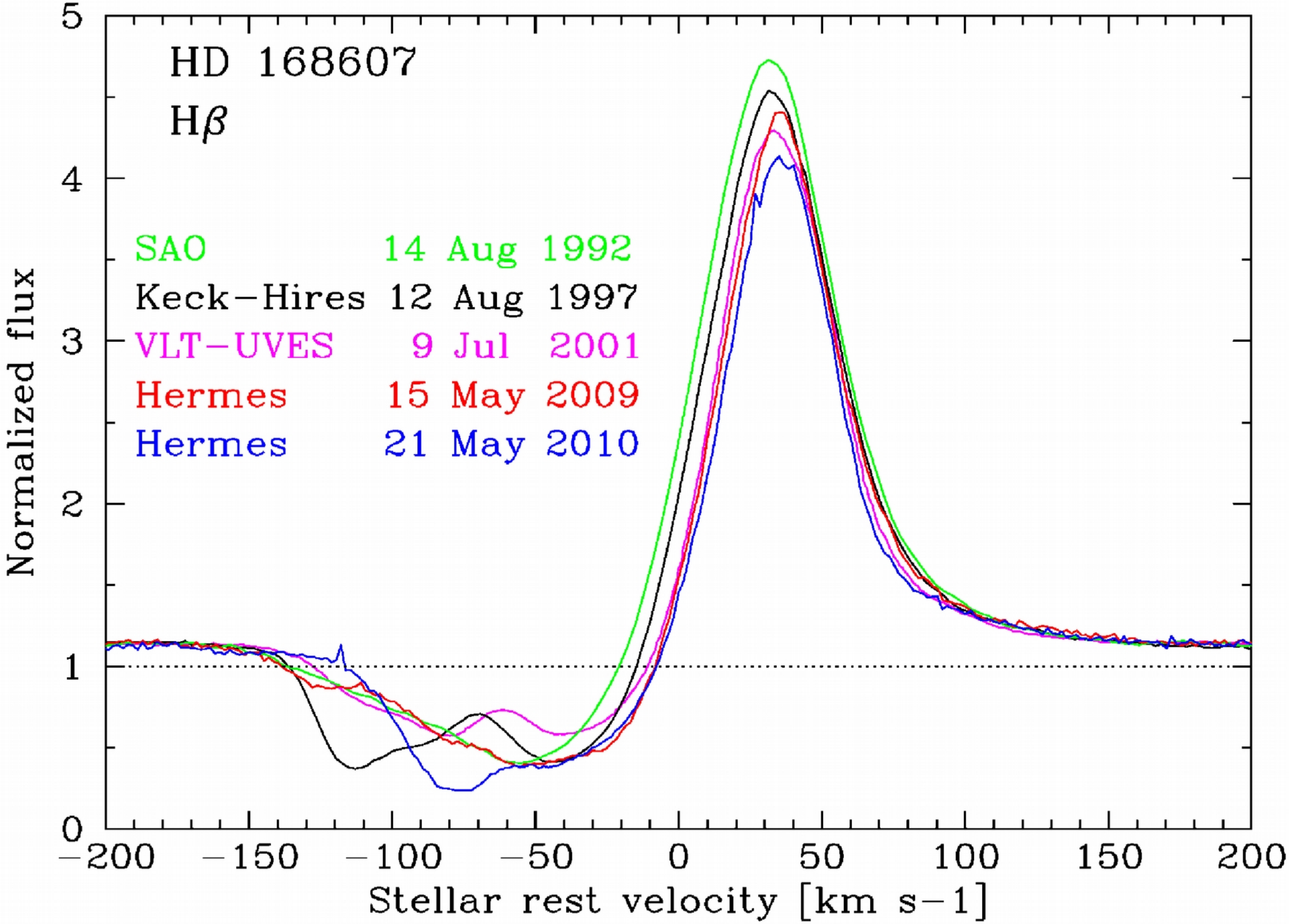

Strong variability of Hβ absorption observed with Mercator-HERMES, VLT-UVES, Keck-Hires (see also Chentsov+, A&A 2003).

J Puppis observed Si IV λ1394 line

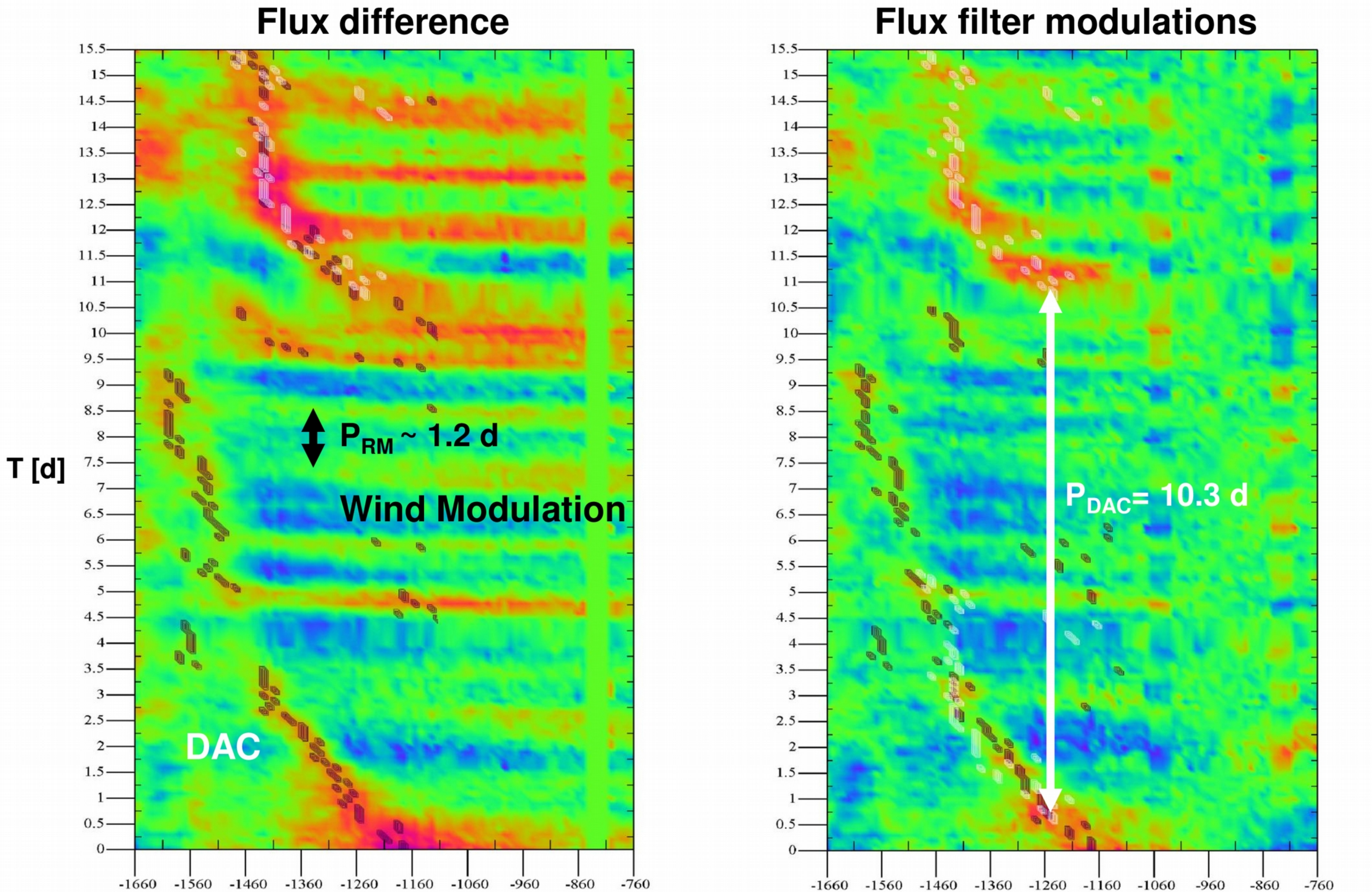

P_{DAC} = 10.3 ± 0.5 d is period between 2 spots at base of wind causing wind structures that produce DACs.

CIRs or Co-rotating Interaction Regions are rotating density waves in the equatorial wind of massive hot stars

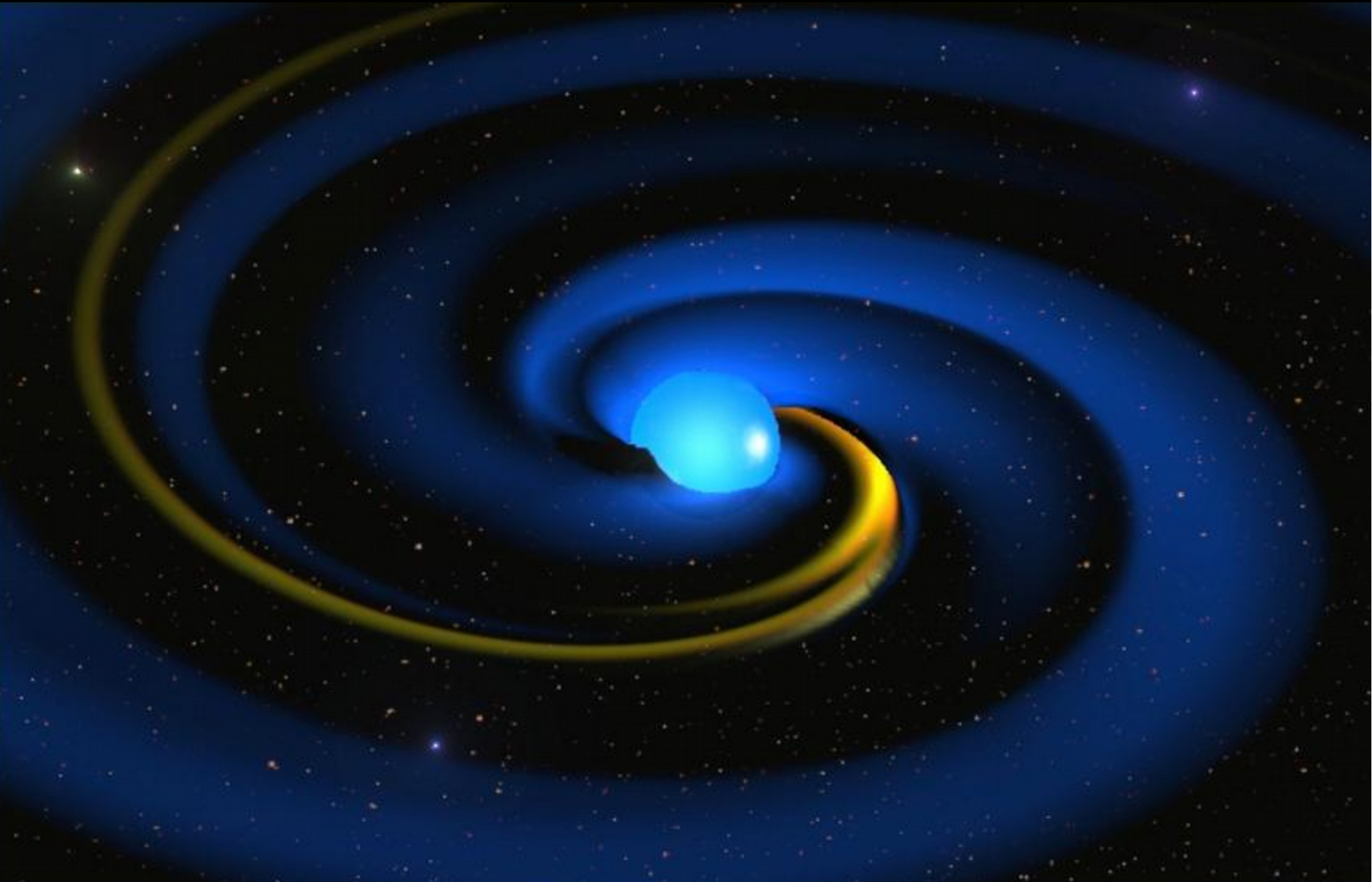

Multi-D hydrodynamic wind modelling

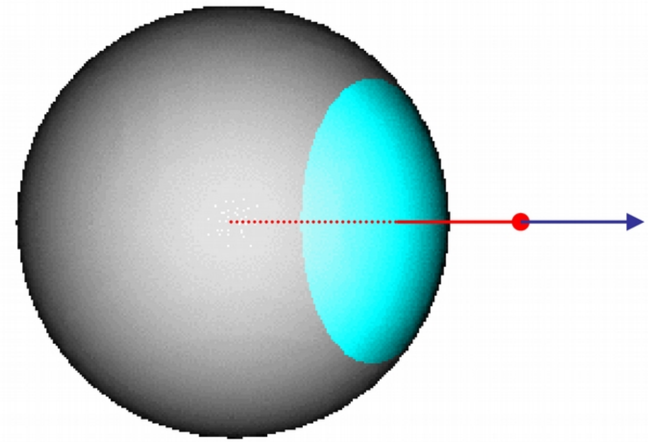

- Zeus3D code
  - Stone & Norman (1992)
  - Clarke (2007)
- Used in 3-D RT by Lobel & Blomme (2007)
  - 3-D hydro equations limited to equatorial plane
  - Rotation of the star and stellar wind
  - Acceleration by spectral lines included (CAK)
  - Spots on the stellar surface
  - Spots could result from NRP, magnetic fields …

J Pup CIR model with Zeus3D hydrodynamics code

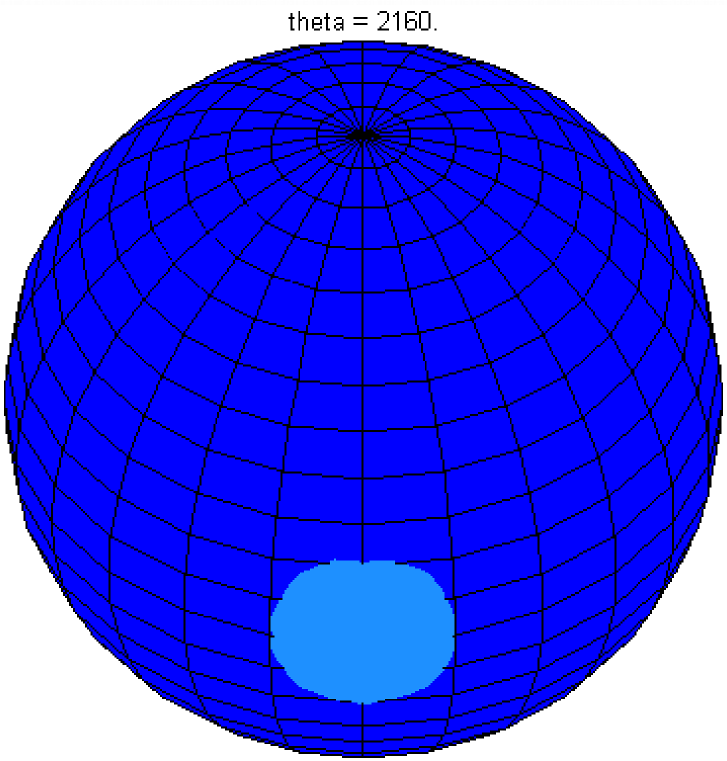

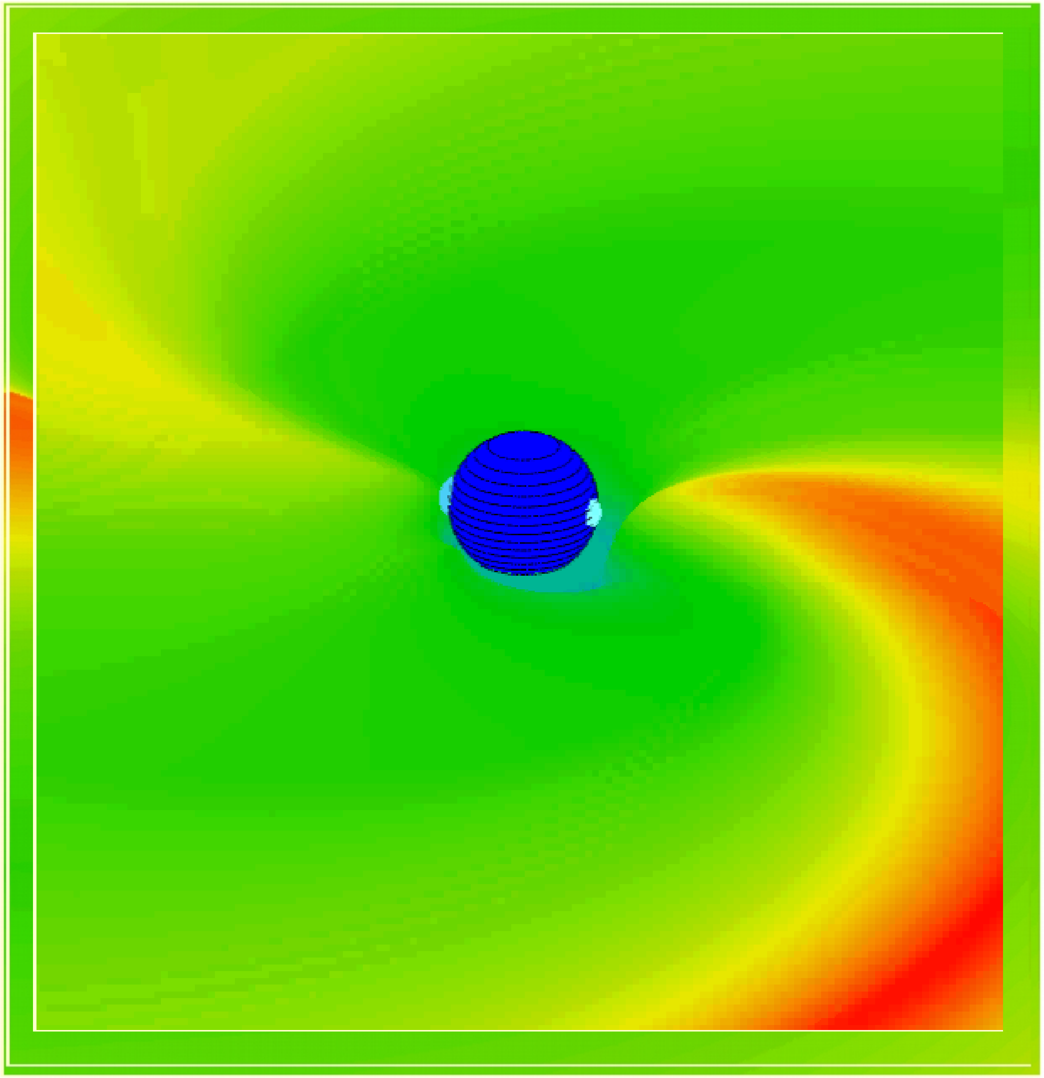

CIRs caused by 2 unequally bright equatorial spots that rotate 5 times slower than stellar surface rotation

P_{rot} = 4.12 d P_{spot} = 20.6 d

Development of 3-D radiation transport code Wind3D

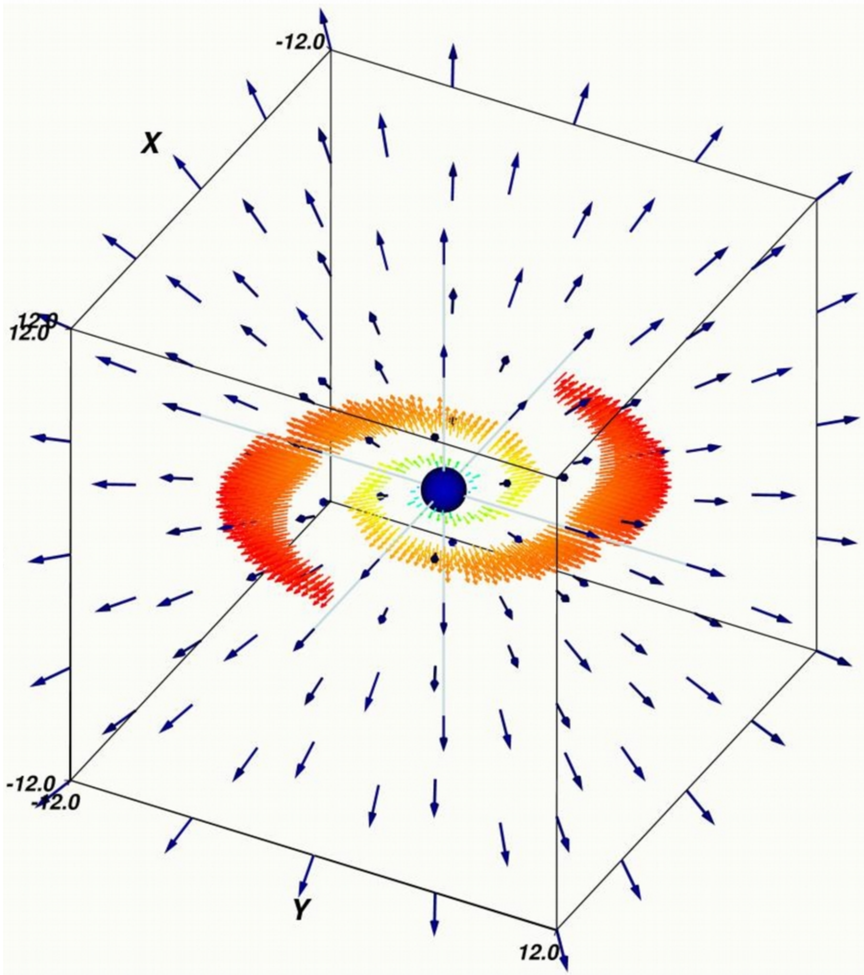

Hot star smooth wind with **'large scale'** internal wind structures input for Wind3D

- implements **Cartesian** radiative transport scheme with short-characteristics method
- accepts **arbitrary 3-D wind-density and -velocity** structures
- exact **lambda iteration** of source function **starting from Sobolev** approximation in 3-D smooth wind model
- lambda iteration to **non-Sobolev** 3-D source function
- 100^3 source function points with 80^2 solid angles for 3-D intensity integral
- **non-LTE** radiative transfer equation is solved for density and velocity points with **3-D source function interpolation** technique
- **two-level atom** approx. for scattering dominated winds
- **fully parallelized** code with excellent load balancing
- 2010-2023: module implementation for parameterized structured wind models of radiatively-driven rotating winds. Also accepts hydrodynamic structured wind models computed with Zeus3D code.

⇒ **Detailed modelling of DACs observed in UV P Cyg lines of J Pup (B0.5 Ib)**

Detailed best fit to DAC shapes using 2 unequal spots with 3D Radiative Transfer Wind3D

2-spot hydrodynamic wind model with

$V_{spot} = V_{rot} / 5$
$A_{sp} = 0.2$ & $\Phi_{sp} = 20°$
$A_{sp} = 0.08$ & $\Phi_{sp} = 30$

Density contrast:

minimum $\rho / \rho_0 = 0.87$
maximum $\rho / \rho_0 = 1.31$

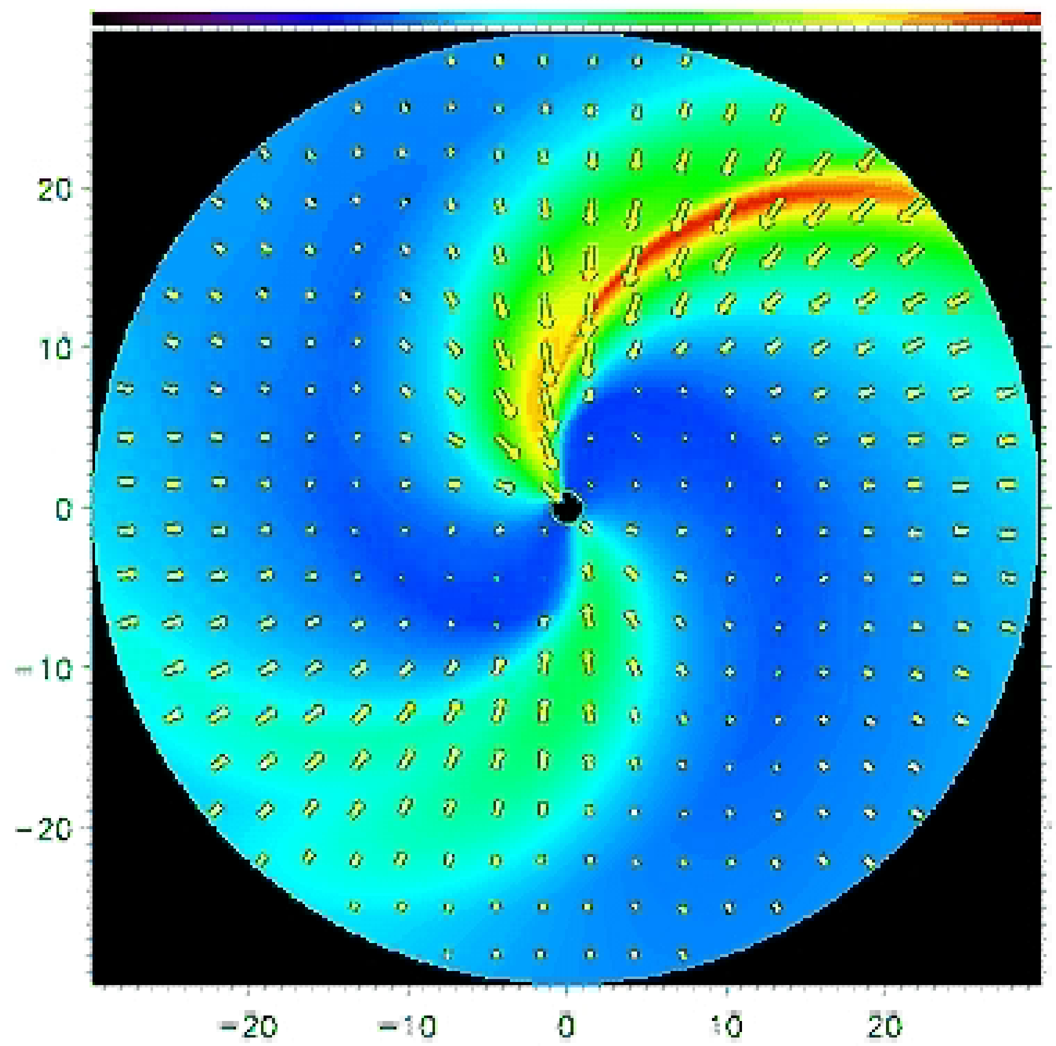

Hydrodynamic wind model with CIR lagging behind rotation of the stellar surface

Si IV λ1394 computed with Wind3D

$\rho / \rho_0 = 0.985$ **Density contrast** $\rho / \rho_0 = 1.2$

Normalized flux

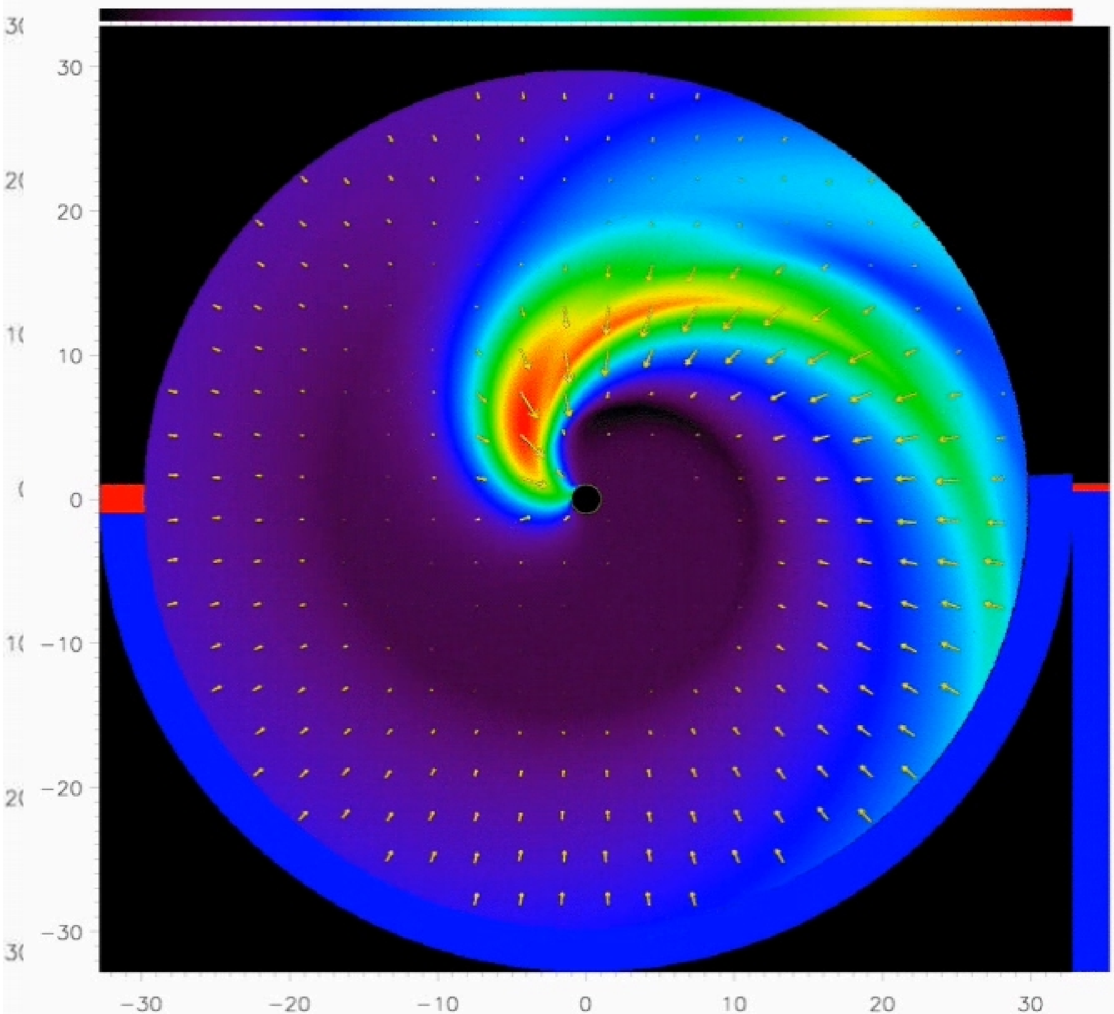

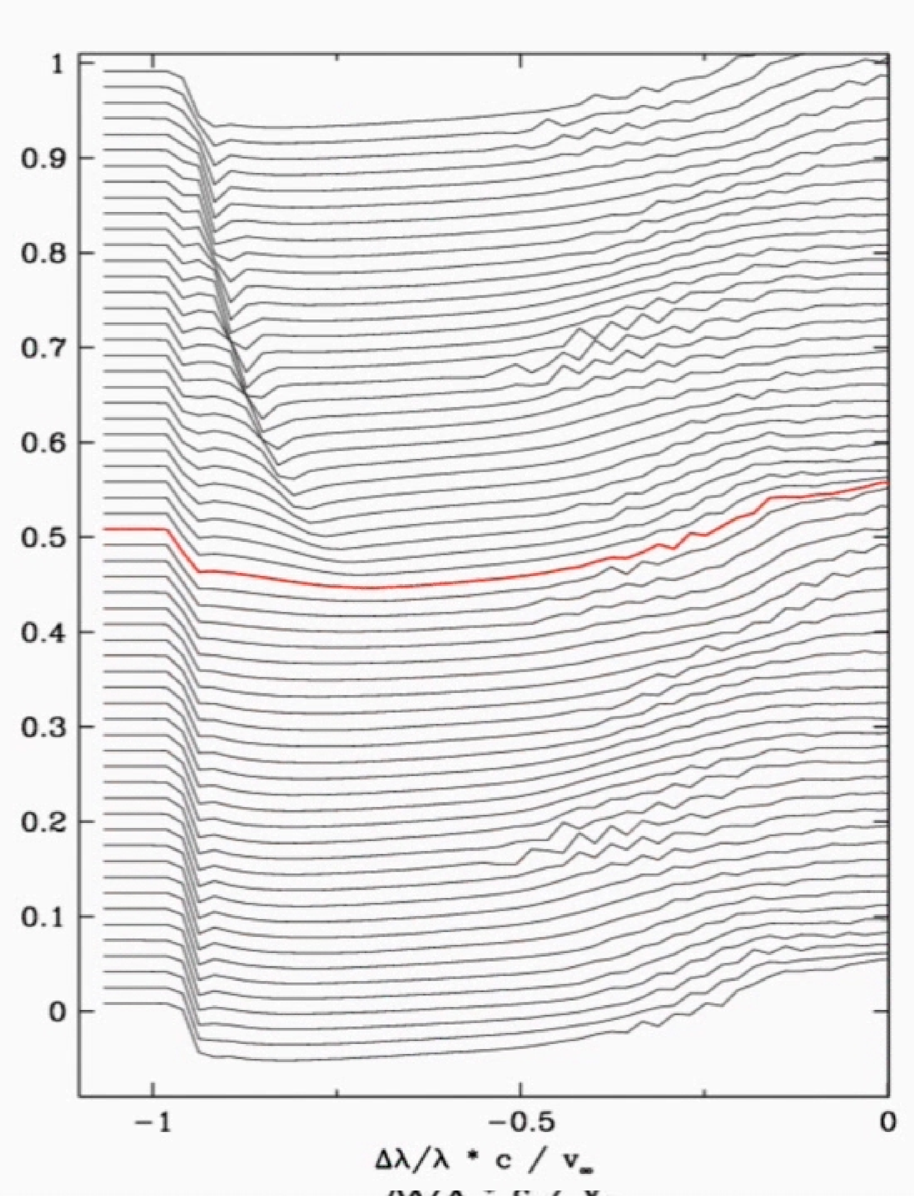

$A_{sp}=0.1$ $\Phi_{sp}=50^o$ $V_{spot} < V_{rot}$

Hydrodynamic wind model with CIR lagging behind rotation of the stellar surface

Si IV λ1394 computed with Wind3D

$\rho / \rho_0 = 0.985$ **Density contrast** $\rho / \rho_0 = 1.2$

Flux difference

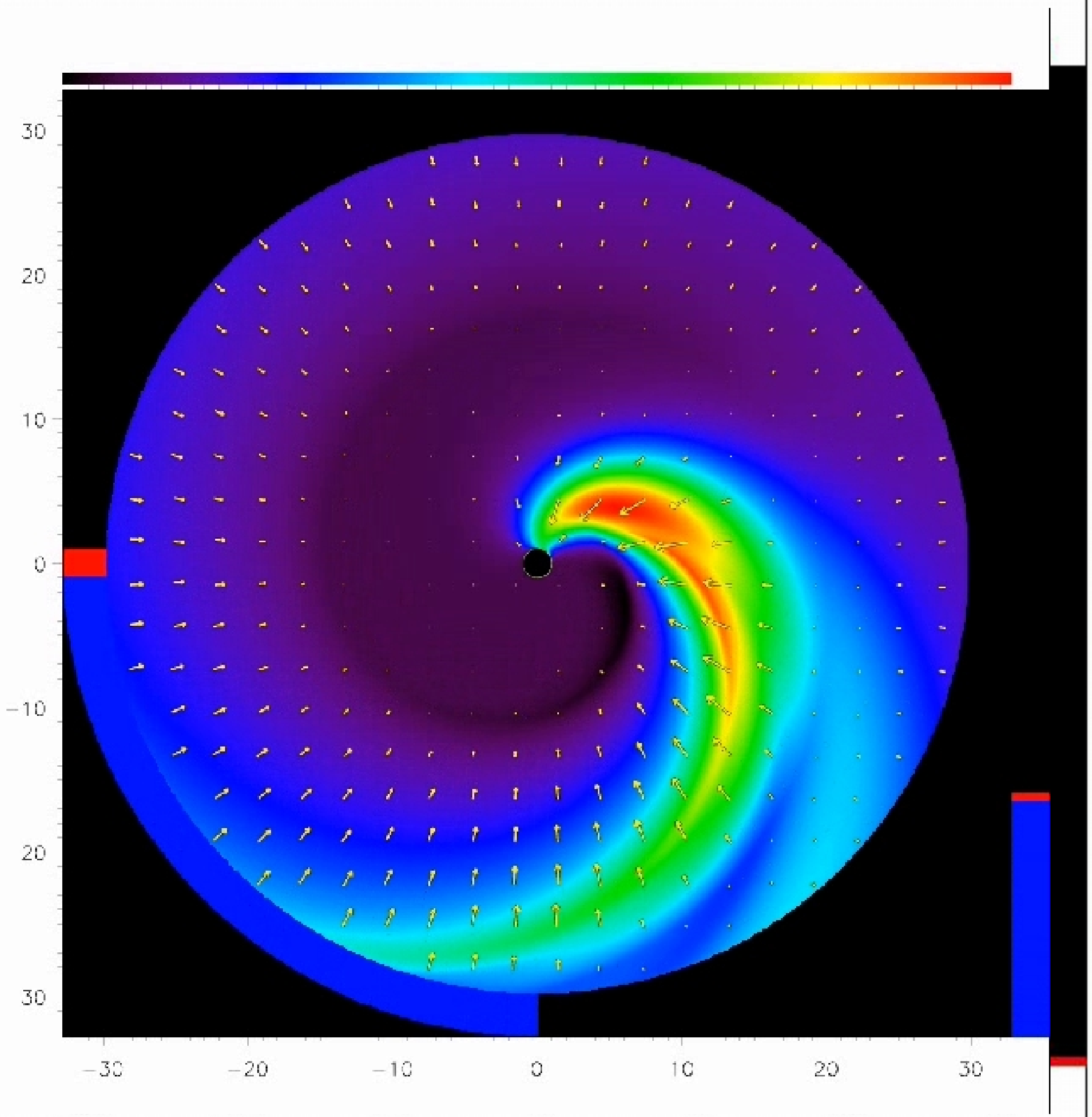

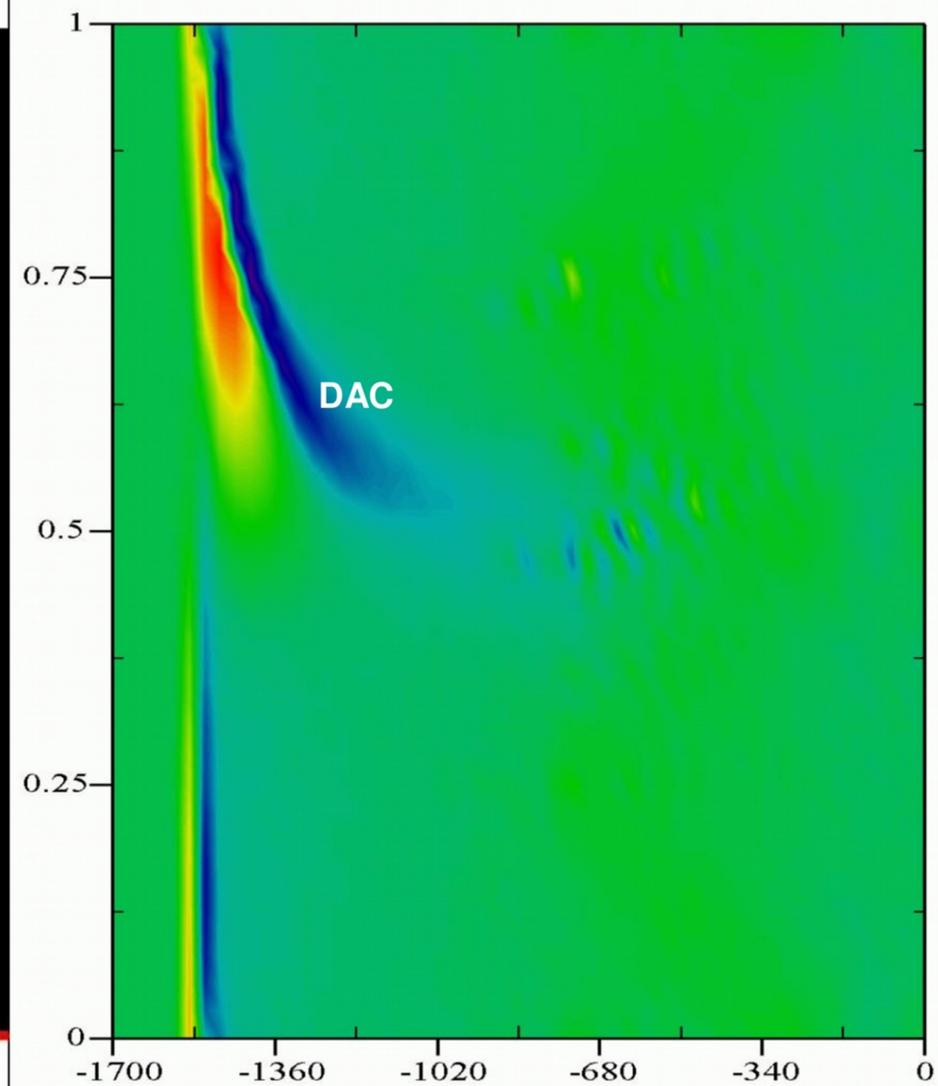

CIR causes DAC because of increased wind density contrasts and velocity plateaus

$A_{sp}=0.1$ $\Phi_{sp}=50^o$ $V_{spot} < V_{rot}$

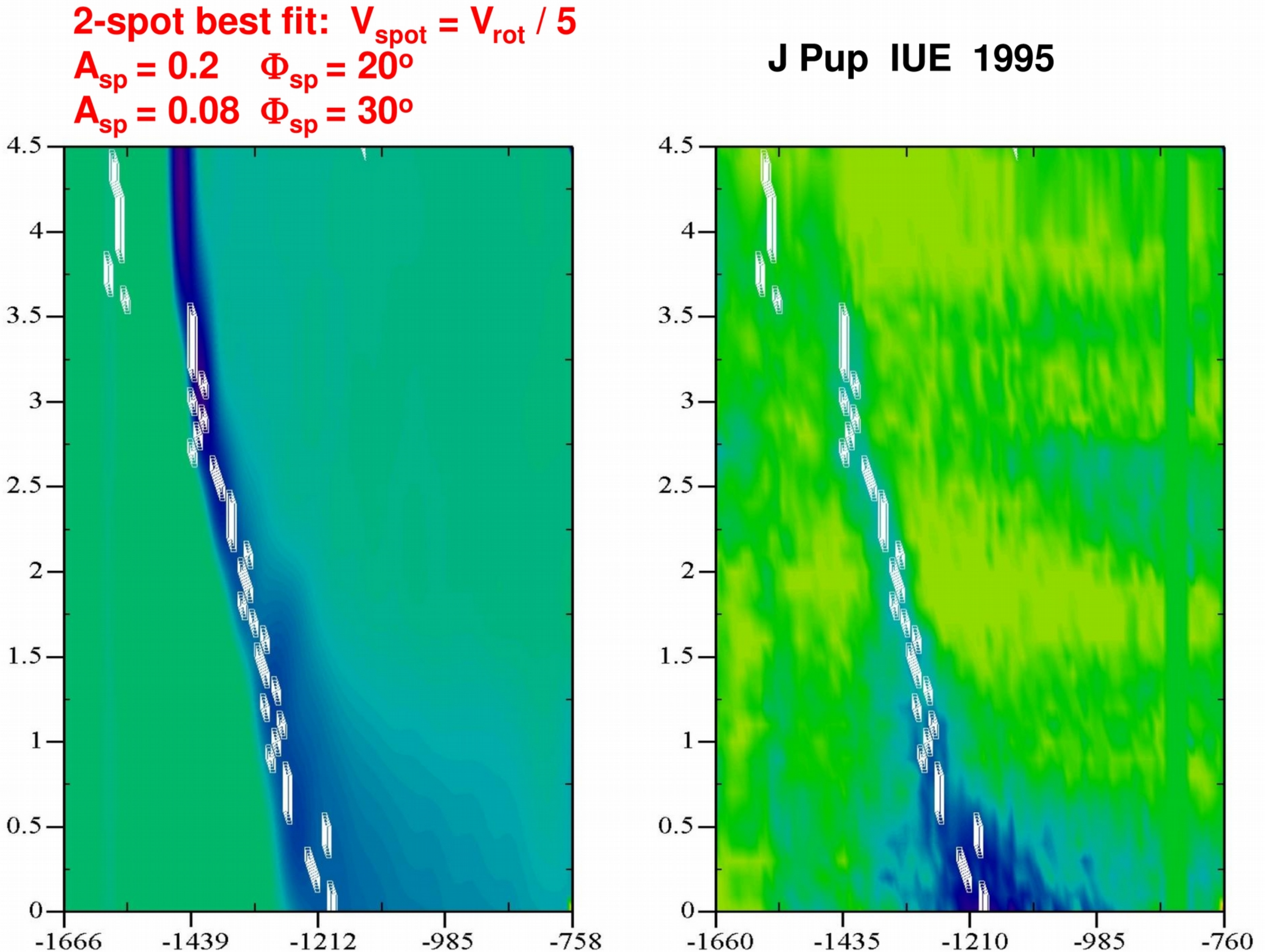
2-spot best fit: $V_{spot} = V_{rot} / 5$
$A_{sp} = 0.2$ $\Phi_{sp} = 20^o$
$A_{sp} = 0.08$ $\Phi_{sp} = 30^o$
J Pup IUE 1995
4.5
4
3.5
3
2.5
2
1.5
1
0.5
0
-1666
-1439
-1212
-985
-758
-1660
-1435
-1210
-985
-760

Modelling the asymmetric wind of LBV binary MWC 314

LBVs and candidate LBVs

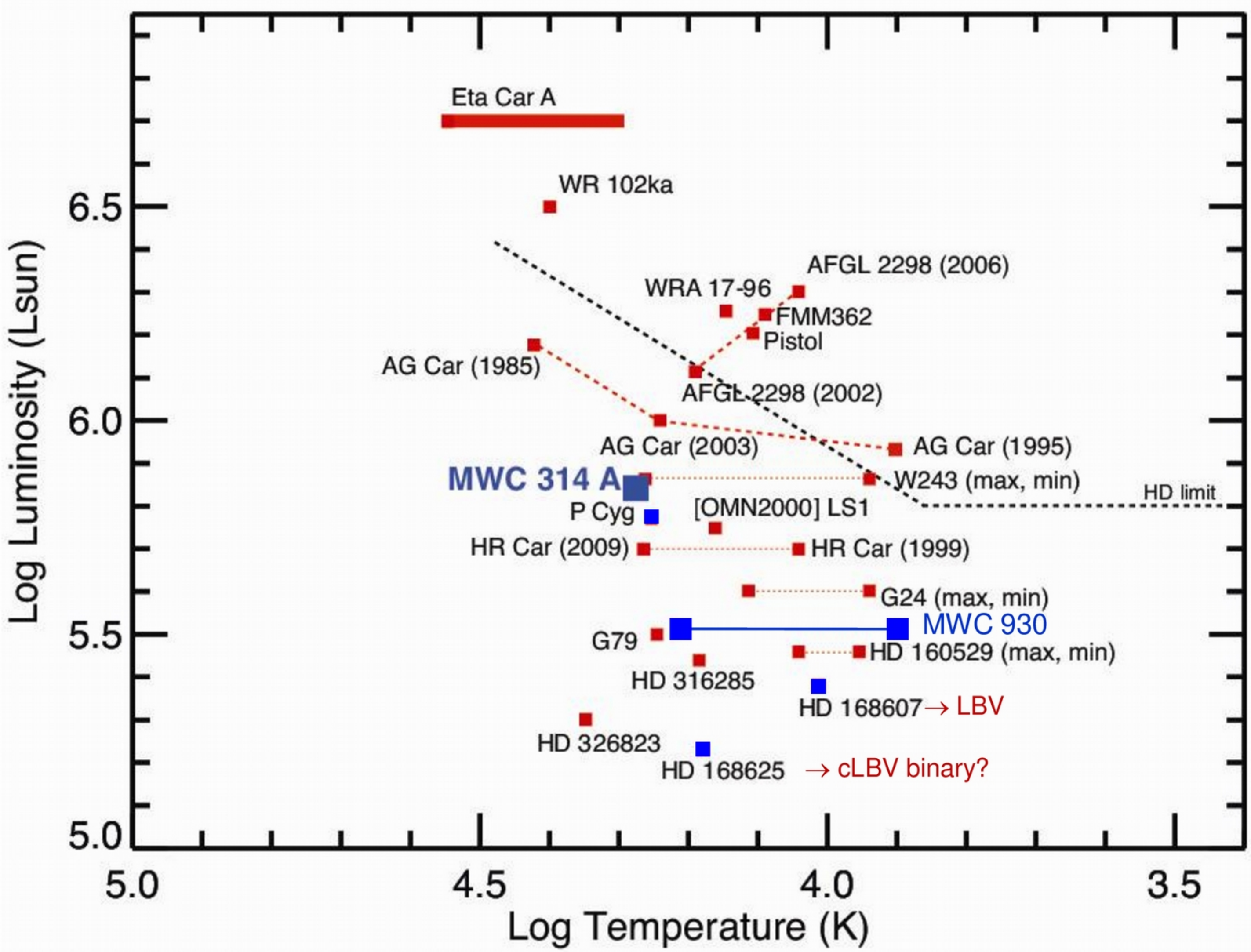

Mercator-HERMES long-term spectroscopic monitoring 2009-2023

MWC 314 A

Teff = 18000 K

log g = 2.26

log $L_* / L_\odot$ = 5.8

$\dot{M}$ = 3 10^{-5} $M_\odot$/yr

Bi-polar Hα nebula of MWC 314

A. P. Marston and B. McCollum: Extended shells around B[e] stars 197

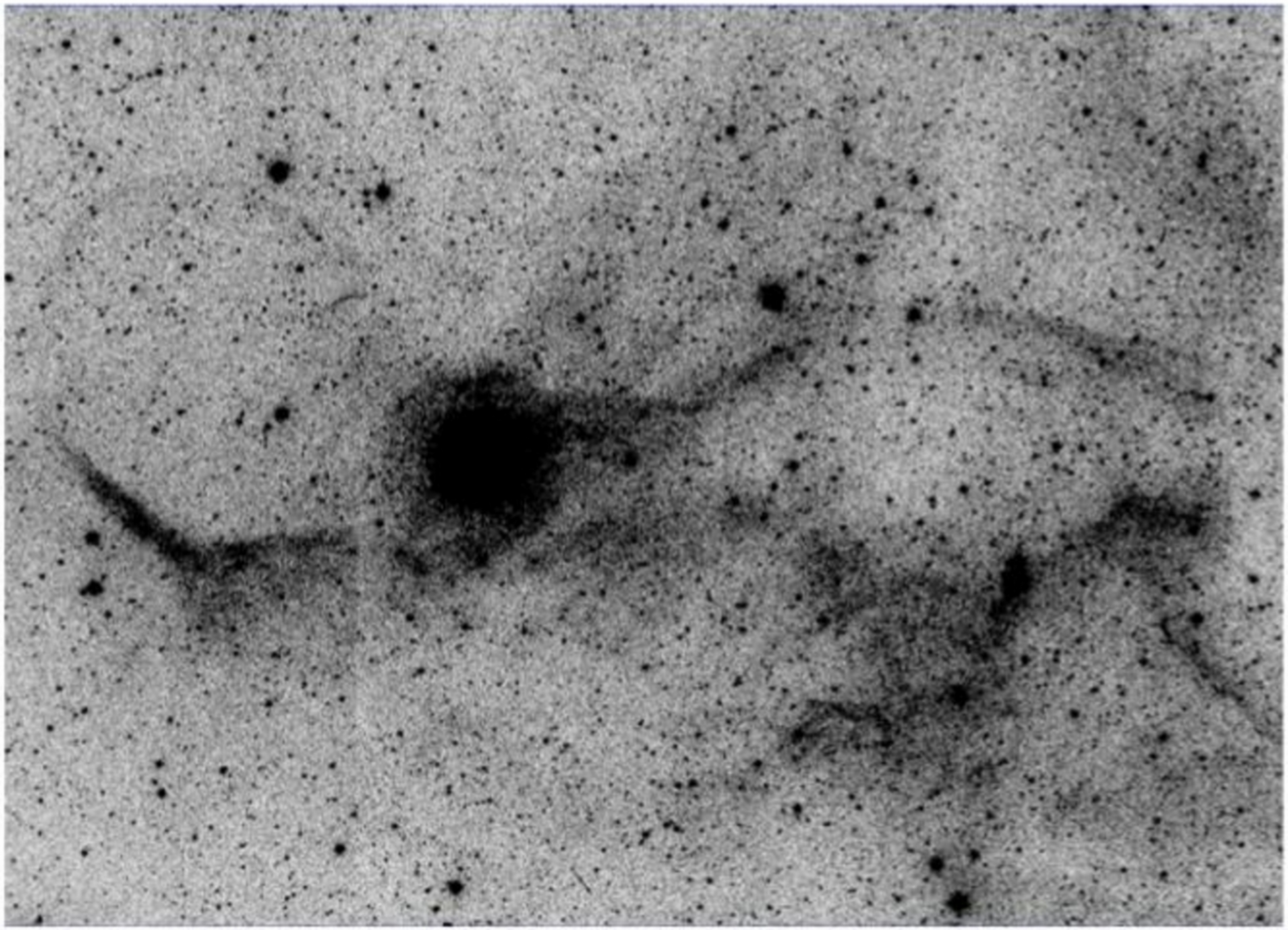

Fig. 1. Narrow band Hα image of the environments of MWC 314 showing the large east-west bipolar feature around the star. The figure is 12.′5 vertically. For all figures, north is up and east to the left.

(Marston & McCollum A&A, 2008)

Very large bi-polar Hα nebula formed 10^5 years ago.

Giant eruption in LBV phase?

Bi-polar Hα nebula of MWC 314

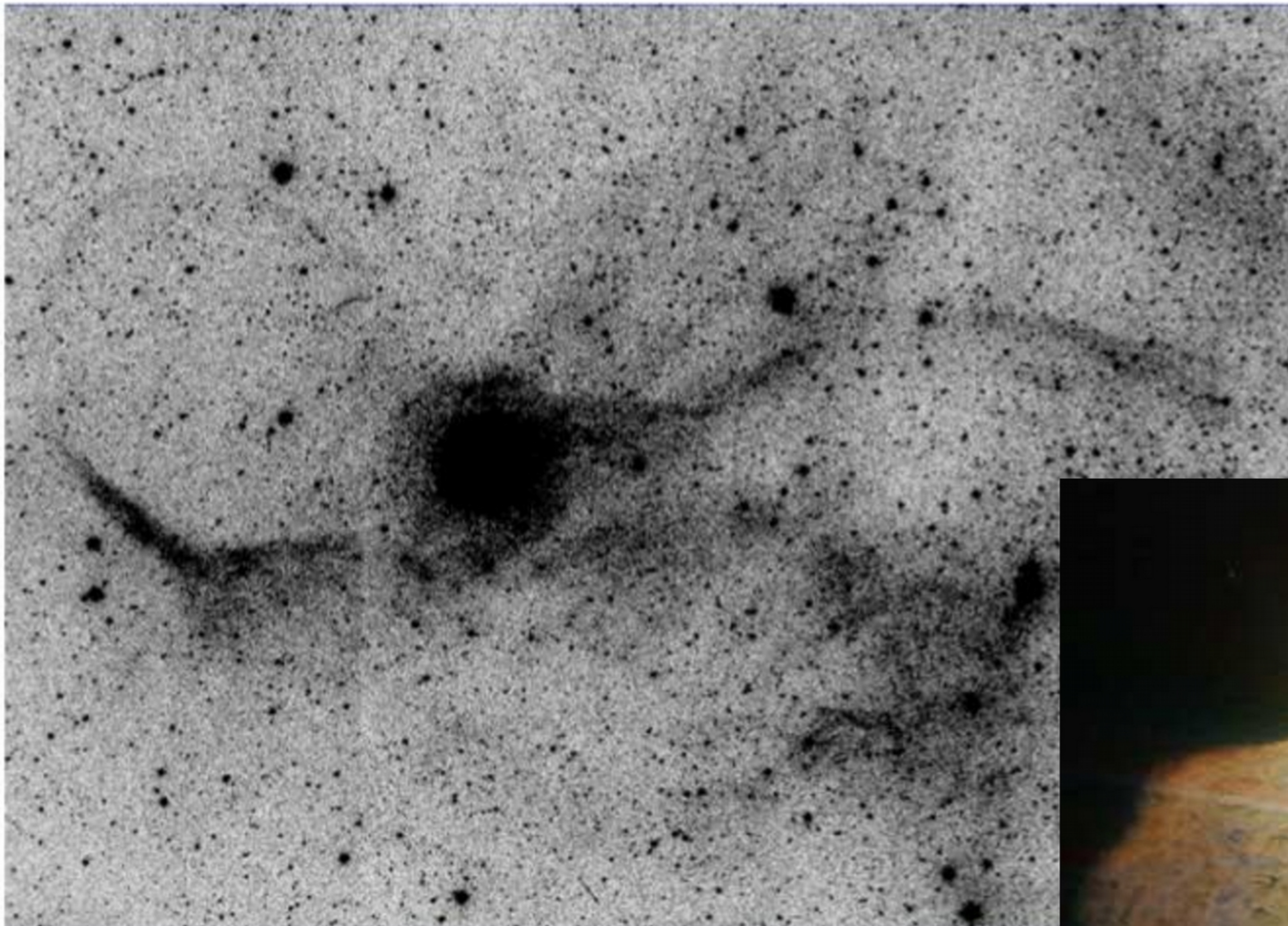

Fig. 1. Narrow band Hα image of the environments of MWC 314 showing the large east-west bipolar feature
12.′5 vertically. For all figures, north is up and east to the left.

(Marston & McCollum A&A, 2008)

η Carinae
LBV binary P_{orb}= 5.5 yr

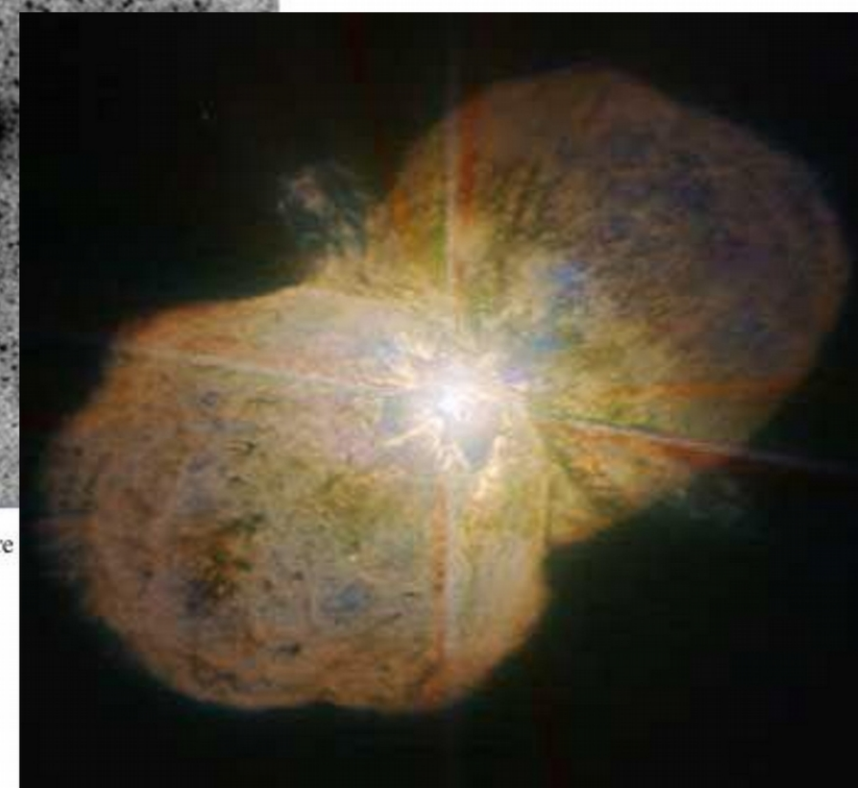

Comparison of He I λ5876 in LBVs

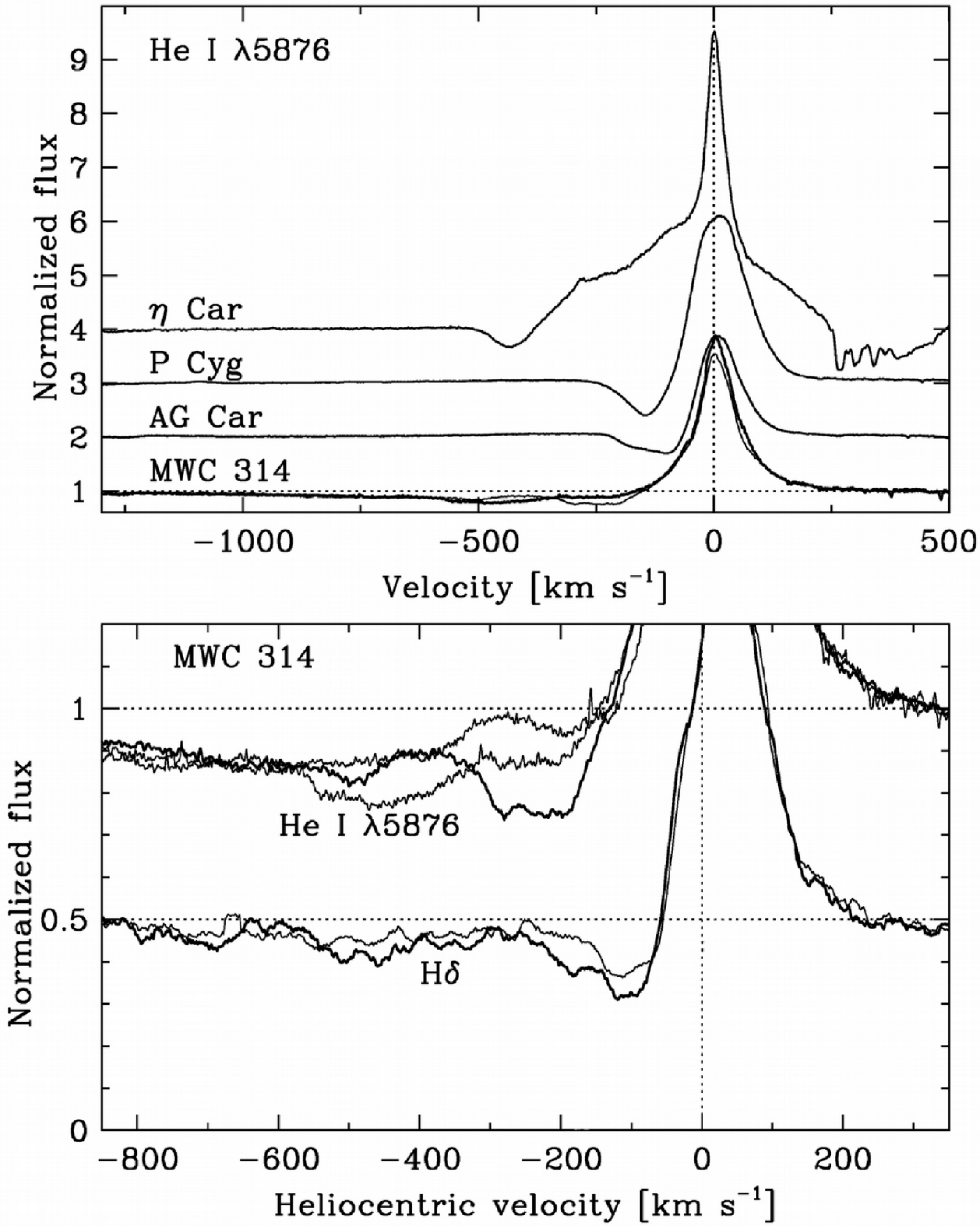

He I P Cyg profiles in MWC 314 with v_∞ > 1200 km/s.

v_∞ ~1500 km/s in He I λ10830 P Cyg line (Groh et al. A&A 2007)

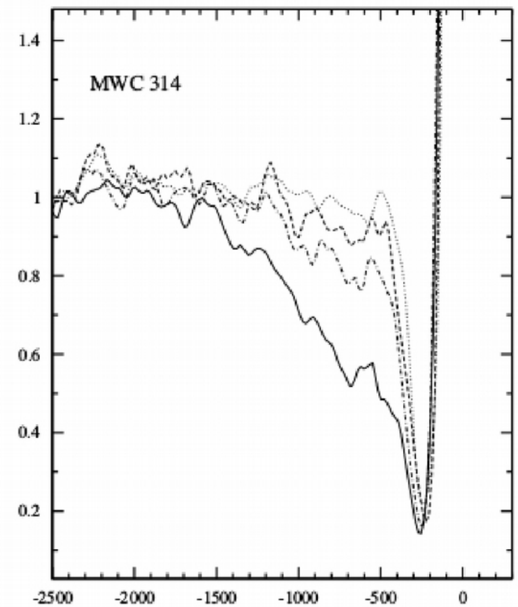

Strong changes in absorption for v_{wind} < 600 km/s, we also observe in the higher H lines.

Photospheric absorption lines with orbital phase

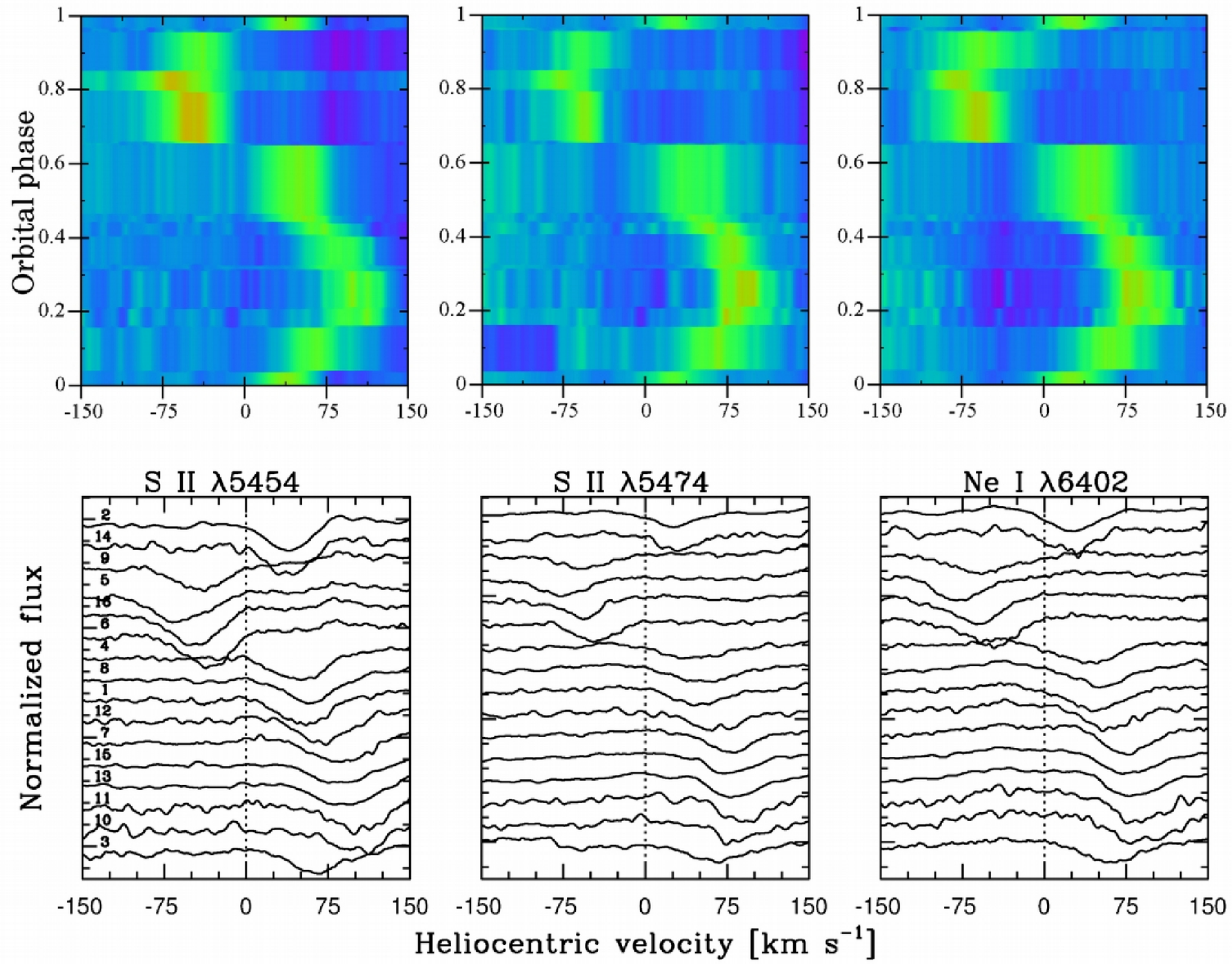

- S-wave observed in high-excitation absorption lines void of emission with amplitude of ~160 km/s. Caused by orbital motion of massive primary.

Orbital variability of He I lines in MWC 314

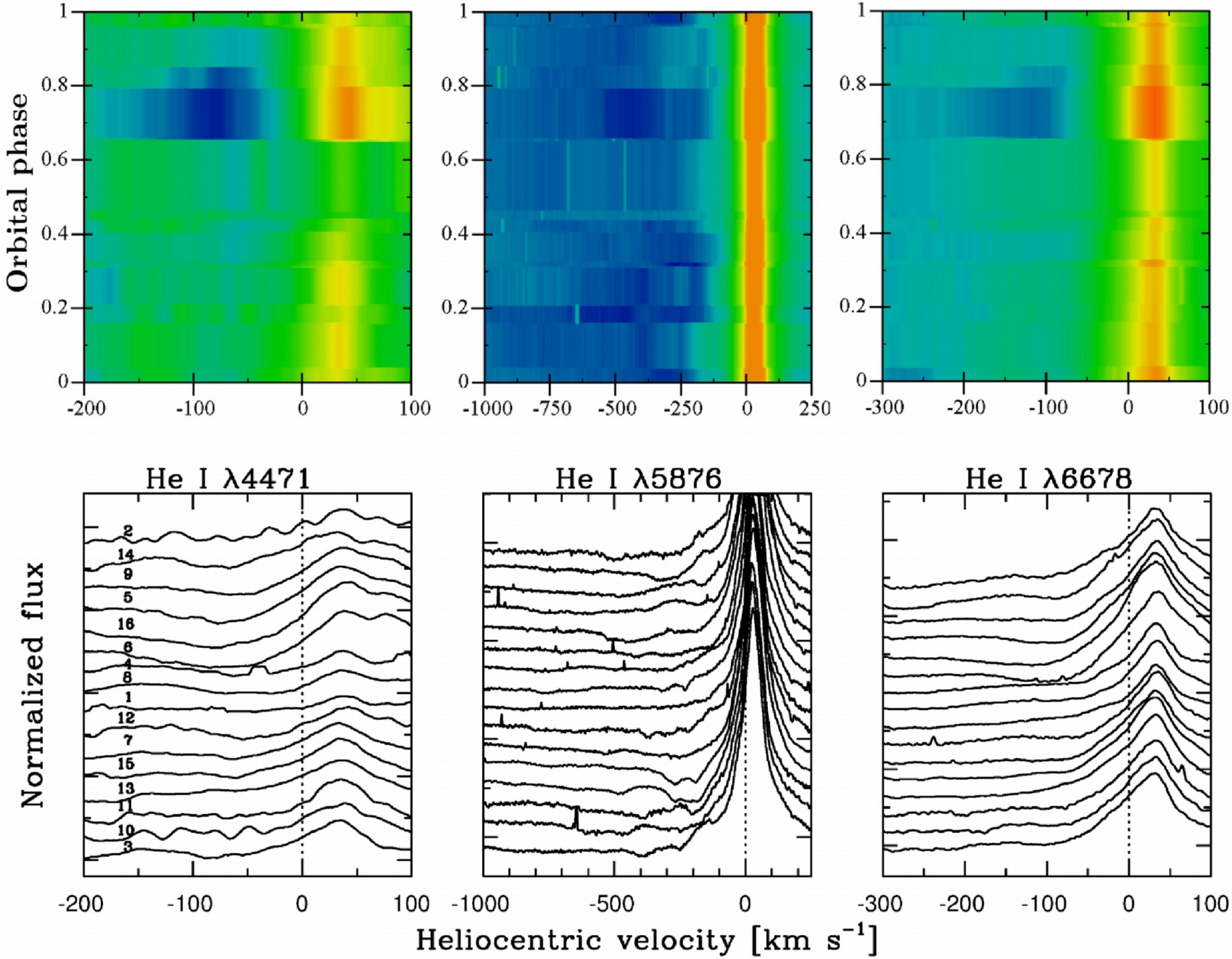

- All He I lines show orbitally modulated wind absorption.
- Maximum wind absorption at ϕ = 0.65 – 0.85; max RV blueshift of primary

Wind3D RT fit to He I λ5876 orbital variability

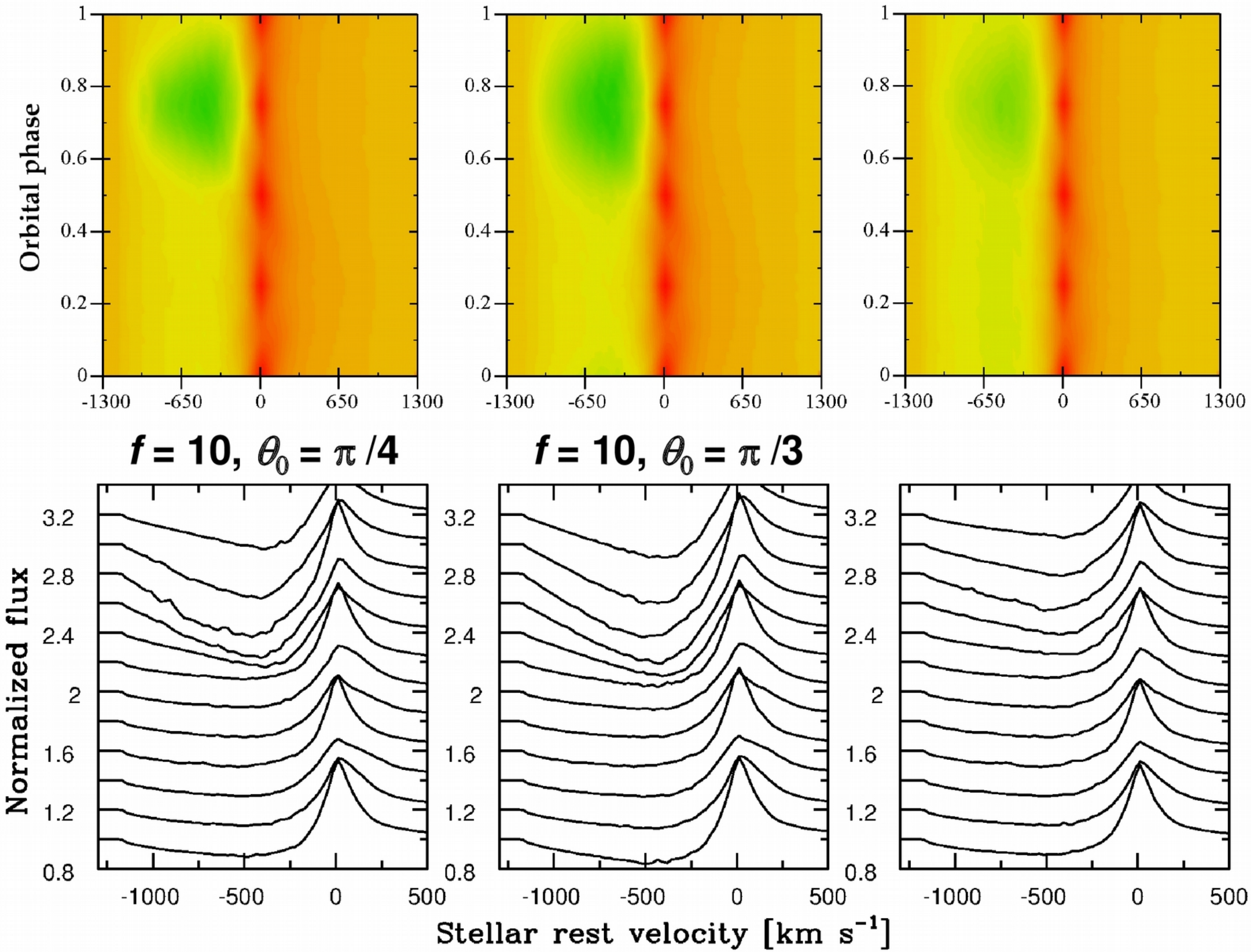

Best fit:
f = 3.3

opening angle $\theta_0 = \pi/4$

K_1 = 84.5 km/s (obs. Vrad)

- **Parametrized 3-D model reproduces enhanced absorption at ϕ=0.65 - 0.85.**
- **3-D RT Wind3D includes convergence of 3-D line source function with ϕ.**

Asymmetric 3-D wind model of MWC 314

primary at apastron

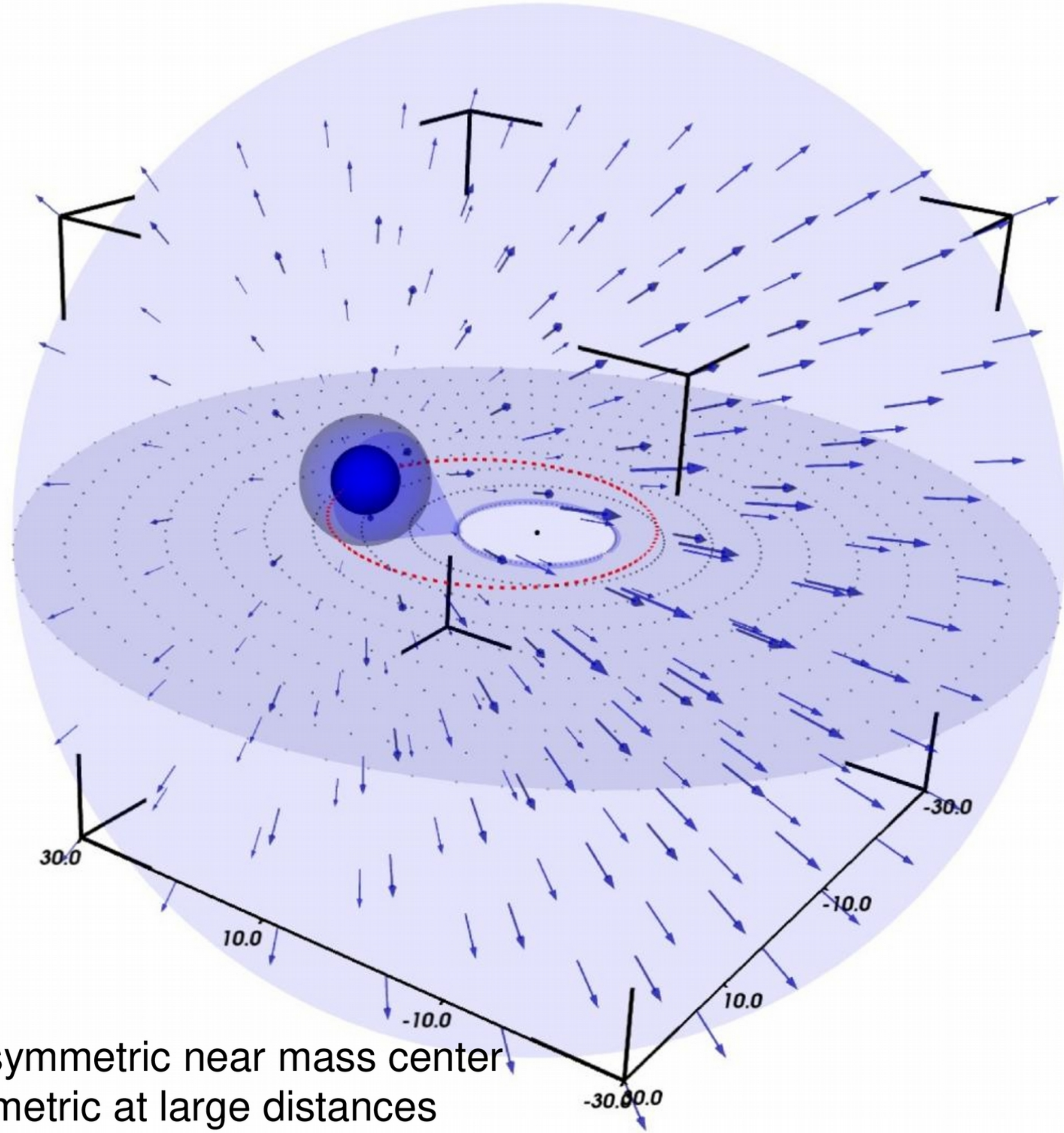

β-law wind model is asymmetric near mass center
and becomes symmetric at large distances

Wind3D RT fit to He I λ5876 orbital variability

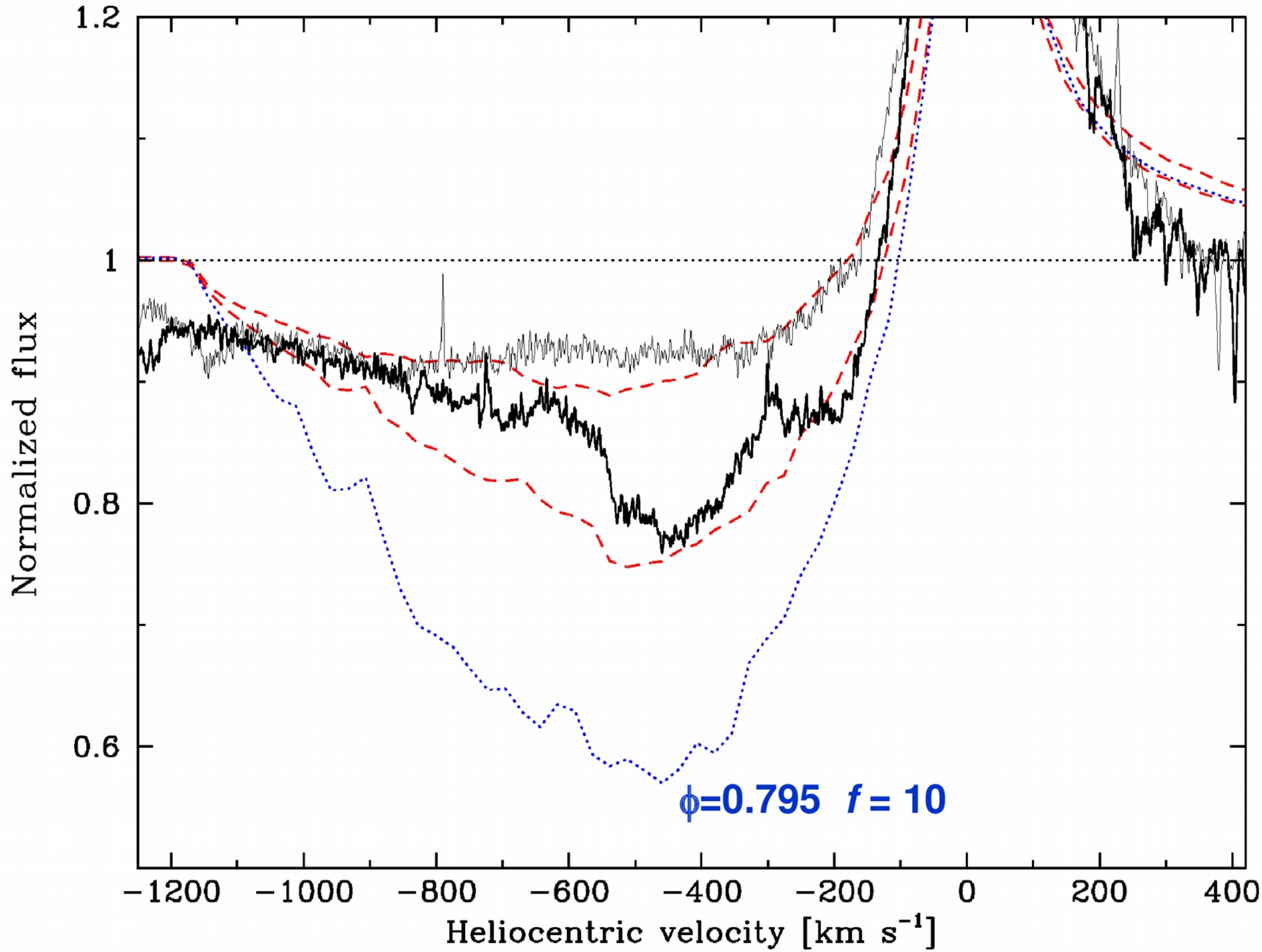

• 3-D best RT fit with Wind3D for wind density enhancement factor *f* = 3.3.

Summary

- **Long-term spectroscopic and photometric monitoring of Yellow Hypergiants and Luminous Blue Variables provides essential information about fundamental properties of the atmospheric dynamics and wind physics in these exceptional stars.**

- **Notorious YHGs such as Rho Cas, HR 5171A , HR 8752 are best suited for long-term monitoring programs since they reveal outburst events, large Teff variability, and strong changes of mass-loss rates.**

- **More research required for understanding the physics of outbursts in terms of pulsation properties, atmospheric velocity fields, and instability mechanisms. Comparison of common YHG properties. Search for links with LBV wind / pulsation variability.**

- **Outbursts are observed in cool and hot hypergiants. Are variable emission lines excited by propagating shock waves? Advanced hydro-dynamic and multi-D RT modelling is needed.**